

Enrichment of Tetracycline Residues in Honey by Magnetic Solid Phase Extraction
using Natural Reagent based-Nanoparticle prior to High Performance Liquid
Chromatography

Tammanoon Nilnit

A Thesis Submitted in Partial Fulfillment of Requirements for
degree of Master of Science in Chemistry

May 2024

Copyright of Mahasarakham University

การเพิ่มความเข้มข้นของเตตราไซคลินตกค้างในน้ำผึ้งโดยการสกัดวัฏภาคของแข็งแม่เหล็กโดยใช้
อนุภาคนาโนที่มีฐานจากรีเอเจนต์ธรรมชาติก่อนการวิเคราะห์ด้วยโครมาโทกราฟีของเหลว

สมรรถนะสูง

วิทยานิพนธ์

ของ

ธรรมนุญ นิลนิตย์

พูน ปลูกโต ชีเว

เสนอต่อมหาวิทยาลัยมหาสารคาม เพื่อเป็นส่วนหนึ่งของการศึกษาดูตามหลักสูตร

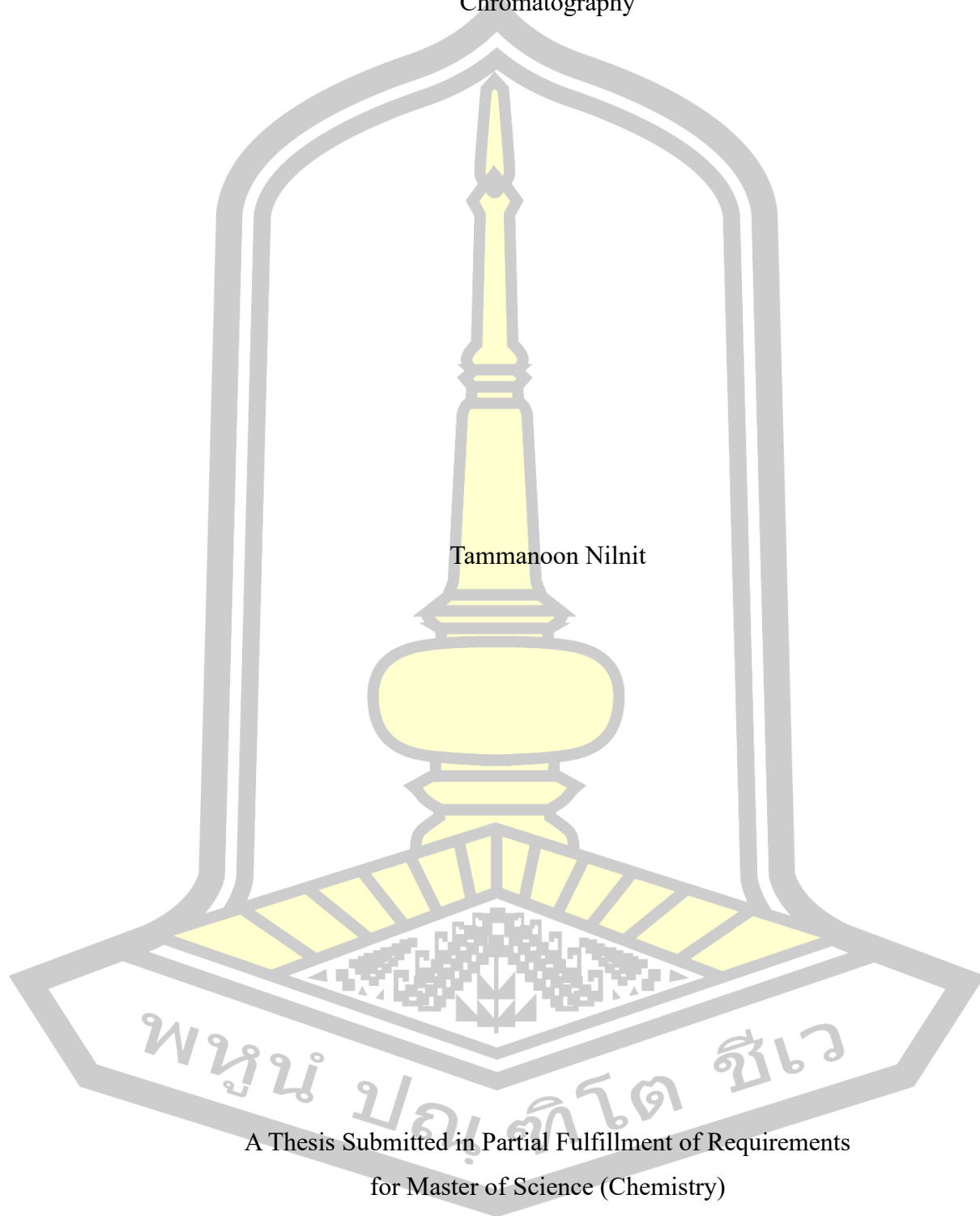
ปริญญาวิทยาศาสตรมหาบัณฑิต สาขาวิชาเคมี

พฤษภาคม 2567

ลิขสิทธิ์เป็นของมหาวิทยาลัยมหาสารคาม

Enrichment of Tetracycline Residues in Honey by Magnetic Solid Phase Extraction
using Natural Reagent based-Nanoparticle prior to High Performance Liquid
Chromatography

Tammanoon Nilnit



A Thesis Submitted in Partial Fulfillment of Requirements
for Master of Science (Chemistry)

May 2024

Copyright of Mahasarakham University



The examining committee has unanimously approved this Thesis, submitted by Mr. Tammanoon Nilnit , as a partial fulfillment of the requirements for the Master of Science Chemistry at Mahasarakham University

Examining Committee

Chairman

(Assoc. Prof. Rodjana Burakham ,
Ph.D.)

Advisor

(Asst. Prof. Kraingkrai Ponghong ,
Ph.D.)

Co-advisor

(Asst. Prof. Sam-ang Supharoek ,
Ph.D.)

Committee

(Asst. Prof. Senee Kruanetr , Ph.D.)

Committee

(Asst. Prof. Orrasa Prasitnok ,
Ph.D.)

Mahasarakham University has granted approval to accept this Thesis as a partial fulfillment of the requirements for the Master of Science Chemistry

(Prof. Pairot Pramual , Ph.D.)
Dean of The Faculty of Science

(Assoc. Prof. Krit Chaimoon , Ph.D.)
Dean of Graduate School

มหาวิทยาลัยราชภัฏรำไพพรรณี

TITLE	Enrichment of Tetracycline Residues in Honey by Magnetic Solid Phase Extraction using Natural Reagent based-Nanoparticle prior to High Performance Liquid Chromatography		
AUTHOR	Tammanoon Nilnit		
ADVISORS	Assistant Professor Kraingkrai Ponhong , Ph.D. Assistant Professor Sam-ang Supharoek , Ph.D.		
DEGREE	Master of Science	MAJOR	Chemistry
UNIVERSITY	Maharakham University	YEAR	2024

ABSTRACT

Tetracyclines (TCs) are widely used for treating and preventing bacterial infections in beekeeping, leading to presence of TC residues in honey. Therefore, natural phenolic-coated Fe₃O₄ magnetic nanoparticles (MNPs) were synthesized using phenolic compounds extracted from the bark of *Hevea brasiliensis* Muell. Arg.. Ultrasound-assisted continuous-flow techniques was utilized to improve synthesis efficiency and reduce the size distribution of MNPs. These MNPs were employed as sorbents in magnetic solid phase extraction (MSPE) to enrich of tetracycline (TC), chlortetracycline (CTC), oxytetracycline (OTC), and doxycycline (DC) residues in honey samples prior to HPLC-UV analysis. The effects of physical and chemical parameters on MNPs synthesis and the extraction method were investigated. The synthesized MNPs were characterized by Zetasizer, TEM, FT-IR, XRD, BET and VSM. The results demonstrated that the shape of the natural phenolic-coated Fe₃O₄ MNPs was spherical and exhibited superparamagnetic behavior, with a saturation magnetization of 87.8 emu g⁻¹. Under the optimum d-SPE conditions, the developed method exhibited limits of detection (LOD) and limits of quantification (LOQ) of 0.50 and 0.70–1.00 µg L⁻¹, respectively, which are lower than the EURL Guidance on minimum method performance requirements for the analysis of TC residues in honey and the maximum residue limits. Additionally, this method demonstrated good linearity ($R^2 = 0.9953$) and a high enrichment factor (32–91). The proposed method was successfully applied to extract and enrich TC residues in honey samples, with recoveries ranging from 81.3% to 117.9%.

Keyword : Tetracyclines, Magnetic nanoparticle, HPLC, Magnetic solid phase extraction, *Hevea brasiliensis* Muell. Arg., Honey

ACKNOWLEDGEMENTS

I would like to express my sincere gratitude to my advisor, Asst. Prof. Kraingkrai Ponghong, and my co-advisor, Asst. Prof. Sam-ang Supharoek, for their invaluable mentorship, supervision, constructive feedback, and the best support throughout my course of study. I am deeply thankful to the Chairman, Assoc. Prof. Rodjana Burakham, from the Department of Chemistry, Faculty of Science, Khon Kaen University, and the committee, Asst. Prof. Sene Kruanetr and Asst. Prof. Orrasa Prasitnok, from the Department of Chemistry, Faculty of Science, Mahasarakham University, for their kindness and valuable advice.

Furthermore, I extend my heartfelt appreciation to the Center of Excellence for Innovation in Chemistry (PERCH-CIC), Ministry of Higher Education, Science, Research, and Innovation for the financial support provided, and to the Department of Chemistry, Faculty of Science, Mahasarakham University, for granting access to chemicals, instruments, and all necessary facilities during my study.

Last but not least, I am profoundly grateful to my parents and family for their unwavering motivation and encouragement, which have been instrumental in making this study a successful and joyful journey.

Tammanoon Nilnit

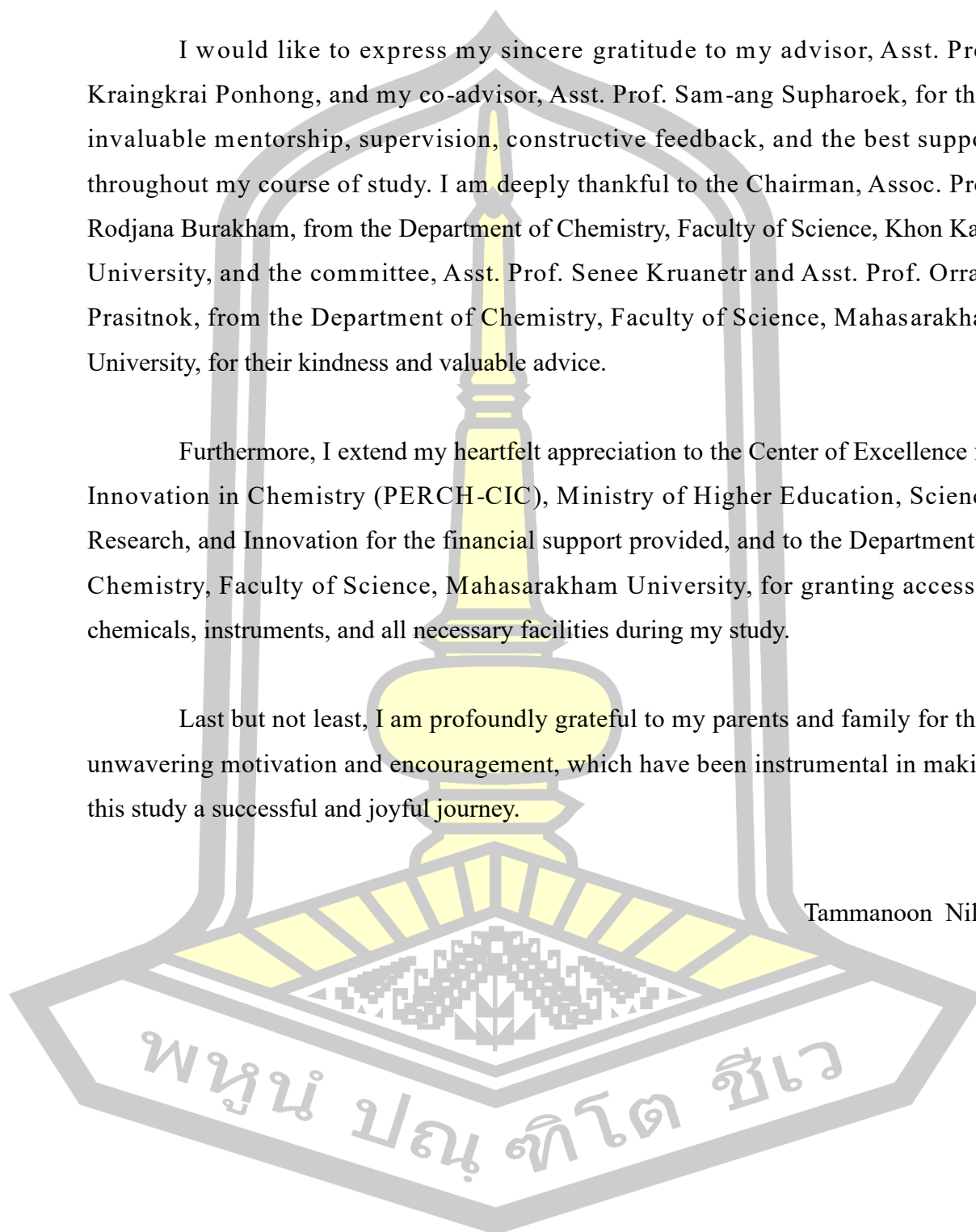


TABLE OF CONTENTS

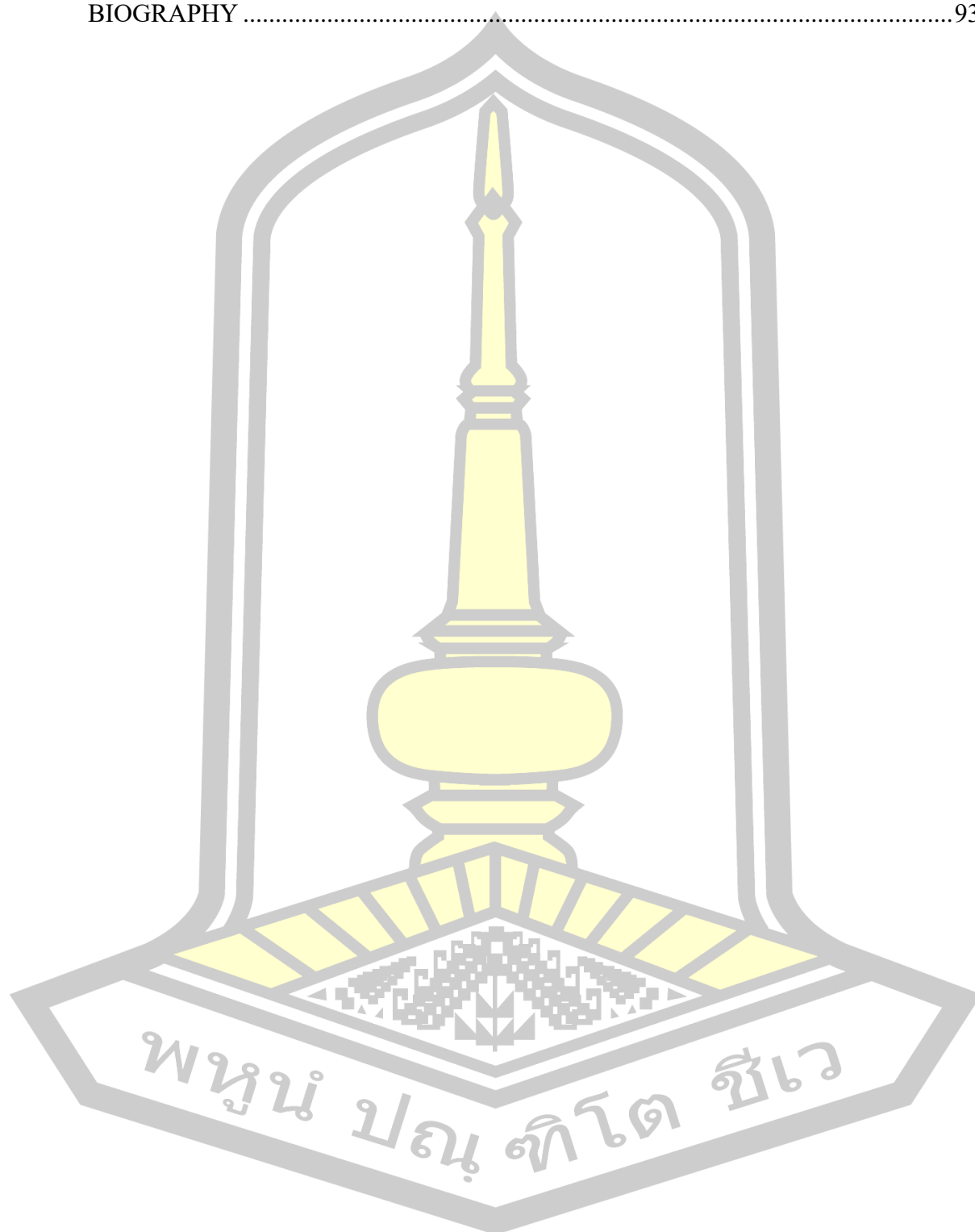
	Page
ABSTRACT.....	D
ACKNOWLEDGEMENTS.....	E
TABLE OF CONTENTS.....	F
LIST OF TABLES	K
LIST OF FIGURES	L
CHAPTER I.....	1
INTRODUCTION	1
1.1 Problems and provenance	1
1.2 Objectives	2
1.3 Scope of this work	2
1.4 Benefit of research	3
1.5 Venue of the study.....	3
CHAPTER II.....	4
LITERATURES REVIEW.....	4
2.1 Tetracyclines	4
2.1.1 Chemical structure of tetracyclines	4
2.1.2 Acid dissociation constants of tetracyclines.....	6
2.1.3 Application and Maximum Residue Limit of tetracyclines.....	8
2.2 Phenolic compounds.....	10
2.2.1 Tannins	10
2.2.1.1 Hydrolyzable tannins.....	10
2.2.1.2 Condensed tannins.....	11
2.3 Para rubber.....	12
2.3.1 Phenolic compounds in the Para rubber tree	12
2.4 Extraction technique	13

2.4.1 Dispersive solid phase extraction	15
2.4.2 Sorbent.....	16
2.4.2.1 Magnetic sorbent	16
2.4.2.2 Tannic acid-iron nanoparticles.....	21
2.4.3 Application of dispersive solid phase extraction for the determination of tetracyclines	22
2.5 High Performance Liquid Chromatography	26
CHAPTER III	30
MATERIALS AND METHODS	30
3.1 Chemicals and reagents	30
3.2 Instrumentation	31
3.3 Experimental.....	31
3.3.1 Preparation of a stock standard solution of 1000 mg L ⁻¹ TCs	31
3.3.2 Preparation of 0.10 mol L ⁻¹ iron(III) solution.....	31
3.3.3 Preparation of 0.10 mol L ⁻¹ iron(II) solution.....	31
3.3.4 <i>Hevea brasiliensis</i> Muell. Arg. bark preparation.....	32
3.3.5 Preparation of a natural reagent solution.....	32
3.3.6 Preparation of a 0.05 mol L ⁻¹ acetate buffer solution, pH 5.0	32
3.3.7 Preparation of 9% TFA in ACN.....	32
3.3.8 Preparation of the mobile phase	32
3.4 Magnetic nanoparticle-based natural reagent synthesis	33
3.5 d-SPE using magnetic nanoparticle-based natural reagents for enrichment TCs	34
3.6 Optimization of magnetic nanoparticle synthesis parameters	36
3.6.1 Batch and flow technique for magnetic nanoparticle synthesis	36
3.6.2 Tool for temperature control.....	36
3.6.3 The effect of the molarity concentration ratio of FeCl ₃ and FeSO ₄ ·7H ₂ O	37
3.6.4 The effect of flow rate	37
3.6.5 The effect of temperature.....	37

3.6.6 The effect of pH.....	37
3.6.7 The effect of stirring time.....	37
3.6.8 Characterization of magnetic nanoparticle-based natural reagents.....	37
3.7 Optimization of the d-SPE extraction parameter.....	38
3.7.1 Effect of honey sample weight.....	38
3.7.2 Effect of pH.....	38
3.7.3 Effect of total volume.....	38
3.7.4 Effect of buffer solution volume.....	38
3.7.5 Effect of magnetic nanoparticle volume.....	38
3.7.6 Effect of ionic strength.....	38
3.7.7 Effect of vortex time.....	38
3.7.8 Effect of magnetic nanoparticle collection time.....	39
3.7.9 Effect of concentration and volume of desorption solvent.....	39
3.8 Method validation.....	39
3.8.1 Linearity.....	39
3.8.2 Limits of detection and limit of quantification.....	39
3.8.3 Precision.....	40
3.8.4 Accuracy.....	40
3.9 Real sample.....	40
3.10 Data analysis.....	40
3.10.1 Mean (\bar{x}).....	40
3.10.2 Standard deviation (SD).....	40
3.10.3 Relative standard deviation (%RSD).....	41
3.10.4 Relative recoveries (%RR).....	41
CHAPTER IV.....	42
RESULTS AND DISCUSSION.....	42
4.1 Performance of natural phenolic-coated Fe ₃ O ₄ MNPs for enrichment of TCs..	42
4.2 Optimization of natural phenolic-coated Fe ₃ O ₄ MNPs synthesis by continuous flow synergistic with ultrasound-assisted.....	43

4.2.1 Batch and flow technique for magnetic nanoparticle synthesis	43
4.2.2 Tool for temperature control.....	44
4.2.3 Effect of $\text{FeCl}_3\text{:FeSO}_4$ molarity concentration ratio.....	45
4.2.4 Effect of flow rate.....	46
4.2.5 Effect of temperature	47
4.2.6 Effect of pH	48
4.2.7 Effect of stir time.....	49
4.3 Characterization of ultrasound-assisted continuous flow-synthesized natural phenolic-coated Fe_3O_4 MNPs.....	51
4.4 Optimization of the d-SPE procedure to TCs extraction using ultrasound-assisted continuous flow-synthesized natural phenolic-coated Fe_3O_4 MNPs ...	56
4.4.1 Effect of honey weight	56
4.4.2 Effect of pH	57
4.4.3 Effect of total volume	58
4.4.4 Effect of buffer solution volume	59
4.4.5 Effect of MNP volume	60
4.4.6 Effect of ionic strength (salt type)	61
4.4.7 Effect of ionic strength (salt concentration)	62
4.4.8 Effect of vortex time.....	63
4.4.9 Effect of MNP collection time.....	64
4.4.10 Effect of concentration of desorption solvent	65
4.4.11 Effect of desorption solvent volume.....	66
4.5 Method validation.....	68
4.6 Stability of the natural phenolic-coated Fe_3O_4 MNP.....	70
4.7 Application of the developed method to honey samples	71
4.8 Comparison of the analytical performance of the developed sample preparation with the previous method	75
CHAPTER V	79
CONCLUSION.....	79
REFERENCES	80

REFERENCES	81
BIOGRAPHY	93



LIST OF TABLES

	Page
Table 1 Tetracyclines.....	5
Table 2 Some chemical and physical properties of 4 tetracyclines antimicrobials [22].	7
Table 3 Some chemical and physical properties of four tetracyclines antimicrobials...	9
Table 4 Application of analytical methods for the determination of tetracycline residues in honey samples.....	14
Table 5 Application of magnetic nanoparticles for tetracyclines analysis.	20
Table 6 Application of dispersive solid phase extraction for determination of tetracyclines.	25
Table 7 Previously published journals related to the determination of tetracyclines using HPLC.....	28
Table 8 List of all chemicals used in this research.....	30
Table 9 The optimum condition of natural phenolic-coated Fe ₃ O ₄ magnetic nanoparticle synthesis for use as an adsorbent in dispersive solid phase extraction to extract tetracyclines.	50
Table 10 The optimum condition of dispersive solid phase extraction for the extraction of tetracyclines using natural phenolic-coated Fe ₃ O ₄ MNP sorbent from ultrasound-assisted continuous flow-synthesis.....	68
Table 11 Method validation of the proposed method in terms of limit of detection, limit of quantitation, linear range, R ² , enrichment factor, and precision for the determination of tetracyclines in honey matrix.	69
Table 12 Application of the developed method for determination of TCs in real honey samples.....	73
Table 13 Comparison of the analytical performance method between the proposed methods and other previously reported methods for using magnetic nanoparticles for tetracycline analysis.	77

LIST OF FIGURES

	Page
Figure 1 The chemical structure of Tetracyclines.	4
Figure 2 Structures and pKa sites of tetracyclines [21].	6
Figure 3 a) Structure of gallotannin, b) Structure of ellagitannin [39].	11
Figure 4 Basic structure of a condensed tannin [40].	11
Figure 5 The latex obtained from the tapping of the rubber tree.	12
Figure 6 Scheme of dispersion methodology by dispersive solid phase extraction [60].	16
Figure 7 The coordination of ferric ion and tannic acid [78].	22
Figure 8 The components of the HPLC system [84].	27
Figure 9 Schematic procedure of nanoparticle synthesis using ultrasound-assisted continuous flow technique.	33
Figure 10 Diagram of the magnetic nanoparticle synthesis procedure.	34
Figure 11 Schematic procedure of the d-SPE for extracting TCs in honey samples. ...	35
Figure 12 Diagram of dispersive solid phase extraction procedure for extracting TCs in honey samples.	36
Figure 13 Peak area of all TCs after being extracted and enriched by batch- synthesized Fe ₃ O ₄ MNPs (Batch Fe ₃ O ₄), batch-synthesized natural-phenolic-coated Fe ₃ O ₄ MNPs (Batch Fe ₃ O ₄ @phenolic), and ultrasound-assisted continuous flow- synthesized natural-phenolic-coated Fe ₃ O ₄ MNPs (Flow Fe ₃ O ₄ @phenolic).	43
Figure 14 Peak area of all TCs after being extracted and enriched by batch- synthesized MNPs and continuous flow-synthesized MNPs.	44
Figure 15 Peak area of all TCs after being extracted and enriched by MNPs synthesized using a continuous-flow technique combined with an ultrasonic bath. ...	45
Figure 16 Effect of molarity concentration ratio of FeCl ₃ :FeSO ₄ . Conditions: 2g of Hevea brasiliensis Muell. Arg. bark, flow rate at 4 mL min ⁻¹ , temperature at 65 °C, pH 10.5, stir time of 1 hr., and 500 µg L ⁻¹ of each tetracycline.	46
Figure 17 Effect of flow rate. Conditions: concentration ratio of FeCl ₃ :FeSO ₄ was 0.1 M:0.1 M, 2g of Hevea brasiliensis Muell. Arg. bark, temperature at 65 °C, pH 10.5, stir time of 1 hr., and 500 µg L ⁻¹ of each tetracycline.	47

Figure 18 Effect of temperature. Conditions: concentration ratio of $\text{FeCl}_3\text{:FeSO}_4$ was 0.1 M:0.1 M, 2g of <i>Hevea brasiliensis</i> Muell. Arg. bark, flow rate at 4 mL min^{-1} , pH 10.5, stir time of 1 hr., and $500 \mu\text{g L}^{-1}$ of each tetracycline.	48
Figure 19 Effect of pH. Conditions: concentration ratio of $\text{FeCl}_3\text{:FeSO}_4$ was 0.1 M:0.1 M, 2g of <i>Hevea brasiliensis</i> Muell. Arg. bark, flow rate at 4 mL min^{-1} , temperature at 65°C , stir time of 1 hr., and $500 \mu\text{g L}^{-1}$ of each tetracycline.....	49
Figure 20 Effect of stir time. Conditions: concentration ratio of $\text{FeCl}_3\text{:FeSO}_4$ was 0.1 M:0.1 M, 2g of <i>Hevea brasiliensis</i> Muell. Arg. bark, flow rate at 4 mL min^{-1} , temperature at 65°C , pH 10.5, and $500 \mu\text{g L}^{-1}$ of each tetracycline.	50
Figure 21 FTIR spectra of flow-synthesized bare Fe_3O_4 MNPs and natural phenolic-coated Fe_3O_4 MNPs before and after TCs extraction.	53
Figure 22 (a) XRD patterns of flow-synthesized bare and natural phenolic-coated Fe_3O_4 MNPs, (b) VSM magnetization of flow-synthesized bare and natural phenolic-coated Fe_3O_4 MNPs.	54
Figure 23 Gaussian distribution curves of (a) flow-synthesized and (b) batch-synthesized natural phenolic-coated Fe_3O_4 MNPs.	54
Figure 24 (a and b) TEM images of flow-synthesized natural phenolic-coated Fe_3O_4 MNPs before and after TCs extraction, respectively, and (c) N_2 adsorption-desorption isotherms of flow-synthesized natural phenolic-coated Fe_3O_4 MNPs.....	55
Figure 25 The summarized graphitic layer extraction mechanism between ultrasound-assisted continuous flow-synthesized natural phenolic-coated Fe_3O_4 MNPs and TCs analytes.	56
Figure 26 Effect of honey weight. Conditions: $100 \mu\text{L}$ of MNPs, 0.05 M acetate buffer pH 5.0, total volume was 10 mL, vortex 60 s, MNPs collection time was 2 min, $100 \mu\text{L}$ of 9% TFA in ACN, and $500 \mu\text{g L}^{-1}$ of each tetracycline.	57
Figure 27 Effect of pH. Conditions: 2 g of honey, $100 \mu\text{L}$ of MNPs, total volume was 10 mL, vortex 60 s, MNPs collection time was 2 min, $100 \mu\text{L}$ of 9% TFA in ACN, and $500 \mu\text{g L}^{-1}$ of each tetracycline.	58
Figure 28 Effect of total volume. Conditions: 2 g of honey, $100 \mu\text{L}$ of MNPs, 0.05 M acetate buffer pH 5.0, vortex 60 s, MNPs collection time was 2 min, $100 \mu\text{L}$ of 9% TFA in ACN, and $500 \mu\text{g L}^{-1}$ of each tetracycline.	59
Figure 29 Effect of buffer solution volume. Conditions: 2 g of honey, $100 \mu\text{L}$ of MNPs, 0.05 M acetate buffer pH 5.0, vortex 60 s, MNPs collection time was 2 min, $100 \mu\text{L}$ of 9% TFA in ACN, and $500 \mu\text{g L}^{-1}$ of each tetracycline.	60

Figure 30 Effect of MNP volume. Conditions: 2 g of honey, 0.05 M acetate buffer pH 5.0, total volume was 40 mL, vortex 60 s, MNPs collection time was 2 min, 100 μL of 9% TFA in ACN, and 500 $\mu\text{g L}^{-1}$ of each tetracycline.61

Figure 31 Effect of salt type. Conditions: 2 g of honey, 180 μL of MNPs, 0.05M acetate buffer pH 5.0, total volume was 40 mL, vortex 60 s, MNPs collection time was 2 min, 100 μL of 9% TFA in ACN, and 500 $\mu\text{g L}^{-1}$ of each tetracycline.62

Figure 32 Effect of NaCl concentration. Conditions: 2 g of honey, 180 μL of MNPs, 0.05M acetate buffer pH 5.0, total volume was 40 mL, vortex 60 s, MNPs collection time was 2 min, 100 μL of 9% TFA in ACN, and 500 $\mu\text{g L}^{-1}$ of each tetracycline.63

Figure 33 Effect of vortex time. Conditions: 2 g of honey, 180 μL of MNPs, 0.05M acetate buffer pH 5.0, total volume was 40 mL, 0.1% NaCl, MNPs collection time was 2 min, 100 μL of 9% TFA in ACN, and 500 $\mu\text{g L}^{-1}$ of each tetracycline.64

Figure 34 Effect of vortex time. Conditions: 2 g of honey, 180 μL of MNPs, 0.05M acetate buffer pH 5.0, total volume was 40 mL, 0.1% NaCl, vortex 10 s, 100 μL of 9% TFA in ACN, and 500 $\mu\text{g L}^{-1}$ of each tetracycline.65

Figure 35 Effect of concentration of desorption solvent. Conditions: 2 g of honey, 180 μL of MNPs, 0.05M acetate buffer pH 5.0, total volume was 40 mL, 0.1% NaCl, vortex 10 s, 100 μL of TFA in ACN, and 500 $\mu\text{g L}^{-1}$ of each tetracycline.66

Figure 36 Effect of concentration of desorption solvent. Conditions: 2 g of honey, 180 μL of MNPs, 0.05M acetate buffer pH 5.0, a total volume was 40 mL, 0.1% NaCl, vortex 10 s, and 500 $\mu\text{g L}^{-1}$ of each tetracycline.67

Figure 37 Chromatogram of tetracyclines standard solution analysis by direct injection method and preconcentrated by the proposed method (500 $\mu\text{g L}^{-1}$ of each tetracycline).....70

Figure 38 Peak area of all TCs after being extracted and enriched over a 15-day period by intra-batch-synthesized MNPs.71

Figure 39 Representation chromatograms of honey samples spiked with standard TCs at 1.00, 3.00, and 5.00 $\mu\text{g L}^{-1}$75

CHAPTER I

INTRODUCTION

1.1 Problems and provenance

Honey is a product derived from bees that humans prefer to use as food and medicine due to its antimicrobial properties [1]. However, bee mortality rates are currently rising due to threats from diseases such as American foulbrood (AFB) and European foulbrood (EFB), caused by the gram-positive bacteria *Penibacillus larvae* and *Melissococcus plutonius* [2]. Antibiotics like tetracyclines are therefore commonly used to treat or prevent bee diseases [3] because tetracyclines have an inhibitory effect on both gram-positive and gram-negative bacteria [4], resulting in possible tetracycline residues in honey. Overuse and misuse of antibiotics can lead to adverse health effects, including drug resistance to pathogens and serious allergies [5]. Therefore, the European Union has recommended content for screening total of tetracycline (TC), oxytetracycline (OTC), and chlortetracycline (CTC) concentration in honey at $20 \mu\text{g kg}^{-1}$, and many countries have been established the maximum residue limits (MRLs) for tetracyclines in honey in order to ensure the safety of consumers, for example: Belgium and Switzerland have been set the limit at $20 \mu\text{g kg}^{-1}$, while France and China were regulated at 10 and $50 \mu\text{g kg}^{-1}$, respectively [6]. Additionally, the European Union have been set the EURL Guidance on minimum method performance requirements (MMPRs) for the analysis of tetracycline residues in honey at $10 \mu\text{g kg}^{-1}$ [7].

However, residual antibiotics are found at low concentrations in a complicated matrix and contain many interferences. Therefore, the sample preparation process prior to analysis is very important. Because it can increase the extraction efficiency and reduce the effect of interference. Currently, there are various sample preparation methods that can effectively preconcentrate tetracyclines for analysis, including dispersive liquid-liquid microextraction (DLLME) [8], solid phase extraction (SPE) [9], cloud-point extraction (CPE) [10], and dispersed solid phase extraction (d-SPE). Among these preparation methods, the d-SPE technique is simple, has a short extraction time, and has low solvent consumption [11]. Magnetic Fe_3O_4 nanoparticles

are one of the commonly used as the sorbents for tetracyclines extraction due to their small size and high surface area, resulting in high extraction efficiency. The superparamagnetic properties of Fe_3O_4 nanoparticles led to the quick and easy collection of sorbents by using an external magnetic field. It causes avoids time-consuming centrifugation or filtration procedures [12][13]. However, magnetic particles are toxic to biological systems and the environment, which can be avoided the toxicity by complexing with green polymers like tannin [14].

Therefore, in this research, we are interested in the synthesis of magnetic nanoparticles using natural reagents from *Hevea brasiliensis* Muell. Arg. bark and further use as sorbents in dispersive magnetic solid phase extraction in combination with high performance liquid chromatography (HPLC) for enrichment and determination of four tetracyclines, including tetracycline (TC), doxycycline (DC), oxytetracycline (OTC), and chlortetracycline (CTC) residues in honey samples. Ultrasound synergized with a flow system was utilized to synthesize magnetic nanoparticle-based natural reagents. This proposed method provided high sensitivity, high accuracy, and rapid.

1.2 Objectives

- 1.2.1) To synthesize the magnetic nanoparticle-based natural reagent from *Hevea brasiliensis* Muell. Arg. bark. as an adsorbent for extraction using a flow system synergized with ultrasonication
- 1.2.2) To develop an extraction method for the enrichment of tetracyclines in honey samples using dispersive solid phase extraction followed by high performance liquid chromatography
- 1.2.3) To apply the developed method for quantification of tetracycline residues in honey samples obtained from Maha Sarakham, Roi-Et, and Kalasin provinces

1.3 Scope of this work

- 1.3.1) Investigation of parameters that influence on magnetic nanoparticle synthesis such as the concentration ratio of $\text{FeCl}_3:\text{FeSO}_4 \cdot 7\text{H}_2\text{O}$, flow rate, ultrasonic temperature, pH, and stir time

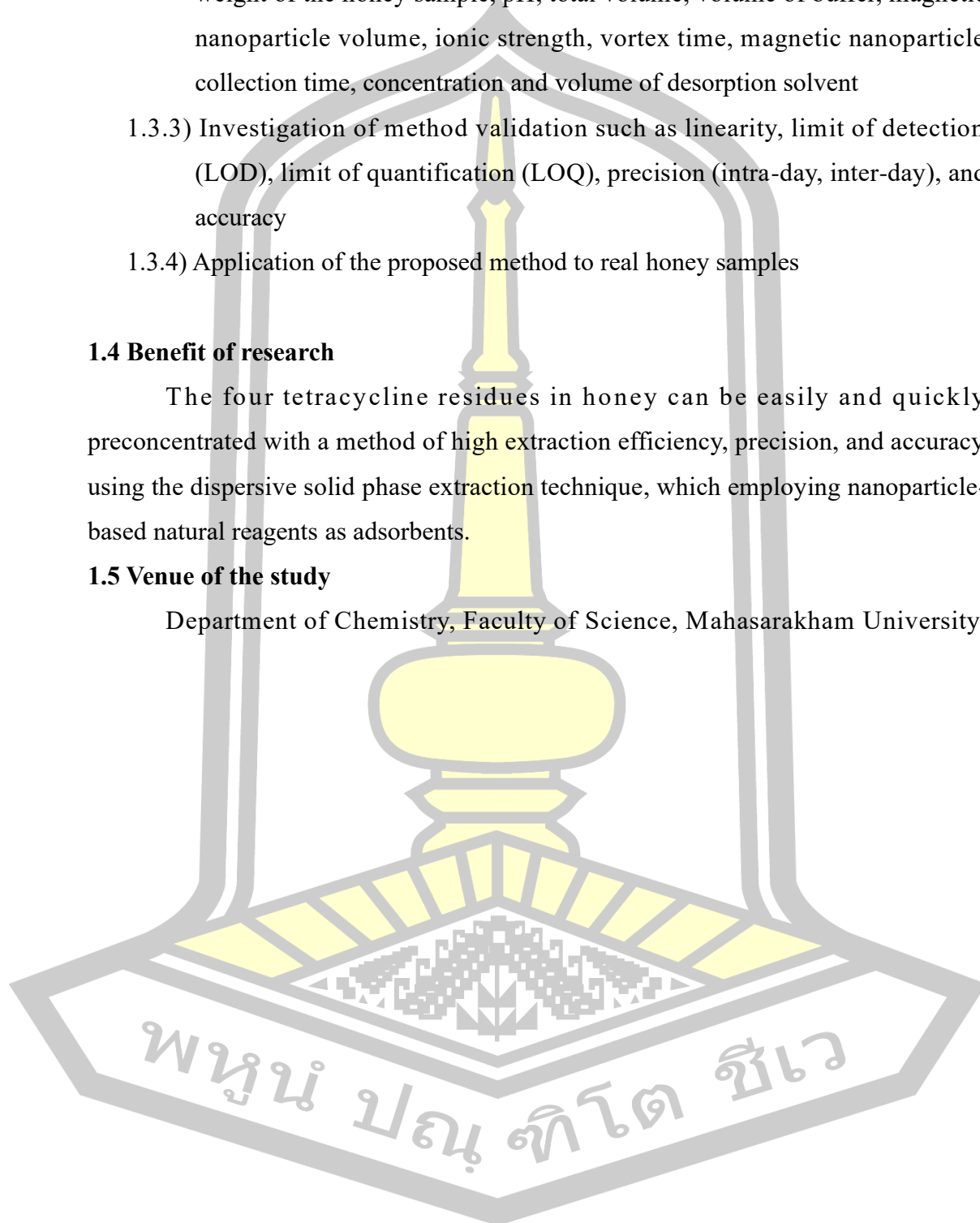
- 1.3.2) Investigation of parameters that influence the extraction efficiency, such as weight of the honey sample, pH, total volume, volume of buffer, magnetic nanoparticle volume, ionic strength, vortex time, magnetic nanoparticle collection time, concentration and volume of desorption solvent
- 1.3.3) Investigation of method validation such as linearity, limit of detection (LOD), limit of quantification (LOQ), precision (intra-day, inter-day), and accuracy
- 1.3.4) Application of the proposed method to real honey samples

1.4 Benefit of research

The four tetracycline residues in honey can be easily and quickly preconcentrated with a method of high extraction efficiency, precision, and accuracy using the dispersive solid phase extraction technique, which employing nanoparticle-based natural reagents as adsorbents.

1.5 Venue of the study

Department of Chemistry, Faculty of Science, Mahasarakham University.



CHAPTER II

LITERATURES REVIEW

2.1 Tetracyclines

Tetracyclines are a class of antibiotics that can be produced by *Streptomyces* spp. Chlortetracycline and oxytetracycline are the first tetracycline antibiotics discovered by Dr. Benjamin Duggar and Alexander Finlay in the 1948s and 1950s, respectively. Tetracyclines are an active agent against the activity of gram-positive and gram-negative bacteria, as well as chlamydia, mycoplasmas, rickettsia, and protozoan parasites. Tetracyclines are transported into the bacterial cell and bind to the 30S subunit of the ribosomal to prevent the binding of tRNA to the ribosomal acceptor, which results in inhibition of bacterial protein synthesis [15]–[17]. The tetracyclines antibiotics can be divided into three generations according to their synthesis. The first generation includes tetracycline, chlortetracycline, oxytetracycline, and demeclocycline, which are obtained by biosynthesis or naturally occurring. The second generation includes doxycycline, lymecycline, meclocycline, methacycline, minocycline, and rolitetracycline, which are derivatives of semi-synthesis. The third generation includes tigecycline, which is obtained by total synthesis [18].

2.1.1 Chemical structure of tetracyclines

Each antibiotic in the tetracyclines class has a very similar chemical structure. Four fused rings of the common hydronaphthacene nucleus are the core chemical structure, as shown in Figure 1 and Table 1, which present the chemical name and substituent group of the hydronaphthacene nucleus [19].

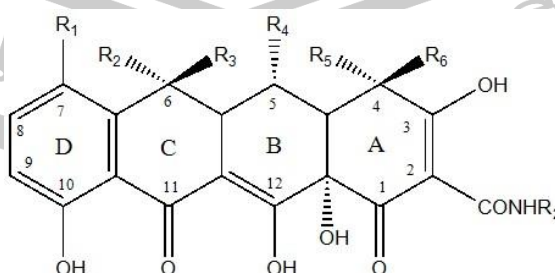
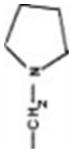


Figure 1 The chemical structure of Tetracyclines.

Table 1 Tetracyclines.

TCs name	Chemical name	R ₁	R ₂	R ₃	R ₄	R ₅	R ₆	R ₇
Tetracycline (TC)	4-(Dimethylamino)-1,4,4a,5,5a,6,11,12a-octahydro-3,6,10,12,12a-pentahydroxy-6-methyl-1,11-dioxo-2-naphthacene carboxamide monohydrochloride.	H	CH ₃	OH	H	N(CH ₃) ₂	H	H
Chlortetracycline (CTC)	7-chloro-tetracycline	Cl	CH ₃	OH	H	N(CH ₃) ₂	H	H
Oxytetracycline (OTC)	5-hydroxy-tetracycline	H	CH ₃	OH	OH	N(CH ₃) ₂	H	H
Methacycline (MTC)	6-methylene-5-hydroxy tetracycline	H	-CH ₂	-CH ₂	OH	N(CH ₃) ₂	H	H
Minocycline (MNC)	7-dimethylamino-6-demethyl-6-deoxy-tetracycline	N(CH ₃) ₂	H	H	H	N(CH ₃) ₂	H	H
Doxycycline (DC)	6-deoxy-5-hydroxy-tetracycline	H	-CH ₂	H	OH	N(CH ₃) ₂	H	H
Demeclocycline (DMCT)	Demethylchlortetracycline	Cl	H	OH	H	N(CH ₃) ₂	H	H
Meclocycline (MCC)	Chlormethylenecycline	Cl	-CH ₂	-	OH	N(CH ₃) ₂	H	H
Rolitetraacycline (RTC)	Pyrrolidinomethyltetracycline	H	CH ₃	OH	H	N(CH ₃) ₂	H	

2.1.2 Acid dissociation constants of tetracyclines

Acid dissociation constant (pK_a) values indicate the acidity of molecules. The tetracyclines provide 3 values of pK_a from 3 sites of the structure, as shown in Figure 2. pK_{a1} is 3–4, pK_{a2} is 7–8, and pK_{a3} is 9–10, which is unique to each tetracycline. It depends on the functional groups and their position. If the TCs are presented at a pH below 3, they are positively charged. At a pH between 3 and 8, they are neutral, and at a pH higher than 8, they have a negative charge [20] [21].

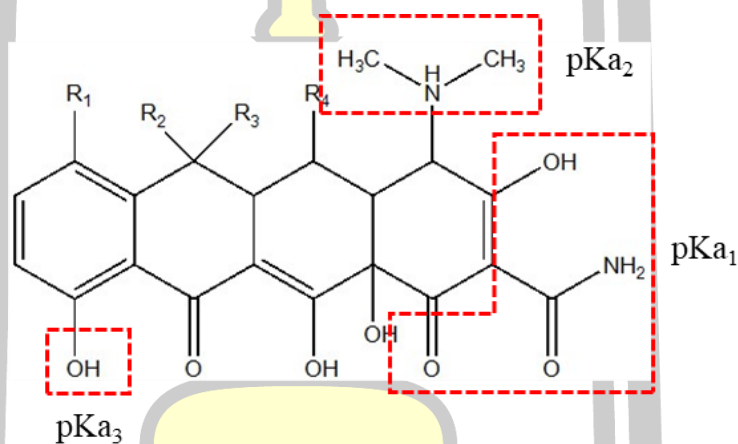
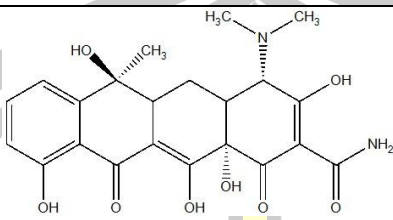
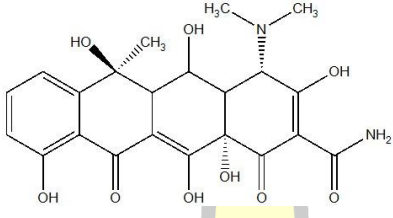
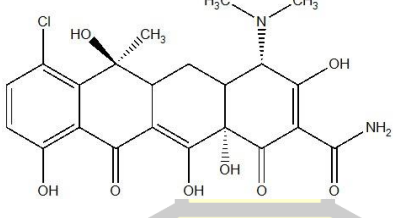
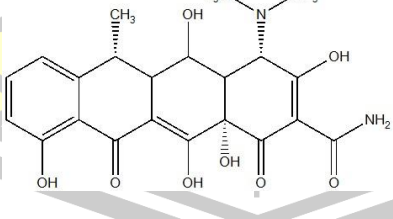


Figure 2 Structures and pK_a sites of tetracyclines [21].

The target analytes of tetracyclines for this research work include tetracycline, chlortetracycline, oxytetracycline, and doxycycline, which have physical and chemical properties listed in Table 2 [22].

พหุ ประสิทธิภาพ

Table 2 Some chemical and physical properties of 4 tetracyclines antimicrobials [22].

Antimicrobial	Chemical structure	Acidity (pKa)	Polarity (Log P)	Molecular mass (g/mol)
Tetracycline (TC)		pKa ₁ 3.3 pKa ₂ 7.7 pKa ₃ 9.7	-1.3	444.4
Oxytetracycline (OTC)		pKa ₁ 3.2 pKa ₂ 7.5 pKa ₃ 8.9	-3.6	460.4
Chlortetracycline (CTC)		pKa ₁ 4.5 pKa ₂ 7.8 pKa ₃ 9.8	-0.62	478.8
Doxycycline (DC)		pKa ₁ 3.0 pKa ₂ 7.9 pKa ₃ 9.2	-1.9	444.4

2.1.3 Application and Maximum Residue Limit of tetracyclines

Tetracyclines are broad-spectrum antibiotics that are readily available, inexpensive, and have effective antibacterial activity. Therefore, TCs are commonly used in livestock such as cattle, pigs, poultry, and fish for the prevention or treatment of animal infections by directly injection or mixed in food or drinking water for animals and used as food additives to promote the growth of animals [23], [24]. However, excessive use of TCs may cause residues of this antibiotic in animal-derived products such as meat, eggs, honey, and milk, which may cause adverse effects on human health such as allergic reactions, tooth discoloration and pigmentation, carcinogenesis in a fetus, and drug resistance to pathogens [25]. Therefore, many countries have established maximum residue limits (MRLs) for tetracyclines in food products of animal origin to ensure consumer safety, as shown in Table 3 [22]. Importantly, tetracycline residues in honey have been instituted the MRLs in many nations; for example, $20 \mu\text{g kg}^{-1}$ in Belgium and Switzerland, while France and China were controlled at 10 and $50 \mu\text{g kg}^{-1}$, respectively. And the recommended content for screening the total concentration of tetracycline (TC), oxytetracycline (OTC), and chlortetracycline (CTC) in honey has been established at $20 \mu\text{g kg}^{-1}$ by the European Union [6]. Additionally, the European Union has set the EURL Guidance on minimum method performance requirements (MMPRs) for the analysis of tetracycline residues in honey at $10 \mu\text{g kg}^{-1}$ [7].

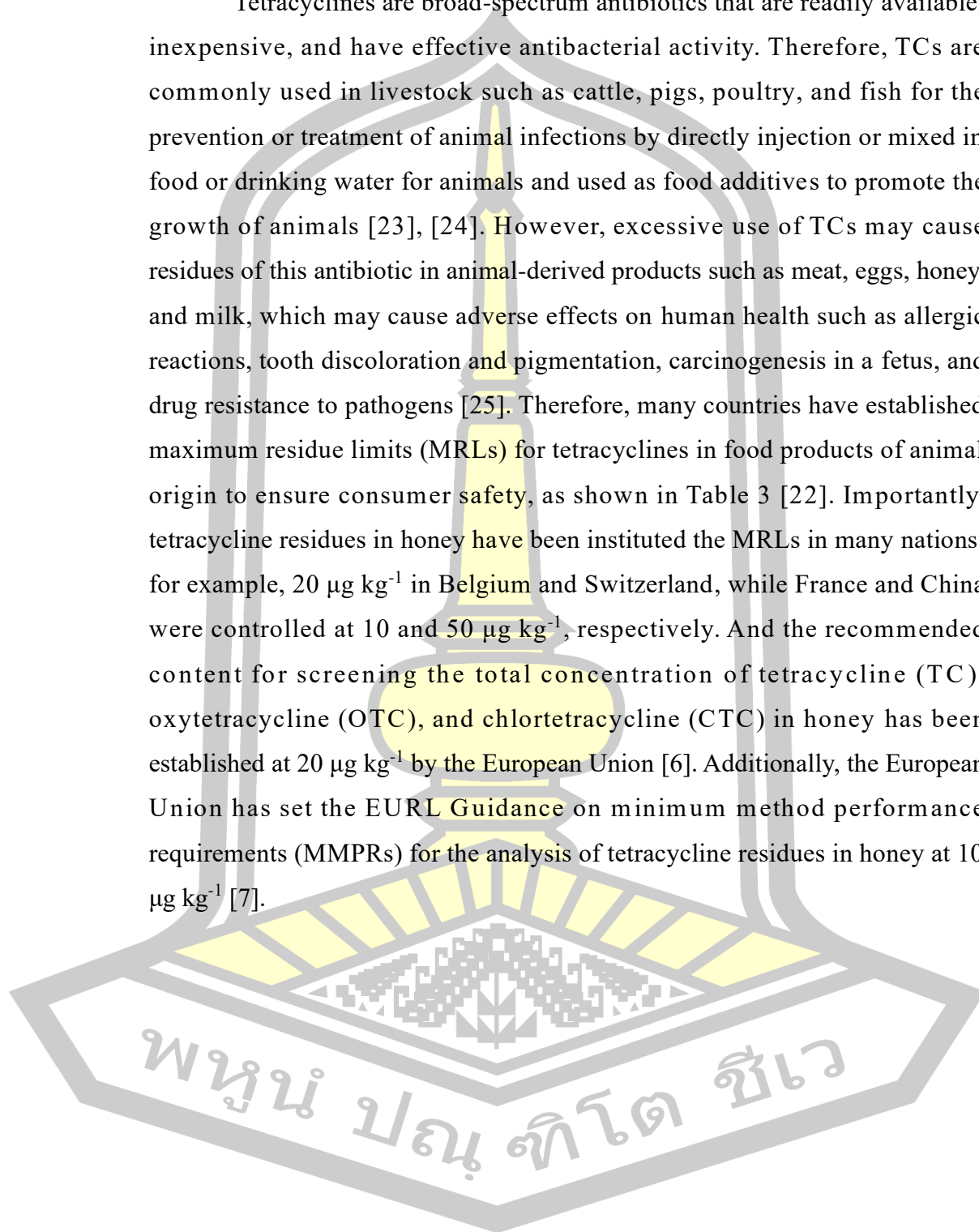


Table 3 Some chemical and physical properties of four tetracyclines antimicrobials.

Authority	Animal group	Target food	MRL ($\mu\text{g kg}^{-1}$)	Ref.
Codex Alimentarius	Poultry	Eggs	400	[26]
	Poultry	Muscle	200	
	Poultry	Liver	600	
	Cattle	Milk	100	
	Cattle and Swine	Muscle	200	
	Cattle and Swine	Liver	600	
	Fish	Muscle	200	
Canadian	Poultry	Eggs	400	[27]
	Poultry	Muscle	200	
	Poultry	Liver	600	
	Cattle	Milk	100	
	Cattle and Swine	Muscle	200	
	Cattle and Swine	Liver	600	
European Union	Poultry	Eggs	200	[28]
	Poultry, Cattle and Swine	Muscle	100	
	Poultry, Cattle and Swine	Liver	300	
	Cattle	Milk	100	
Chinese	Poultry	Eggs	200	[29]
	All Animal Source Foods	Muscle	100	
	All Animal Source Foods	Liver	300	
	Cattle and Lamb	Milk	100	
Brazilian (PNCRC)	Poultry	Eggs	-	[30]
	Poultry, Cattle and Swine	Muscle	200	
	Poultry, Cattle and Swine	Liver	-	
	Cattle	Milk	100	

2.2 Phenolic compounds

Phenolic compounds are secondary metabolites synthesized via the shikimic acid and phenylpropanoid pathways. The ability of phenolic compounds is bioactive, as antioxidants by chelating with metals involved in the formation of radicals or scavenging free radicals by donating hydrogen atoms or electrons. Phenolic compounds can be found in plant tissues such as fruits, seeds, leaves, roots, and stems. Phenolic compounds in plants have more than 8000 structures, and the general chemical structure of phenolic compounds consists of at least one aromatic ring with one or more substituent hydroxyl groups, which allows them to be divided into several subgroups such as phenolic acids, flavonoids, tannins, lignans, quinones, stilbenes, coumarins, and curcuminoids [31]–[33].

2.2.1 Tannins

Tannins or tannic acid are classified as water-soluble phenolic compounds. Tannins molecular mass was between 500-3000 Da and can be found in various parts of plants such as bark, leaves, stems, fruit, seed, and root [34][35]. Tannins have binding properties to proteins, macromolecules, pigments, and metal ions and can act as antioxidants. Considering the structural characteristics of the molecules, tannins can be divided into hydrolyzable tannins and condensed tannins [36].

2.2.1.1 Hydrolyzable tannins

Hydrolyzable tannins are derived from esterification between polyols such as D-glucose (mostly), fructose, xylose, saccharose, and structures like hamamelose with gallic acid or hexahydroxydiphenic acid. Hydrolyzable tannins can release gallic acid and/or ellagic acid when hydrolyzed by dilute acid. Hydrolyzable tannins can be divided into gallotannin and ellagitannin [34][37][38], whose structures are shown in Figure 3.

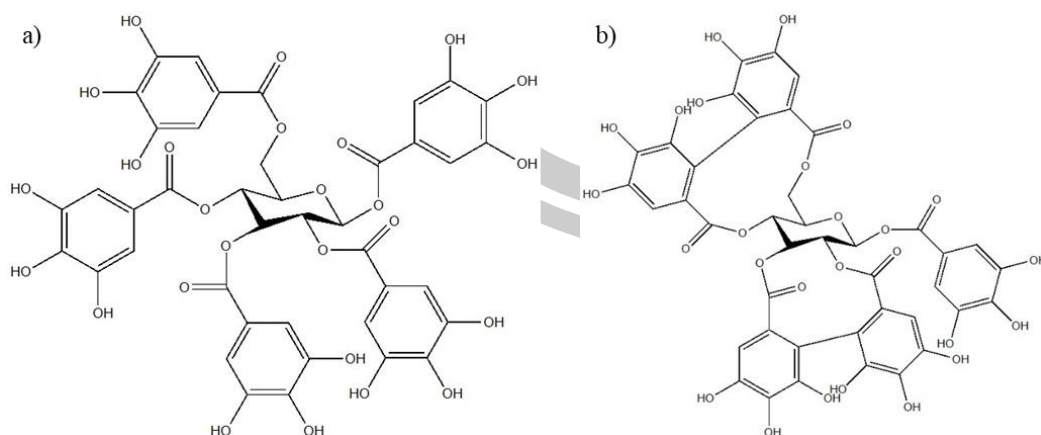


Figure 3 a) Structure of gallotannin, b) Structure of ellagitannin [39].

2.2.1.2 Condensed tannins

Condensed tannins or proanthocyanidins, are the most abundant natural phenolic compounds. Condensed tannins have a more complex structure than hydrolyzable tannins. The structure of condensed tannins consists of products obtained by oligomerization of flavan-3-ol units, where two flavan-3-ol units form carbon-carbon bonds between carbon-4 and carbon-8 of each flavan-3-ol unit, which is a highly stable bond. Examples of flavan-3-ol such as catechin and/or epicatechin and epigallocatechin [34][37][38]. The structure of condensed tannins is shown in Figure 4.

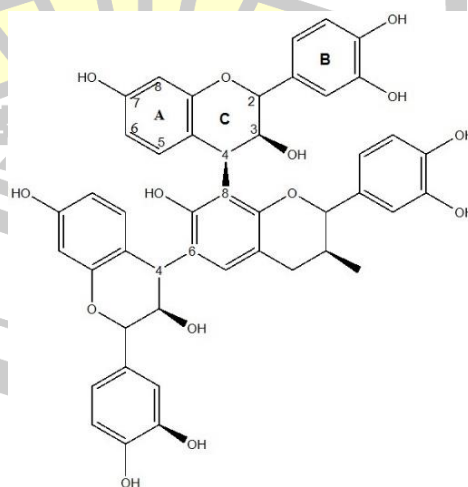


Figure 4 Basic structure of a condensed tannin [40].

2.3 Para rubber

The Para rubber tree or *Hevea brasiliensis* Muell. Arg., is a native plant in the tropical forests of the Amazon basin, Brazil, which belongs to the family Euphorbiaceae. The para rubber tree produced natural rubber latex, as shown in Figure 5. Natural rubber can be used to make a wide range of finished goods, such as tires, paints, pharmaceuticals, plastics, rain protection cloth, and pipes for transporting gases and liquids. As a result, the rubber tree is an important economic crop around the world. More than 10 million hectares of rubber trees are planted in Southeast Asia (92%), Africa (9%), and Latin America (2%), where the most profitable rubber industry countries are Malaysia, Thailand, India, Vietnam, Indonesia, and Cambodia [41]–[43].



Figure 5 The latex obtained from the tapping of the rubber tree.

2.3.1 Phenolic compounds in the Para rubber tree

Phenolic compounds are essential for the growth and reproduction of plants. They can be produced to defend injured plants against pathogens. Additionally, phenolic compounds are strong antioxidants against free radicals and other reactive oxygen species [44]. *Hevea brasiliensis* Muell. Arg. or Para rubber tree is one of the plants reported to contain phenolic compounds. Which can be found in the latex, wood, leaves, and seeds of the Para rubber tree. The

leaves of *Hevea brasiliensis* Muell. Arg. are the part with a higher amount of phenolic content than the seeds, explaining the reason that, the leaves are the site for the biosynthesis of these phenolic compounds and they are transferred from the leaves to the site of storage via the xylem or phloem tissues through long distance translocation [45]–[47].

2.4 Extraction technique

Tetracyclines are antibiotics used in beekeeping around the world to prevent and treat bacterial diseases. Thus, there may be residual TCs in the honey that cause adverse effects on consumer health, such as allergies. To ensure the safety of the public, many countries have established the maximum residue limits (MRLs) for tetracycline residues in honey; for example, Belgium and Switzerland have been set the limit at $20 \mu\text{g kg}^{-1}$, while France and China were regulating at 10 and $50 \mu\text{g kg}^{-1}$, respectively. Additionally, $20 \mu\text{g kg}^{-1}$ is the recommended content for screening the sum of tetracycline (TC), oxytetracycline (OTC) and chlortetracycline (CTC) in honey for the European Union [6]. Moreover, the European Union have been set the EURL Guidance on minimum method performance requirements (MMPRs) for the analysis of tetracycline residues in honey at $10 \mu\text{g kg}^{-1}$ [7]. Because of the low concentration of MRLs and MMPRs at the ppb level, a sample preparation method is needed to enrich TCs before analysis, which is essential for the determination of tetracycline residues in honey samples [48]. Sample preparation typically consists of sampling, extraction, clean-up, and preconcentration prior to analysis. Sampling is the process to obtain the sample smaller but representative of the whole sample. The clean-up is a procedure to remove or reduce the effect of the interference. Extraction is the separation of the analyte from the matrix based on differences in chemical and physical properties such as charge, polarity, and solubility. Moreover, the preconcentration of analyte concentration increases the detection ability and reduces the limit of detection and quantitation. The sample preparation procedure depends on the composition of the sample, such as the matrix, concentration, and properties of the target analyte contained in the sample. Especially when performing ultra-trace level analysis, the uncertainty increases as the concentration of the analyte decreases.

Therefore, the extraction and preconcentration steps in the sample preparation method are important to reduce or eliminate possible errors and uncertainties [49].

Nowadays, many methods for extraction and preconcentration have been developed. The application of the analytical method for the determination of tetracycline residues in honey samples is summarized in Table 4, which presents the main sample preparation methods, separation techniques, and method efficiency.

Table 4 Application of analytical methods for the determination of tetracycline residues in honey samples.

Sample preparation	Technique	Linear range	Sensitivity	Recovery (%)	Ref.
Dissolution with the mixture of McIlvaine buffer- Na_2EDTA and followed by extraction with SPE cartridge.	HPLC-FLD	25-500 $\mu\text{g kg}^{-1}$	LOD 8 $\mu\text{g kg}^{-1}$ LOQ 25 $\mu\text{g kg}^{-1}$	86-111	[50]
Dissolution with Na_2EDTA -McIlvaine buffer (pH 4.0) and analyzed with on-line SPE-HPLC.	HPLC-UV	50-1000 ng g^{-1}	LOD 5-12 ng g^{-1} LOQ 17-40 ng g^{-1}	84.2-120.6	[51]
Dissolution with Na_2EDTA -McIlvaine buffer and extracted with d-SPE method.	HPLC-MS/MS	0.25-500 ng g^{-1}	LOD 0.073-0.435 ng g^{-1} LOQ 0.239-1.449 ng g^{-1}	88.7-126.2	[52]
Extraction with QuEChERS method	UPLC-MS/MS	0.05-50 ng L^{-1} and 0.1-100 ng L^{-1}	LOD 0.05-1.02 $\mu\text{g kg}^{-1}$ LOQ 0.17-3.40 $\mu\text{g kg}^{-1}$	70.5-119.8	[53]
Precipitated the proteins with ACN and dissolved with DI water before Magnetic-SPE extraction.	HPLC-UV	10-3000 $\mu\text{g L}^{-1}$	LOD 2.5 $\mu\text{g L}^{-1}$ LOQ 10 $\mu\text{g L}^{-1}$	82.9-107.3	[54]
Dissolution with water before being extracted with miniaturized SPE method.	UHPLC-Q-TOF/MS	0.010-0.89 $\mu\text{g mL}^{-1}$	LOD 0.61-10.34 $\mu\text{g kg}^{-1}$ LOQ 2.02-34.46 $\mu\text{g kg}^{-1}$	81.5-101.4	[55]

Sample preparation	Technique	Linear range	Sensitivity	Recovery (%)	Ref.
Extraction with McIlvaine- Na_2EDTA buffer (pH 4) and clean-up with HLB cartridge.	HPLC-FLD	5-1000 ng mL^{-1}	LOD 0.29-4.69 $\mu\text{g kg}^{-1}$ LOQ 0.96-15.62 $\mu\text{g kg}^{-1}$	81.52-97.25	[56]
Liquid extraction with acetone.	Voltammetry	0.40-3.00 μM	LOD 0.15 μM	91.46-105.54	[57]
Homogenization with DI water and extraction with fatty acid-based ternary deep eutectic solvents for vortex assisted microextraction method	UV-vis spectrophotometry	3.3-450 $\mu\text{g L}^{-1}$	LOD 1.0 $\mu\text{g L}^{-1}$ LOQ 3.3 $\mu\text{g L}^{-1}$	95.6-103.4	[58]

2.4.1 Dispersive solid phase extraction

Dispersive solid phase extraction (d-SPE) is an extraction technique developed from solid phase extraction (SPE) methodology to overcome the problems of time-consuming extraction, cartridge clogging, and the difficulty of simultaneous extraction operation of the conventional SPE [59]. The advantages of d-SPE are its short extraction time, simplicity, adaptability, and ease of handling in comparison with traditional techniques. The principle of d-SPE involves the direct addition of solid sorbent to the sample or analytical solution, followed by its dispersion throughout the solution through shaking or agitation, thereby increasing the contact surface area between the sorbent and the analyte. After the sorbent dispersion step is completed, the sorbent containing the analyte is collected using centrifugation, filtration, or an external magnetic field in case the sorbent has magnetic properties. Finally, the analyte is desorbed with a suitable desorption solvent before being analyzed by the appropriate instrument. The schematic of the sorbent dispersion method and the extraction procedure of the d-SPE method are shown in Figure 6 [60][61].

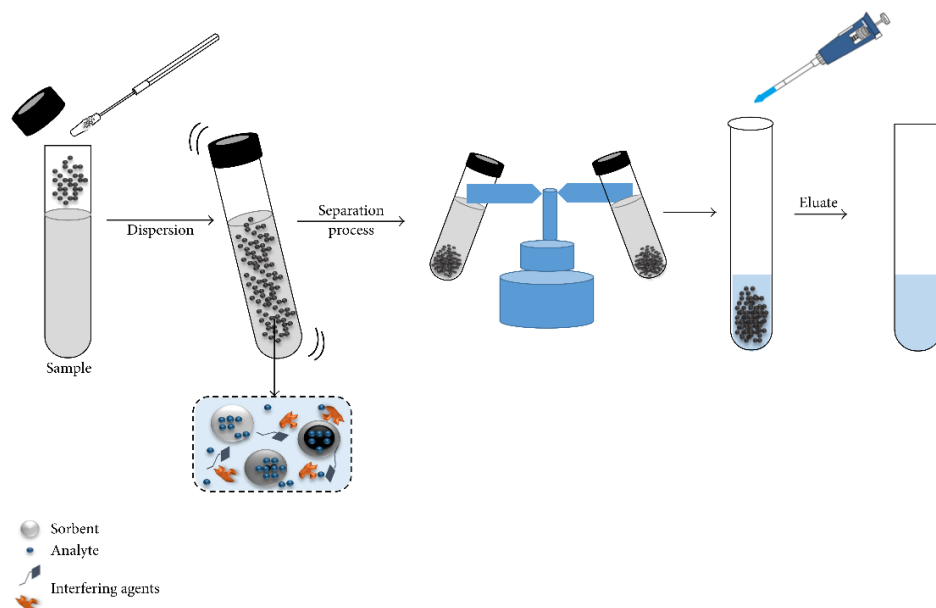


Figure 6 Scheme of dispersion methodology by dispersive solid phase extraction [60].

2.4.2 Sorbent

The sorbent plays an important role in the efficiency of the d-SPE method. The sorbent used in this technique has a high sorption capacity, high specificity, low cost, non-toxicity, reusability, and excellent chemical and physical stability. As a result, selecting the sorbent for the d-SPE method is critical. Both of the chemical and physical properties are considered to maximize the interaction between the sorbent and the analyte [62].

2.4.2.1 Magnetic sorbent

Magnetic sorbents are magnetic nanoparticles (MNPs) with a magnetic core such as iron, cobalt, nickel, and their oxides, which iron oxide ($\gamma\text{-Fe}_2\text{O}_3$, Fe_3O_4) is the most widely used as MNPs. MNPs are functionalized with other materials to improve the sorption capacity, target analyte selectivity, and stability in acidic media such as metal organic frameworks (MOFs), layered double hydroxide (LDHs), covalent organic frameworks (COFs), molecularly imprinted polymers (MIPs), and carbon nanotubes (CNTs) as magnetic nanocomposites.

In recent years, magnetic sorbents have attracted considerable interest as adsorbents in extraction techniques to preconcentrate and separate analytes from sample solutions since the magnetic sorbents can be easily and quickly collected and separated from the aqueous solution using an external magnetic field. The filtration or centrifugation steps in the extraction process are eliminated, resulting in a short extraction time, and the magnetic adsorbent also has advantages including recyclability, reusability, eco-friendliness, high extraction efficiency, high extraction capacity, and a significantly higher surface-area-to-volume ratio compared with other sorbents [63][64].

2.4.2.1.1 Magnetic nanoparticle synthesis methods

Several methods were used for efficient synthesis of magnetic nanoparticles to achieve highly stable, uniform particle size and excellent magnetic properties, such as the co-precipitation method, flow-based synthesis, hydrothermal method, sol-gel method, thermal decomposition method, microemulsion method, and aerosol/vapor-phase-based methods.

1) Co-precipitation method

The co-precipitation method relies on the precipitation reaction of two or more cations in a homogeneous solution to obtain a uniform composition. The co-precipitation method is probably the simplest and most convenient way to synthesize magnetic nanoparticles in a chemical pathway and it is one of important methods for the synthesis of composite materials containing two or more metal elements [65]. For example, the synthesis of Fe_3O_4 nanoparticles of suitable diameter under optimal process conditions such as pH and temperature. The

representative chemical reaction is shown in the following equation:



The main advantage of the co-precipitation method is that it synthesized magnetic nanoparticles in large quantities. However, the obtained particles have a wide size distribution, which means that the conditions during the synthesis process should be carefully determined [66].

2) Continuous-flow synthesis

The continuous flow technique relies on the continuous reaction of reagents within a narrow channel, and this technique gained interest in research related to the fields of pharmaceuticals and fine chemistry as a tool for solving synthesis problems. In continuous flow synthesis, a pump is used to carry two or more streams of different reactants along a pipe or tube at a specific flow rate into a mixing junction and through a reactor coil to produce the final product [67][68].

Continuous flow synthesis has several advantages compared to batch synthesis, such as lower cost, ease of scaling up, reduced waste, rapid mixing resulting in reduced particle size distribution, safe handling of hazardous reagents, and fast heat transfer for reactions that require high temperatures [69].

3) Ultrasound-assisted synthesis

Ultrasound-assisted synthesis is one of the most powerful tools in the synthesis of nanostructured materials [70]. The ultrasonic-assisted processes have a key factor involved in cavitation generated by the liquid medium exposed to ultrasonic waves. Cavitation is the formation,

growth, and collapse of bubbles in a liquid medium with high pressure, a high specific temperature, and high energy. The collapse of microscopic bubbles can generate high localized temperatures of $\sim 5000\text{--}10,000\text{ K}$ and a pressure of approximately $100\text{--}200\text{ MPa}$, which results in a transient local hot spot. When the collapse occurs near the surface of a solid substrate, the solid is activated to split larger particles into smaller or deagglomerate nanoparticles [71]–[73].

The main advantages of the ultrasound-assisted synthesis method are that the desired particles have a uniform shape and a narrow size distribution, controllable reaction conditions, potentially low processing costs, and a fast reaction rate [74].

Examples of previously reported studies on the application of magnetic particles for tetracycline analysis are summarized in Table 5.

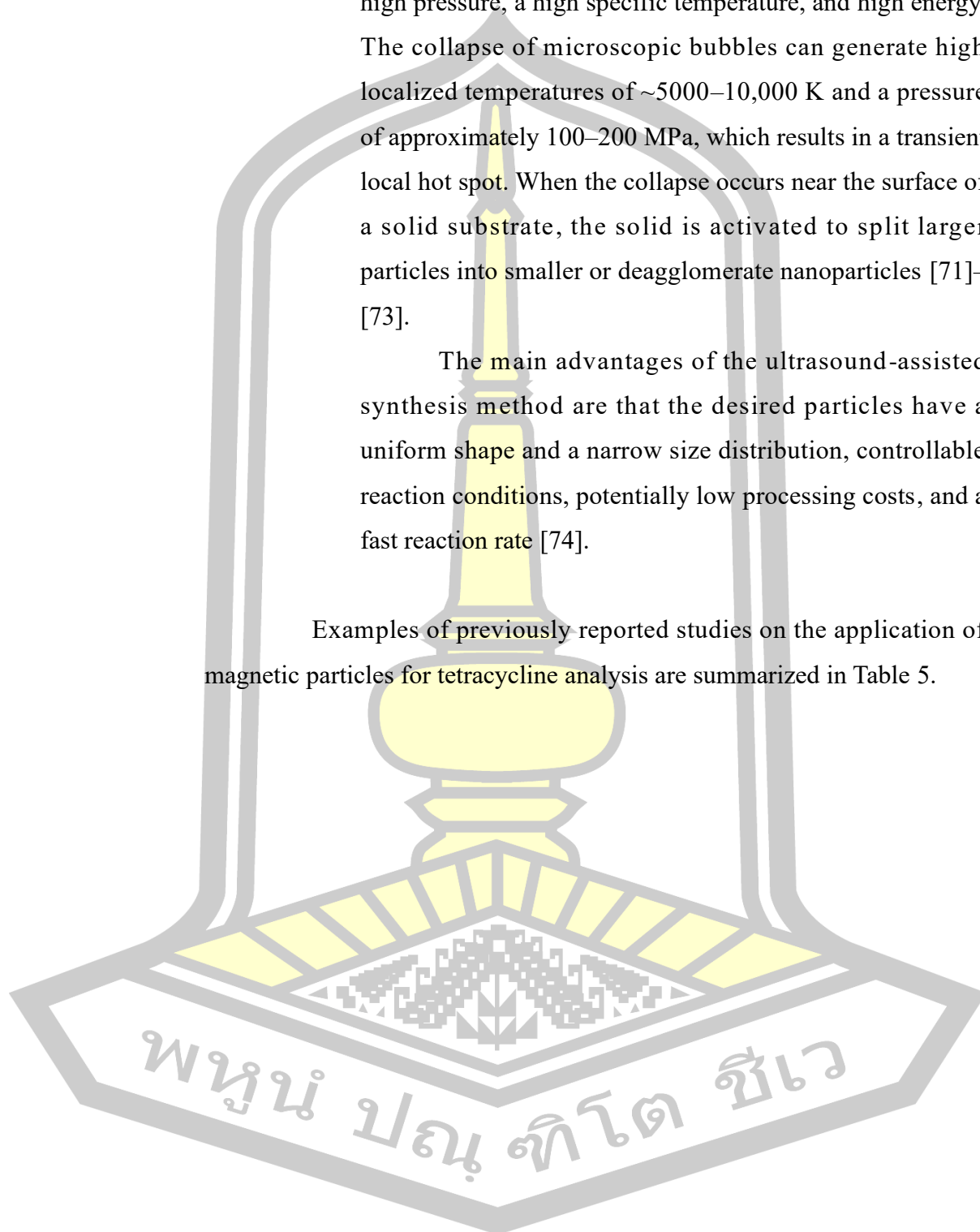


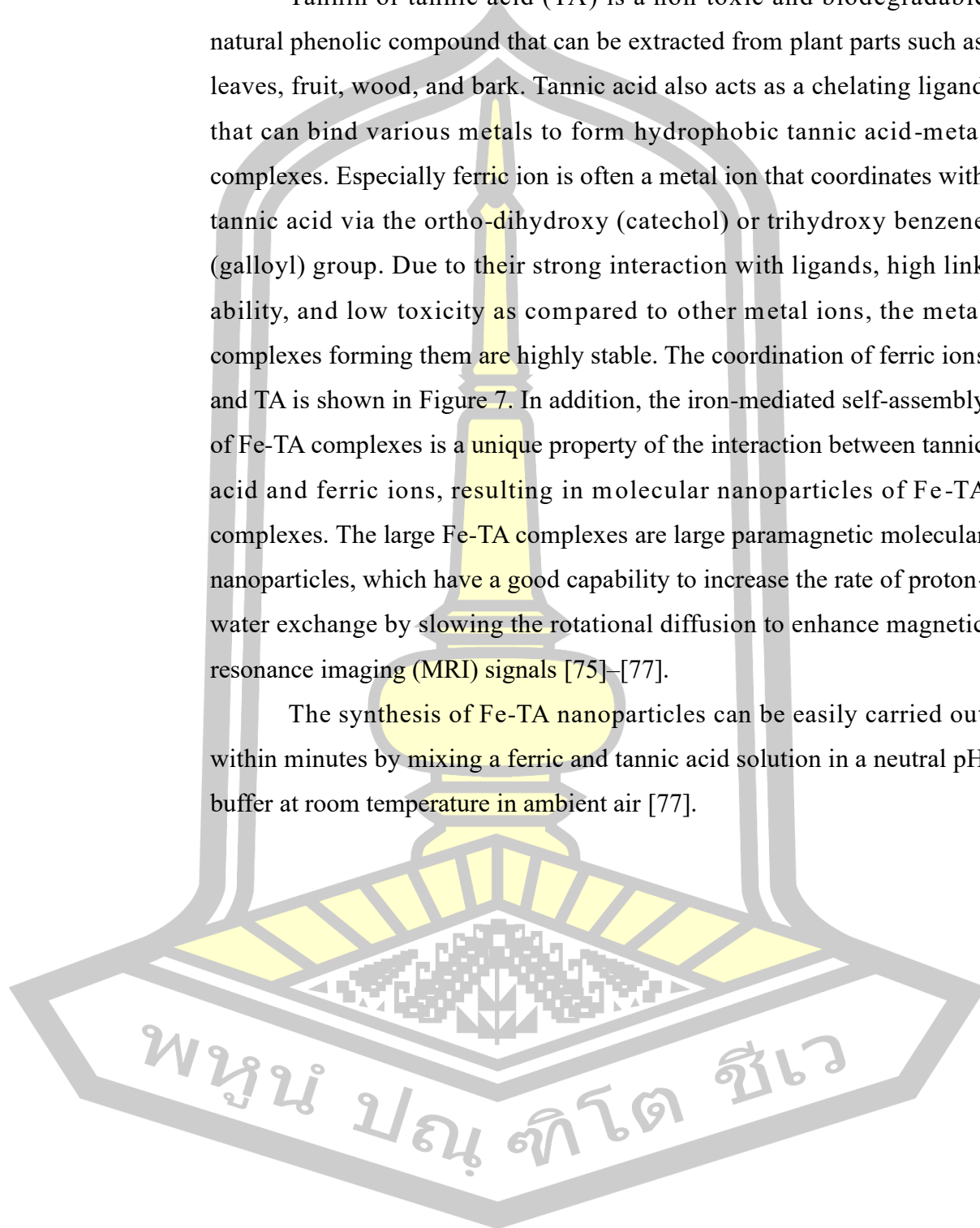
Table 5 Application of magnetic nanoparticles for tetracyclines analysis.

	Reference					
	[12]	[94]	[97]	[98]	[99]	[96]
Matrix samples	Humens serum	Water	Water	Milk	Water	Milk
Analyte	OTC, TC and DC	OTC, TC and CTC	TC, CTC, OTC, DC, DMC and MC	Chloramphenicol (CP) and TC	TC, OTC and CTC	OTC, TC, CTC and DC
Magnetic sorbent	Surfactant-coated Fe ₃ O ₄ MNPs	C ₁₈ /SiO ₂ /Fe ₃ O ₄ MNPs	Carboxyl-modified MNPs	C-nanofiber coated MNPs	Fe ₃ O ₄ @SiO ₂ @FeO magnetic nanocomposite	Water-soluble amino functionalized MNP
MNPs synthesis method	Co-precipitation method	Co-precipitation and Sol-gel	Solvothermal method	Hydrothermal method	Solvothermal method and hydrothermal method	Co-precipitation method
Analytical technique	HPLC-DAD	HPLC-DAD	LC-MS/MS	HPLC-DAD	UPLC-TUV	HPLC-UV
Sensitivity	LOD 0.03-0.08 mg L ⁻¹	LOD 2.0-10.0 µg L ⁻¹ LOQ 8.0-40.0 µg L ⁻¹	LOD 12.0-74.1 ng L ⁻¹ LOQ 40.1-247 ng L ⁻¹	LOD TC 3.52 ng mL ⁻¹ CP 3.02 ng mL ⁻¹ LOD TC 9.83 ng mL ⁻¹ CP 9.63 ng mL ⁻¹	LOD 0.027-0.107 µg L ⁻¹ LOQ 0.133-0.267 µg L ⁻¹	LOD 40 µg L ⁻¹ LOQ 50 µg L ⁻¹
Recovery (%)	90-115	82.2-87.7	95.4-111.1	94.6-105.4	91.0-104.6	88-108
Precision (%)	<8	<10.0	2.9-11.8	<4.0	<4.0	≤2.2

2.4.2.2 Tannic acid-iron nanoparticles

Tannin or tannic acid (TA) is a non-toxic and biodegradable natural phenolic compound that can be extracted from plant parts such as leaves, fruit, wood, and bark. Tannic acid also acts as a chelating ligand that can bind various metals to form hydrophobic tannic acid-metal complexes. Especially ferric ion is often a metal ion that coordinates with tannic acid via the ortho-dihydroxy (catechol) or trihydroxy benzene (galloyl) group. Due to their strong interaction with ligands, high link ability, and low toxicity as compared to other metal ions, the metal complexes forming them are highly stable. The coordination of ferric ions and TA is shown in Figure 7. In addition, the iron-mediated self-assembly of Fe-TA complexes is a unique property of the interaction between tannic acid and ferric ions, resulting in molecular nanoparticles of Fe-TA complexes. The large Fe-TA complexes are large paramagnetic molecular nanoparticles, which have a good capability to increase the rate of proton-water exchange by slowing the rotational diffusion to enhance magnetic resonance imaging (MRI) signals [75]–[77].

The synthesis of Fe-TA nanoparticles can be easily carried out within minutes by mixing a ferric and tannic acid solution in a neutral pH buffer at room temperature in ambient air [77].



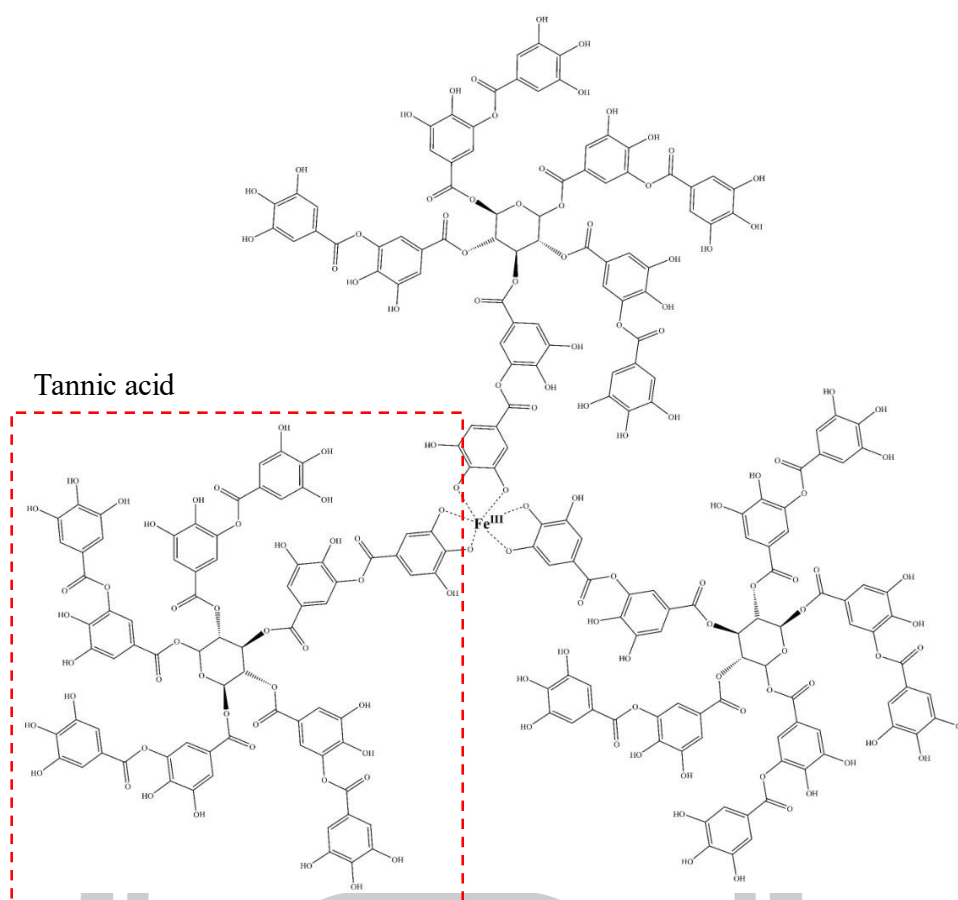


Figure 7 The coordination of ferric ion and tannic acid [78].

2.4.3 Application of dispersive solid phase extraction for the determination of tetracyclines

Mahboob Nemati et al. developed a dispersive solid phase extraction method (d-SPE) for the extraction and preconcentration of four tetracyclines (oxytetracycline, doxycycline, chlortetracycline, and tetracycline) in milk samples prior to analysis with HPLC-DAD. The d-SPE was performed in a home-made extraction device using activated carbon as the sorbent, dispersed in the sample solution with the aid of an air stream, and floated on top of the solution with the aid of air bubbles and lauryl betaine, which acts as a surfactant. The analytes were eluted from sorbents with a tetrabutyl ammonium chloride-propionic acid deep eutectic solvent under sonication, resulting in this developed method that can eliminate the use of organic dispersive and extraction solvents and the centrifugation step of sorbent collection [79].

Yue-Hong Pang et al. developed a dispersive solid phase extraction method (d-SPE) using compounding MOFs of MIL-101 (Cr), MIL-100 (Fe), and MIL-53 (Al) at a ratio of 7:1:2, respectively, as adsorbents for the determination of four tetracyclines (oxytetracycline, doxycycline, chlortetracycline, and tetracycline) in honey samples combined with HPLC-MS/MS. The use of compounding MIL-101 (Cr), MIL-100 (Fe), and MIL-53 (Al) as an adsorbent in the proposed method aimed to improve the adsorption capacity of the four types of TCs based on the differences in adsorption properties of each MOFs with different ligands, crystal structures, and pore sizes [52].

Ehsan Soleimanirad et al. developed a dispersive micro solid-phase extraction (DMSPE) method as a simple and efficient sample preparation method for the simultaneous extraction and cleanup of four antibiotics (azithromycin, amoxicillin, doxycycline, and tetracycline) in human urine and hair samples using chitosan@Fe₃O₄ nanoparticles as a green and magnetic sorbent prior to analysis with HPLC-DAD. The chitosan@Fe₃O₄ nanoparticles were prepared by chemically coating the Fe₃O₄ nanoparticles with chitosan. The antibiotic extraction efficiency of this sorbent was also compared with other sorbents such as ZnO nanoparticles, CuO nanoparticles, and Fe₃O₄ nanoparticles. In addition, the central composite design and the one factor at a time strategy were used in this work to evaluate and optimize the effective factors for antibiotic extraction [80].

Ning Ma et al. reported a novel composite absorbent for the dispersive magnetic solid phase microextraction method for the determination of seven tetracyclines (minocycline, chlortetracycline, tetracycline, oxytetracycline, demeclocycline, doxycycline, and methacycline) in chicken muscle prior to UPLC-PDA analysis. The proposed novel composite was synthesized using polymerization of the molecularly imprinted nano-polymer of minocycline on the surface of the metal organic framework material UiO-66 in order to obtain a high absorption capacity and reusability many times [81].

Yunyun Sun et al. reported the development of the synthesis of magnetic graphene/carbon nanotube composites (M-G/CNTs) for application as

adsorbents of magnetic dispersive solid-phase extraction for the determination of oxytetracycline in sewage water samples in combination with a HPLC-fluorescence detector. M-G/CNTs were synthesized by modifying graphene/carbon nanotubes with Fe_3O_4 nanoparticles in a reduction procedure, which is a simple and time-saving one-pot synthesis method to shorten the synthesis time by avoiding the drying process of graphite oxide. The resulting M-G/CNTs exhibit good magnetic properties, outstanding thermal stability, and excellent adsorption capacity [82].

Details of the application of dispersive solid phase extraction for the determination of tetracyclines are summarized in Table 6.

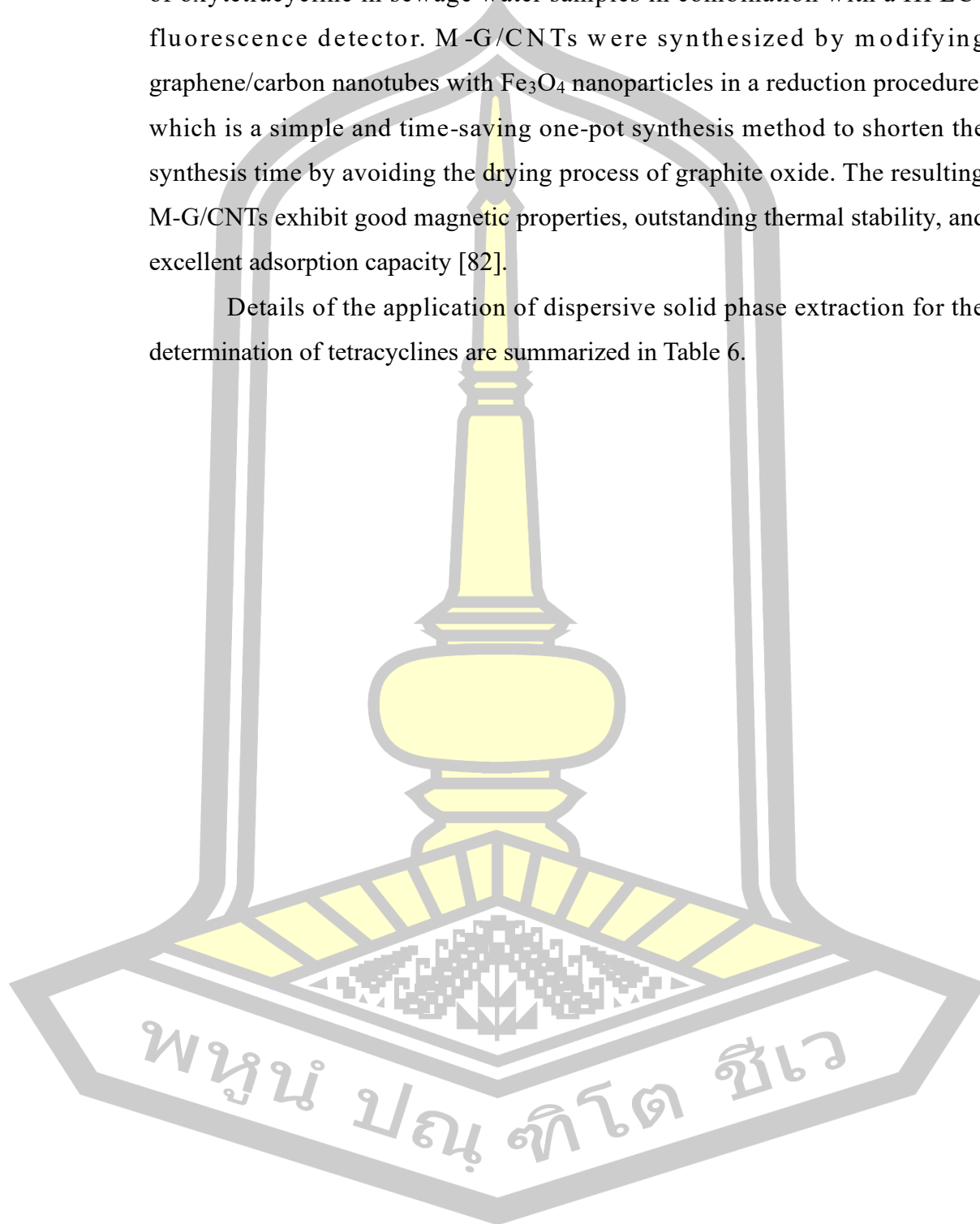


Table 6 Application of dispersive solid phase extraction for determination of tetracyclines.

Reference		[79]	[52]	[80]	[81]	[82]
Matrix samples		Milk	Honey	Human urine and hair samples	Chicken muscle	Sewage water
Analyte		TC, CTC, DC and OTC	OTC, TC, CTC and DC	Azithromycin, amoxicillin, DC and TC	MC, CTC, TC, OTC, DMC, DC and MTC	OTC
Sorbent		Activated carbon	Compounding MOFs of MIL-101 (Cr), MIL-100 (Fe) and MIL-53 (Al)	Chitosan@Fe ₃ O ₄ NPs	MIP-MOF composite	Magnetic graphene/carbon nanotube composites (M-G/CNTs)
Analytical technique		HPLC-DAD	HPLC-MS/MS	HPLC-DAD	UPLC-PDA	HPLC-fluorescence detector
Coefficients of determination		≥0.994	>0.9965	>0.9958	≥0.9334	0.9997
Sensitivity		LOD 0.1-0.3 µg kg ⁻¹ LOQ 0.6-1.0 µg kg ⁻¹	LOD 0.073-0.435 ng g ⁻¹ LOQ 0.239-1.449 ng g ⁻¹	LOD <0.1 µg L ⁻¹ LOQ <3.5 µg L ⁻¹	LOD 0.2-0.6 ng g ⁻¹ LOQ 0.5-2.0 ng g ⁻¹	LOD 3.6 ng mL ⁻¹ LOQ 12 ng mL ⁻¹
Recovery (%)		80-91	88.1-126.2	94.7-106.75	92-97	95.5-112.5
Precision (%)		≤9.8	<9.4	<4.9	<4.7	<5.8

2.5 High Performance Liquid Chromatography

High performance liquid chromatography (HPLC) is a technique of liquid chromatography used for the separation, identification, and quantification of components in mixtures. This technique is ideal for compounds that are non-volatile, thermally unstable, and possess a high molecular mass. The principle of HPLC is based on using a pump to drive the mobile phase to carry the liquid-injected mixture into the column to achieve separation of the individual analytes. The separation relies on different chemical and physical properties of the analytes, such as the polarity and/or size of the molecules, which interact differently with the stationary phase inside the column. As a result, the column ejects each target analyte at different times. The target analytes are detected with the detector, with the chromatogram showing the peak of each target analyte at different retention times [83][84].

Reverse-phase HPLC and normal-phase HPLC separation systems are used mainly for HPLC. Reverse-phase HPLC is the use of a stationary phase column composed of non-polar alkyl hydrocarbons such as C-8 and C-18 chains bound to silica or another inert support. Polar mobile phase such as water, methanol, and acetonitrile were employed, whereas as a result, the more polar analyte is evacuated from the column and reaches the detector before the less polar analyte. And the normal phase HPLC is the use of the polar stationary phase with plain silica or organic compounds such as amino or cyano groups bound to silica as a support, and a non-polar mobile phase such as hexane or heptane. The separation result of the more nonpolar analyte was eluted from the column before the more polar analyte. There are two modes of operation of HPLC, including the isocratic mode (an analysis in which the component ratio of the mobile phase remains constant throughout the analytical run) and the gradient mode (an analysis in which the component ratio of the mobile phase is changed through the programming of the pump). The components of the HPLC system are shown in Figure 8 [83][84].

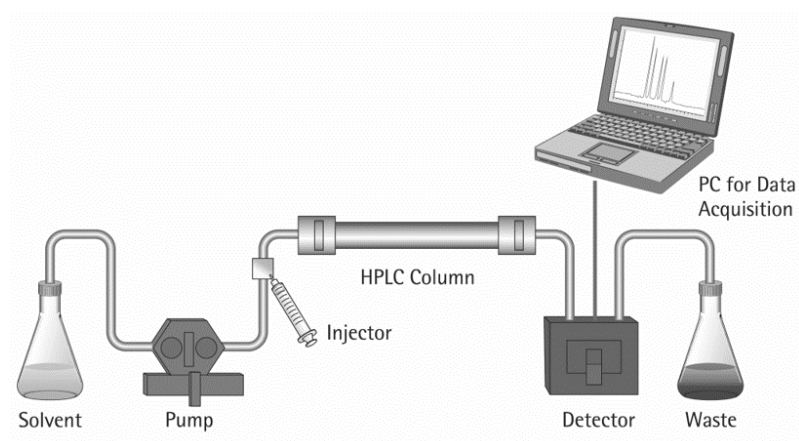


Figure 8 The components of the HPLC system [84].

Examples of previously published research journals involving high-performance liquid chromatography (HPLC) for the determination of tetracyclines are summarized in Table 7.

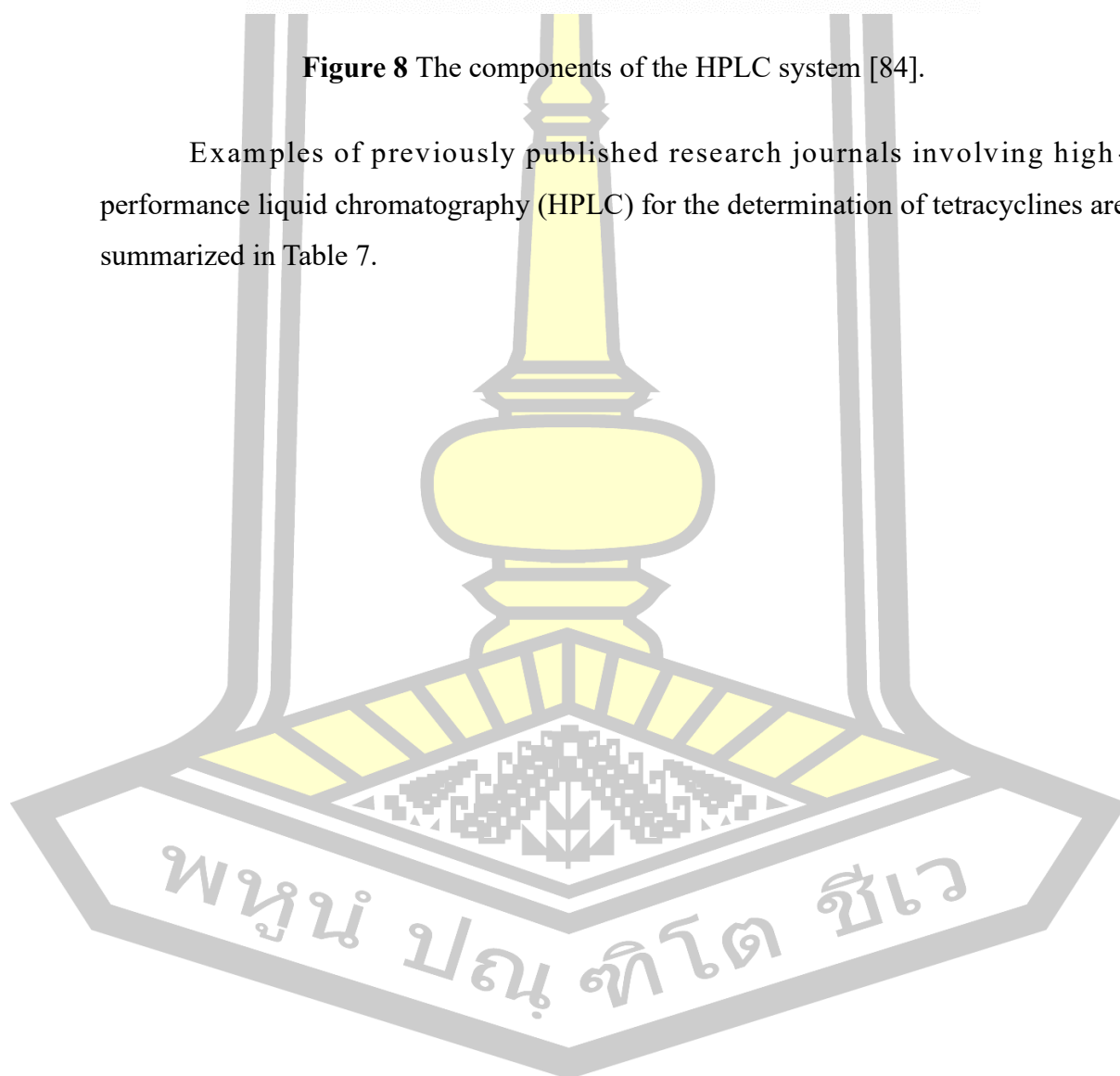


Table 7 Previously published journals related to the determination of tetracyclines using HPLC.

Reference		[100]	[101]	[102]	[103]
Matrix		Milk	Chicken tissue	Milk	Water
Sample size		0.5 g	1.0 g	1.50 mL	20 mL
Analyte		OTC, TC, CTC and DC	OTC, TC, CTC and DC	MNC, OTC, TC, DMCT, CTC, MTC and DC	OTC, TC, DMCT, CTC, MTC and DC
Extraction/ deproteination		Methanol and Oxalic acid	20% (v/v) acetonitrile	20% (w/v) trichloroacetic acid in methanol	NA
Sorbent of SPE		QuEChERS dispersive extraction	Electrospun Graphene Oxide–Doped Nanofiber	Dissolvable layered double hydroxide	Carboxyl Fe ₃ O ₄ magnetic nanoparticle
Column		Orbit 100C4 (5 µm, 250 × 4.0 mm)	Eclipse Plus C18 column (250 × 4.6 mm I.D., 5 µm particle Size)	Gemini-C18 column (150 mm × 4.6 mm, 5 mm)	Phenomenex Gemini-C18 column (150 mm × 4.6 mm, 5 µm)
Mobile phase		0.01 M Oxalic acid – 10 ⁻⁴ M Na ₂ EDTA/ Acetonitrile	Magnesium chloride (0.05 M)–malonic acid (0.1 M)– ammonia buffer solution (pH 6.5)/Methanol	Methanol/acetonitrile/0.01 M oxalic acid	Methanol/acetonitrile/0.01 M oxalic acid
Detector		DAD, 355 nm	FLD (Excitation: 375 nm Emission: 535 nm)	VWD 358 nm	VWD 355, 370, 346 nm
Spike range		100-200 µg/kg	100-500 ng/g	50-150 µg/L	Tap water 0.063-3.29 µg/L; Pond water 0.5-2.5 µg/L
Recovery (%)		83.07-106.3	84.7-106.3	93.5-100	76.2-98.0
Precision (%)		<15.5	<5.0	<10.0	<15.5

Table 7 (continued)

Reference		[104]	[105]	[96]	[79]
Matrix		Water	Bovine milk, eggs and chicken liver	Bovine milk	Milk
Sample size		30 mL	5 g	4 mL	10 mL
Analyte		TC	OTC, TC, CTC and DC	OTC, TC, CTC and DC	OTC, TC, CTC and DC
Extraction/ deproteination		Not shown	EDTA-McIlvaine's buffer	Acetonitrile and perchloric acid	Trichloroacetic acid
SPE		Magnetic adsorbent based on chitosan-kaolin nanocomposite	Microporous covalent triazine-terphenyl polymer (CTP _{CC-TP}) HLB	Water-soluble amino functionalized magnetite nanoparticle (MNP-NH ₂)	Activated carbon
Column		Agilent Zorbax Eclipse Plus C18 column (3.5 μm \times 150 mm \times 4.6 mm)	ZORBAX SB-C18 Column (5 μm , 4.6 \times 150 mm)	SunFire C18-5 μm , 250 mm \times 4.6 mm	Zorbax-SB-Aq C18 (100 mm \times 4.6 mm, 3 μm particles size)
Mobile phase		Methanol/acetoneitrile/0.03 M oxalic acid	0.01 M oxalic acid in water/ acetoneitrile: methanol (1:1)	Acetonitrile/ 0.5% trifluoroacetic acid	0.5% formic acid/ acetoneitrile: methanol, 70:30 v/v
Detector		DAD 351,365 nm	UV 360 nm	PDA 360 nm	DAD 335, 296 nm
Spike range		5-100 $\mu\text{g/L}$	100-1000 $\mu\text{g/kg}$	100-200 $\mu\text{g/L}$	20-100 $\mu\text{g/kg}$
Recovery (%)		89-103	81.3-98.7	87.8-107.5	80-91
Precision (%)		<2.7	<7.7	<2.2	≤ 9.8

CHAPTER III

MATERIALS AND METHODS

3.1 Chemicals and reagents

All chemicals and reagents used in this research were laboratory-grade and analytical-grade. They were used without further purification and are listed in Table 8.

Table 8 List of all chemicals used in this research.

No.	Chemicals	Formula	Grade	Company	Country
1.	Tetracycline hydrochloride	$C_{22}H_{24}N_2O_8 \cdot HCl$	HPLC	Sigma-Aldrich	Germany
2.	Oxytetracycline hydrochloride	$C_{22}H_{24}N_2O_9 \cdot HCl$	HPLC	Sigma-Aldrich	Germany
3.	Chlortetracycline hydrochloride	$C_{22}H_{23}ClN_2O_8 \cdot HCl$	HPLC	Sigma-Aldrich	Germany
4.	Doxycycline hyclate	$C_{22}H_{24}N_2O_8 \cdot HCl \cdot 0.5H_2O \cdot 0.5C_2H_6O$	HPLC	Sigma-Aldrich	Germany
5.	Methanol	CH_3OH	HPLC	Merck	Germany
6.	Acetonitrile	CH_3CN	HPLC	Merck	Germany
7.	Trifluoroacetic acid	$C_2HF_3O_2$	LR	Fisher Scientific	USA
8.	Iron(III) chloride anhydrous	$FeCl_3$	LR	Chem-supply	Australia
9.	Iron(II) sulphate 7-hydrate	$FeSO_4 \cdot 7H_2O$	AR	KemAus	Australia
10.	Sodium acetate 3-hydrate	$CH_3COONa \cdot 3H_2O$	AR	KemAus	Australia
11.	Acetic acid	CH_3COOH	AR	ANAPURE	New Zealand
12.	Sodium hydroxide	$NaOH$	AR	Ajax Finechem	Australia
13.	Sodium chloride	$NaCl$	AR	Ajax Finechem	Australia
14.	Deionized water	-	-	Milli-Q	USA

AR grade means analytical reagent grade

HPLC grade means high performance liquid chromatography grade

LR grade means laboratory reagent grade

3.2 Instrumentation

The HPLC system was equipped with a Waters 1525 Binary HPLC pump (USA) and a Waters 2489 UV-Visible detector. The determination of TCs was performed at 365 nm, and the data acquisition was done using Breeze software version 2.0. The analytical column was a Purospher® STAR RP-18 endcapped column (4.6 x 150 mm, 5.0 μm) (Merck, Germany), and it was carried out at room temperature. The isocratic elution using a mixture of 0.2% (v/v) trifluoroacetic acid in acetonitrile (mobile phase A) and 0.2% (v/v) trifluoroacetic acid (mobile phase B) were used as mobile phase at a ratio of 27:73, respectively, for the TCs separation at a flow rate of 0.7 mL min⁻¹ and the injection volume was 20 μL . The solution was mixed using a vortex mixer (50 Hz, model ZX3, VELP SCIENTIFICA, Italy). Ultrasonic bath (37 Hz, model S 30H, ELMA, Germany) and peristaltic pumps (model ISM 828B, ISMATEC, USA) were used for temperature and flow rate control of the reagents in the magnetic nanoparticle synthesis procedure, respectively.

3.3 Experimental

3.3.1 Preparation of a stock standard solution of 1000 mg L⁻¹ TCs

Individual stock standard solutions of TC, OTC, CTC, and DC (1000 mg L⁻¹) were prepared by dissolving 0.010 g of each standard in 10 mL of methanol and were stored in an amber glass bottle at 4 °C. The daily working TCs mixed standard solutions were prepared by stepwise dilution of the stock solution with deionized water.

3.3.2 Preparation of 0.10 mol L⁻¹ iron(III) solution

A 0.10 mol L⁻¹ iron(III) solution was prepared by dissolving 0.828 g ferric chloride in 50 mL of deionized water.

3.3.3 Preparation of 0.10 mol L⁻¹ iron(II) solution

A 0.10 mol L⁻¹ iron(II) solution was prepared by dissolving 1.390 g ferrous sulfate heptahydrate in 50 mL of deionized water.

3.3.4 *Hevea brasiliensis* Muell. Arg. bark preparation

The bark of *Hevea brasiliensis* Muell. Arg. was collected from a plantation in Kalasin province, Thailand. Then, the latex was removed from the bark, and the air dried in the shade. The dried bark was ground into a fine powder, then sieved into a zip-lock bag and stored in a dry place.

3.3.5 Preparation of a natural reagent solution

The natural reagent solution was prepared by boiling 2 g of *Hevea brasiliensis* Muell. Arg. bark in 50 mL of deionized water on a hot plate at 75 °C for 15 min with constant stirring. The mixture was then filtered with Whatman No. 1 filter paper. Finally, the final volume was adjusted to 50 mL with deionized water.

3.3.6 Preparation of a 0.05 mol L⁻¹ acetate buffer solution, pH 5.0

Acetate buffer solution was prepared by mixing 0.435 g of sodium acetate trihydrate with an appropriate volume of deionized water and 103 µL of glacial acetic acid solution. Then, the final volume was adjusted to 100 mL with deionized water. Finally, the obtained buffer solution was adjusted to pH 5.0 with 1 mol L⁻¹ sodium hydroxide solution.

3.3.7 Preparation of 9% TFA in ACN

TFA 9% in ACN was prepared by pipetting 900 µL of 99% TFA into a 10 mL volumetric flask containing a small amount of ACN. Then, the final volume was adjusted to 10 mL with ACN.

3.3.8 Preparation of the mobile phase

The mobile phase consisted of 0.2% TFA in ACN (mobile phase A) and 0.2% TFA (mobile phase B), which were prepared by pipetting 2 mL of 99% TFA into a 1000 mL volumetric flask and then adjusting the final volume to 1000 mL with ACN and deionized water for the mobile phases A and B, respectively.

3.4 Magnetic nanoparticle-based natural reagent synthesis

The magnetic nanoparticle synthesis process was adapted from previous work [14]. Briefly, the reagents consisting of 50 mL of 0.1 mol L⁻¹ FeCl₃, 50 mL of 0.1 mol L⁻¹ FeSO₄ · 7H₂O, and 50 mL of the extracted natural reagent solution were placed in a temperature-controlled ultrasonic bath at 65 °C. All reagents were pushed and mixed in the mixing coil using peristaltic pumps at a flow rate of 4 mL min⁻¹. Then, the solution was cooled down at ambient temperature (~30 min). The pH of the solution products was adjusted to 10.5 with 1 mol L⁻¹ sodium hydroxide solution and stirred for 1 hour. Magnetic nanoparticles were collected using an external magnet, and the solution was discarded to obtain a final volume of 20 mL. The schematic procedure of nanoparticle synthesis using the ultrasound-assisted continuous flow technique and the diagram of the magnetic nanoparticle synthesis procedure are shown in Figures 9 and 10, respectively.

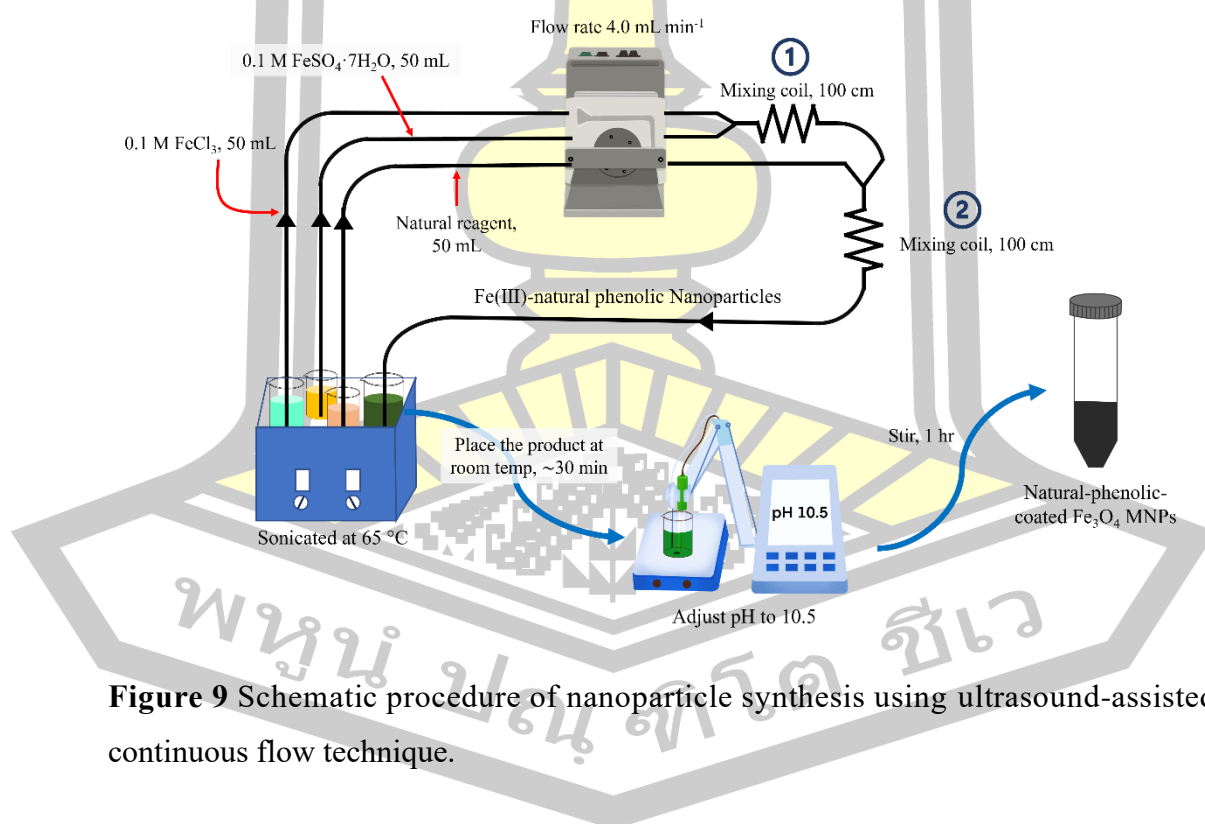


Figure 9 Schematic procedure of nanoparticle synthesis using ultrasound-assisted continuous flow technique.

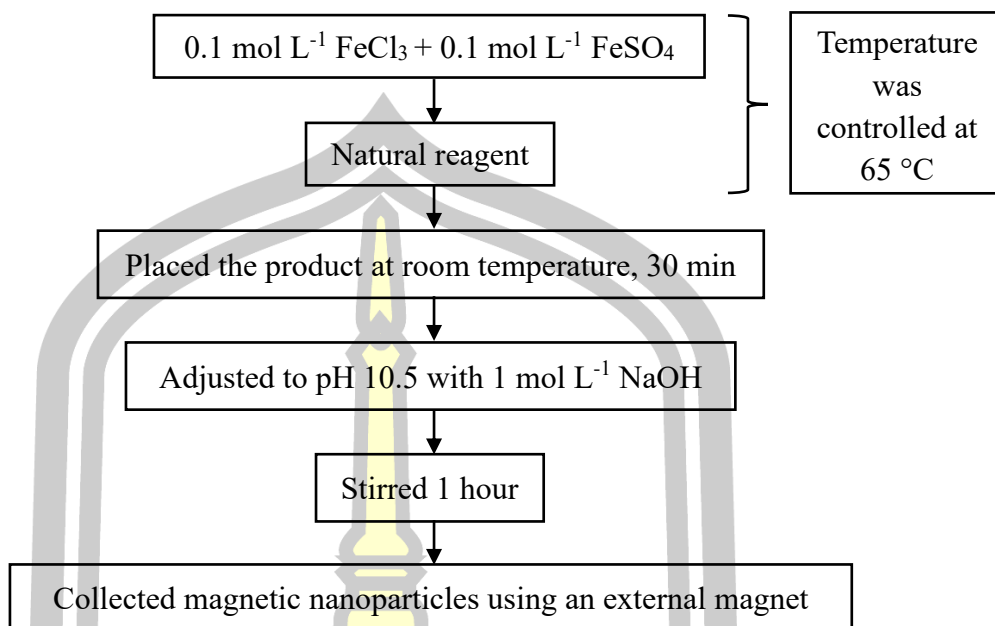


Figure 10 Diagram of the magnetic nanoparticle synthesis procedure.

3.5 d-SPE using magnetic nanoparticle-based natural reagents for enrichment TCs

A d-SPE was performed as follows. Initially, 2.0 g of honey samples were weighed into a 50-mL centrifuge tube. Then, 180 μ L of magnetic nanoparticles and 1 mL of 0.05 mol L⁻¹ acetate buffer pH 5 were added. The volume was adjusted to 40 mL with deionized water and added 0.04 g of NaCl (0.1% w/v). After that, the solution was mixed using a vortex mixer for 10 s. Magnetic nanoparticles were collected using an external magnet for 2 minutes, and the supernatant phase was discarded. TCs were eluted from sorbents using 100 μ L of 9% TFA in ACN. The eluent containing the analytes was then filtered with a 0.20 μ m nylon filter and injected into HPLC-UV for analysis. The schematic procedure of d-SPE for extracting TCs in honey samples and the diagram of the d-SPE procedure for extracting TCs in honey samples are demonstrated in Figures 11 and 12, respectively.

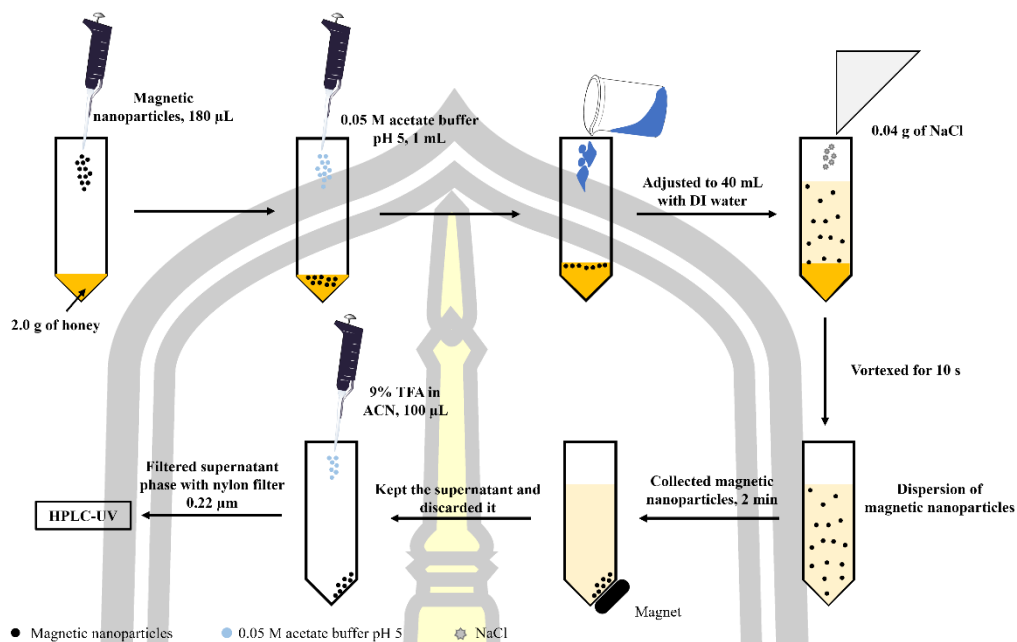


Figure 11 Schematic procedure of the d-SPE for extracting TCs in honey samples.

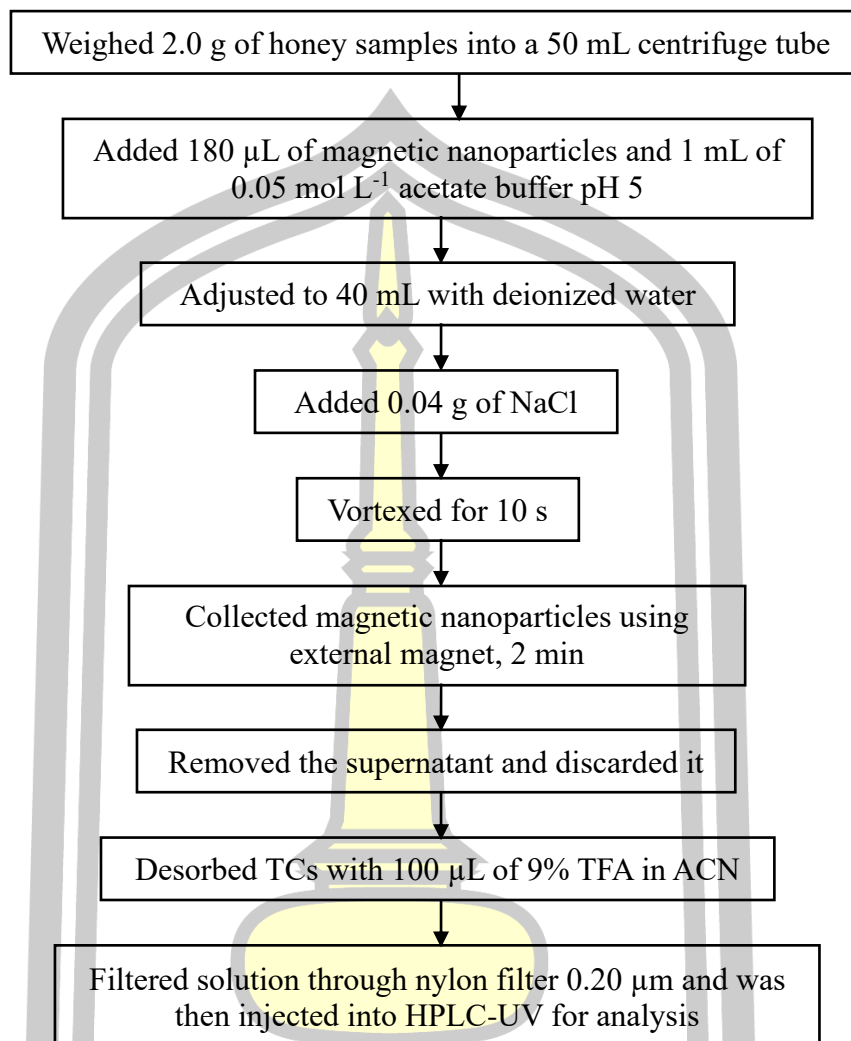


Figure 12 Diagram of dispersive solid phase extraction procedure for extracting TCs in honey samples.

3.6 Optimization of magnetic nanoparticle synthesis parameters

3.6.1 Batch and flow technique for magnetic nanoparticle synthesis

Batch and flow techniques were employed in the synthesis of magnetic nanoparticles.

3.6.2 Tool for temperature control

A tool for temperature control in magnetic nanoparticle synthesis was studied by using a hotplate and an ultrasonic bath for temperature control.

3.6.3 The effect of the molarity concentration ratio of FeCl_3 and $\text{FeSO}_4 \cdot 7\text{H}_2\text{O}$

The effect of the molarity concentration ratio of FeCl_3 and $\text{FeSO}_4 \cdot 7\text{H}_2\text{O}$ was investigated at 0.2 M:0.1 M, 0.1 M:0.1 M, and 0.1 M:0.2 M for $\text{FeCl}_3:\text{FeSO}_4 \cdot 7\text{H}_2\text{O}$, respectively.

3.6.4 The effect of flow rate

The effect of flow rate was investigated in the range of 2.0, 4.0, 6.0, and 8.0 mL min^{-1} .

3.6.5 The effect of temperature

An ultrasonic bath was used to control the temperature of the reagent and obtain a product for rapid and complete nanoparticle formation. The temperature was studied in the range of 55, 60, 65, and 75 $^{\circ}\text{C}$.

3.6.6 The effect of pH

The pH of the solution affects the magnetic properties of nanoparticles. In this work, the effects of pH in the range of pH 5, 6.5, 8.5, 10.5, and 12.5, were investigated.

3.6.7 The effect of stirring time

Stirring time affected the oxidation of Fe ions, which affected the magnetic properties of nanoparticles. Therefore, the stirring times at 30, 60, 90, and 120 min were studied.

3.6.8 Characterization of magnetic nanoparticle-based natural reagents

The ultrasound-assisted continuous-flow synthesized bare, natural phenolic-coated Fe_3O_4 MNPs and the ultrasound-assisted continuous-flow synthesized natural phenolic-coated Fe_3O_4 MNPs before and after TCs extraction were characterized by Zetasizer, TEM, FT-IR, XRD, BET and VSM.

3.7 Optimization of the d-SPE extraction parameter

3.7.1 Effect of honey sample weight

The honey weight was studied in the range of 1–5 g, as this work was performed matrix-matched to eliminate the matrix effect.

3.7.2 Effect of pH

The effect of pH on extraction efficiency was studied in the range of pH 3.0–7.0 using 0.05 mol L⁻¹ acetate buffers (pH 3.0–5.0) and 0.05 mol L⁻¹ phosphate buffers (pH 6.0–7.0).

3.7.3 Effect of total volume

The total volume was studied to reduce the viscosity of the honey. It was studied in the range of 10–50 mL using deionized water to dilute the sample.

3.7.4 Effect of buffer solution volume

The effect of buffer solution volume was studied in the range of 1, 2, 4, 6, 8, and 10 mL.

3.7.5 Effect of magnetic nanoparticle volume

The effect of magnetic nanoparticle volume was studied in the range of 60, 100, 140, 180, and 220 µL.

3.7.6 Effect of ionic strength

The effect of ionic strength was studied for both the type and concentration of salt.

The type of salt was independently studied by adding NaCl, CH₃COONa, NH₄Cl at a concentration of 0.1% w/v and no salt added.

The concentration of salt was studied at 0.01, 0.05, 0.1, 0.15, and 0.20% (w/v).

3.7.7 Effect of vortex time

The vortex was used to achieve homogenization of the solution and to allow the magnetic nanoparticles to disperse throughout the sample solution,

resulting in an increase in the contact area between the magnetic nanoparticles and the target analyte. Therefore, the vortex time was studied at 10, 30, 60, and 90 s.

3.7.8 Effect of magnetic nanoparticle collection time

Magnetic nanoparticles were collected by using an external magnetic field. In this work, the effect of collection time was studied at 0.5, 1, 2, 3, 4, and 5 min.

3.7.9 Effect of concentration and volume of desorption solvent

In this work, TFA in ACN was used as an eluent for the desorption of the target analyte from the sorbents.

The effect of TFA concentration in ACN was studied at 0, 1, 3, 5, 7, and 9% v/v.

The effect of volume of eluent was studied in the range of 100–300 μL .

3.8 Method validation

To confirm the capability and performance of the proposed method, in this work, linear range, detection limits, quantitation limits, precision, and accuracy were studied under optimal conditions of extraction and HPLC.

3.8.1 Linearity

The linear range was studied by the plotting calibration curves of each analyte at least five different concentrations and evaluating the linearity from the calibration curve equation ($y = mx + c$) and the correlation coefficient (R^2) value. The calibration curve was obtained by plotting the peak areas versus the concentration of the mixed standard solution and was constructed by the matrix-matched method using a blank honey sample.

3.8.2 Limits of detection and limit of quantification

The limit of detection (LOD) and limit of quantification (LOQ) were studied to evaluate the sensitivity of the proposed method. The limit of detection (LOD) was considered at concentrations providing a signal-to-noise ratio of 3:1,

and the limit of quantification (LOQ) was considered at concentrations providing a signal-to-noise ratio of 10:1.

3.8.3 Precision

The precision of the method was reported as the relative standard deviation (%RSD), which was studied by analyzing standard solutions mixed at three concentrations within intra-day and inter-day at six concentrations continuously for five days.

3.8.4 Accuracy

The accuracy of the d-SPE method was studied in terms of relative recoveries (%RR) under optimum extraction conditions to achieve the highest relative recoveries (%RR). It can be inferred that the proposed method was capable of extracting the target compounds from the real honey samples.

3.9 Real sample

Honey samples were purchased from convenience stores and department stores in Maha Sarakham and nearby provinces. Samples were extracted according to the procedure in Section 3.5 without sample pretreatment.

3.10 Data analysis

3.10.1 Mean (\bar{x})

The mean of results was calculated by dividing the sum of individual results by the number of individual values (n).

$$\bar{x} = \frac{X_1 + X_2 + X_3 + \dots + X_n}{n}$$

3.10.2 Standard deviation (SD)

The standard deviation (SD) is an indication of how similar the results are to each other, which was calculated as follows:

$$SD = \sqrt{\frac{\sum (x - \bar{x})^2}{n-1}}$$

where

SD is standard deviation.

Σ mean “sum of”.

x is value of individual result.

\bar{x} is mean of results.

n is the number of individual values.

3.10.3 Relative standard deviation (%RSD)

The relative standard deviation (%RSD) was calculated by dividing the standard deviation (SD) by the mean (\bar{x}), as follows:

$$\%RSD = \frac{SD}{\bar{x}} \times 100$$

3.10.4 Relative recoveries (%RR)

The relative recoveries (%RR) were calculated by dividing the difference between the analyte concentration in the spiked sample (C_{spike}) and the analyte concentration in the unspiked sample (C_{unspike}) with the concentration of the standard solution added to the sample (C_{added}), as shown in the following equation.

$$\%RR = \frac{C_{\text{spike}} - C_{\text{unspike}}}{C_{\text{added}}} \times 100$$

พหุ ประถมศึกษา

CHAPTER IV

RESULTS AND DISCUSSION

4.1 Performance of natural phenolic-coated Fe_3O_4 MNPs for enrichment of TCs

To achieve the best extraction efficiency and enrichment of TCs, the development of sorbents was important to obtain sorbents with high adsorption capacity and a large contact surface area. In this research, batch-synthesized bare Fe_3O_4 MNPs (Batch Fe_3O_4) and batch-synthesized natural phenolic-coated Fe_3O_4 MNPs (Batch $\text{Fe}_3\text{O}_4@\text{phenolic}$) were compared to use as magnetic sorbents in d-SPE for TCs extraction. The results in Figure 13 show that the batch-synthesized natural phenolic-coated Fe_3O_4 MNPs provided higher extraction efficiency. This can be attributed to the surface of MNPs was functionalized with natural phenolic compounds, resulting in a functional group of phenolics like hydroxyl groups that enhanced the adsorption capability and stability of MNPs more than MNPs without coated with phenolic compounds [85]. However, when the ultrasound-assisted continuous flow technique was used in the synthesis of MNPs, the performances for extraction and preconcentration of TCs by batch-synthesized natural phenolic-coated Fe_3O_4 MNPs (Batch $\text{Fe}_3\text{O}_4@\text{phenolic}$) and ultrasound-assisted continuous flow-synthesized natural phenolic-coated Fe_3O_4 MNPs (Flow $\text{Fe}_3\text{O}_4@\text{phenolic}$) were compared, and the results are shown in Figure 13. It was found that employing of natural phenolic-coated Fe_3O_4 MNPs as a sorbent obtained from ultrasound-assisted continuous flow-synthesized can provided the extraction efficiency higher than batch-synthesized natural phenolic-coated Fe_3O_4 MNP. Because using of ultrasound-assisted and continuous-flow techniques allowed for the control of MNPs size, leading to a smaller and uniform size [69], [74]. This increased the contact surface area and opportunities for interaction with TCs. Therefore, natural phenolic-coated Fe_3O_4 MNPs from ultrasound-assisted continuous flow-synthesized were employed as magnetic adsorbents in d-SPE for the extraction and enrichment of TCs.

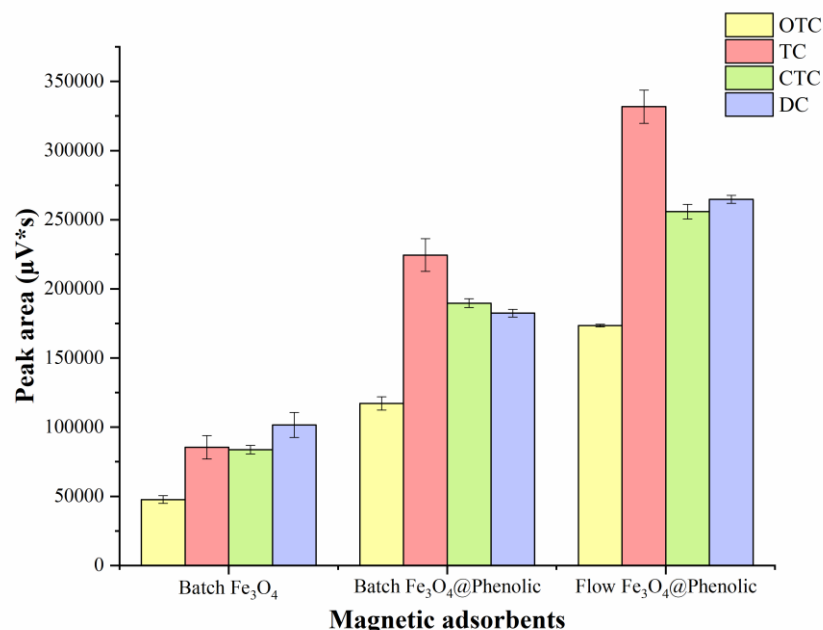


Figure 13 Peak area of all TCs after being extracted and enriched by batch-synthesized Fe₃O₄ MNPs (Batch Fe₃O₄), batch-synthesized natural-phenolic-coated Fe₃O₄ MNPs (Batch Fe₃O₄@phenolic), and ultrasound-assisted continuous flow-synthesized natural-phenolic-coated Fe₃O₄ MNPs (Flow Fe₃O₄@phenolic).

4.2 Optimization of natural phenolic-coated Fe₃O₄ MNPs synthesis by continuous flow synergistic with ultrasound-assisted

The natural phenolic-coated Fe₃O₄ MNPs were synthesized using a continuous flow technique combined with an ultrasound-assisted technique to produce MNPs that are uniform in size and exhibit high magnetism. The parameters affecting MNPs synthesis, such as the concentration ratio of FeCl₃:FeSO₄, flow rate, temperature, pH, and stir time, were optimized. The optimum conditions of each parameter were optimized by the one factor-at-a-time approach with three replicates and were chosen based on the extraction efficiency that was evaluated in terms of peak area.

4.2.1 Batch and flow technique for magnetic nanoparticle synthesis

The magnetic nanoparticle synthesis techniques were studied by comparing the TCs extraction efficiency of solid sorbent obtained from batch-synthesized MNPs and continuous flow-synthesized MNPs as solid sorbent. The results are shown in Figure 14. It was found that continuous flow-synthesized

MNPs provided higher extraction efficiency than batch-synthesized MNPs because the continuous-flow technique can control the size of MNPs better than the batch technique, resulting in continuous flow-synthesized MNPs having a smaller and uniform size, which increased the chance of the interaction between MNPs and TCs analytes [69]. Therefore, the continuous-flow technique was used in the MNP synthesis process.

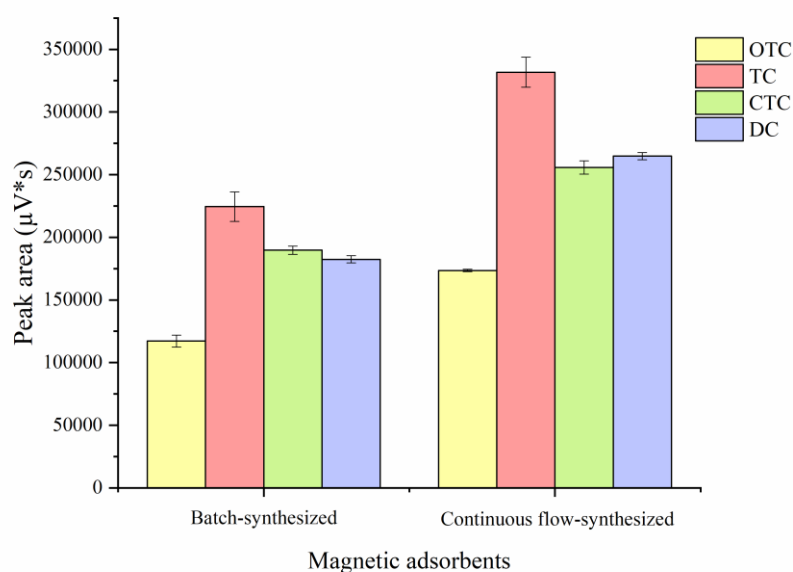


Figure 14 Peak area of all TCs after being extracted and enriched by batch-synthesized MNPs and continuous flow-synthesized MNPs.

4.2.2 Tool for temperature control

A tool for temperature control was investigated by using a hotplate compared with an ultrasonic bath. The results demonstrated that the MNPs synthesized using hotplate provided a very low response to external magnets and that after the extraction process, the MNPs did not respond to external magnets. On the other hand, MNPs synthesized using an ultrasonic bath responded very well to an external magnet, and it can provide high TCs extraction efficiency compared to the direct injection method (500 $\mu g/L$ of mix TCs standard), as shown in Figure 15. This result may be described by using an ultrasonic bath can be temperature controlled better than a hotplate. Additionally, an ultrasonic bath can generate ultrasound wave, resulting in

controllable particle size distribution and an increasing reaction rate [74]. Therefore, an ultrasonic bath was used to control the temperature in the MNP synthesis process.

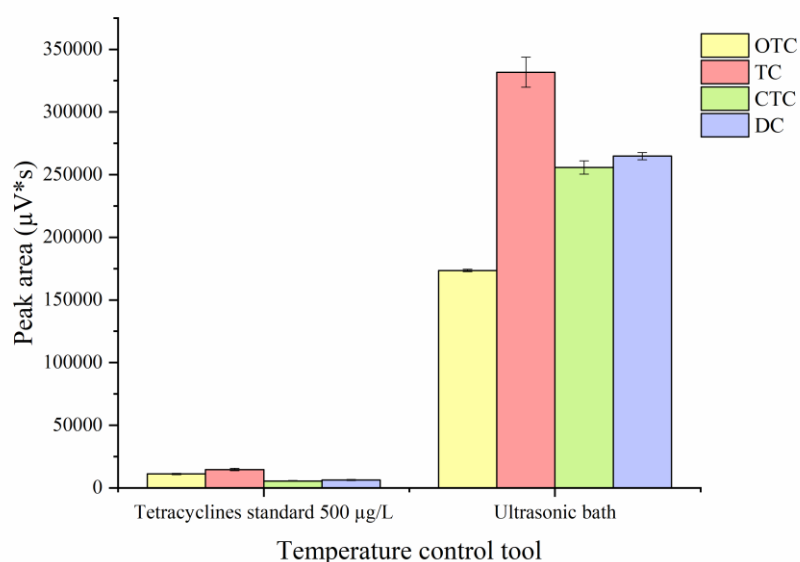


Figure 15 Peak area of all TCs after being extracted and enriched by MNPs synthesized using a continuous-flow technique combined with an ultrasonic bath.

4.2.3 Effect of $FeCl_3:FeSO_4$ molarity concentration ratio

The effect of the molarity concentration ratio of $FeCl_3:FeSO_4$ was studied at 0.2 M:0.1 M, 0.1 M:0.1 M, and 0.1 M:0.2 M. The result indicated that the concentration ratio of $FeCl_3:FeSO_4$ at 0.1 M:0.1 M provided the highest extraction efficiency, as shown in Figure 16. This can be explained by the equal concentration ratio of $Fe^{3+}:Fe^{2+}$, resulting in high-purity Fe_3O_4 precipitation. On the other hand, excess Fe^{3+} and Fe^{2+} precipitate as iron oxide when the concentration ratios of $Fe^{3+}:Fe^{2+}$ are not equal, which results in saturation magnetization decreasing [86]. Therefore, 0.1 M:0.1 M was used as the concentration ratio of $FeCl_3:FeSO_4$ for MNP synthesis.

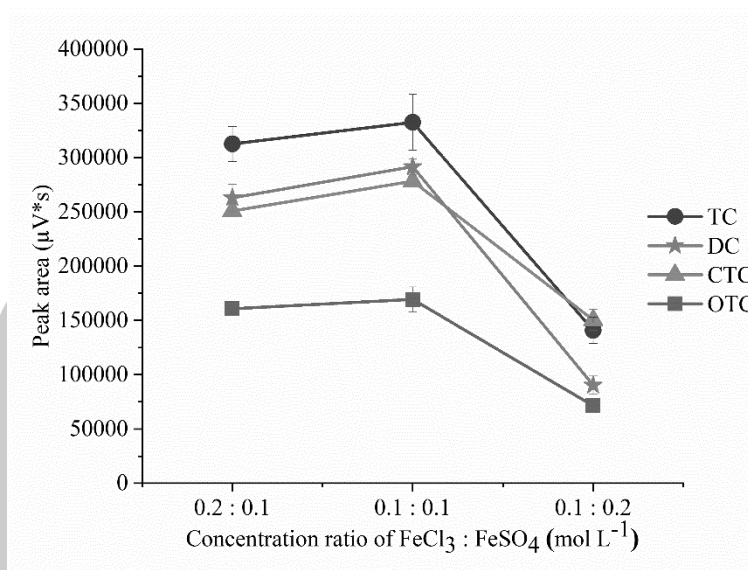


Figure 16 Effect of molarity concentration ratio of FeCl₃:FeSO₄. Conditions: 2g of *Hevea brasiliensis* Muell. Arg. bark, flow rate at 4 mL min⁻¹, temperature at 65 °C, pH 10.5, stir time of 1 hr., and 500 μg L⁻¹ of each tetracycline.

4.2.4 Effect of flow rate

The effect of flow rate on MNP synthesis was evaluated at 2.0, 4.0, 6.0, and 8.0 mL min⁻¹. The results are shown in Figure 17. It was found that flow rates of 2.0, 4.0, and 8.0 mL min⁻¹ were provided the extraction efficiency was not significantly different ($p > 0.05$). Therefore, a flow rate of 4.0 mL min⁻¹ was used for MNP synthesis in the further experiments because using 8 mL min⁻¹ may cause problems during the synthesis process, such as joint leakage caused by excessive pressure. Additionally, the synthesis time using 4.0 mL min⁻¹ (approximately 37 min) is faster than with 2.0 mL min⁻¹ (approximately 71 min).

พหุ ประสิทธิภาพ

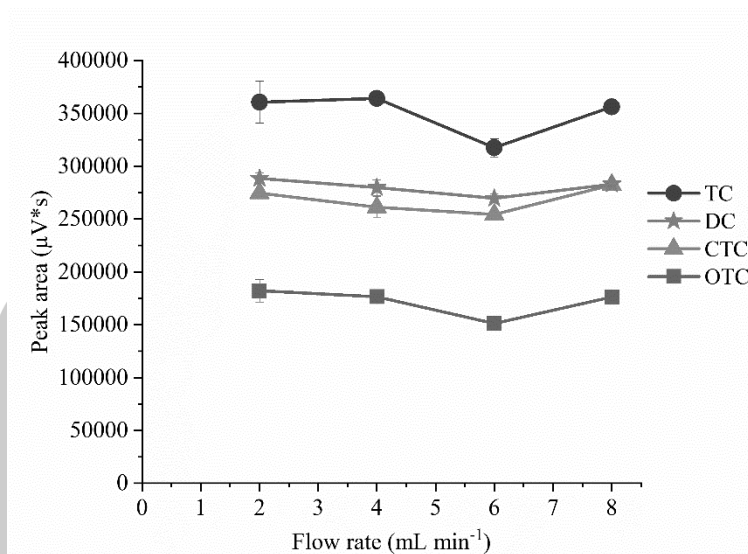


Figure 17 Effect of flow rate. Conditions: concentration ratio of $\text{FeCl}_3\text{:FeSO}_4$ was 0.1 M:0.1 M, 2g of *Hevea brasiliensis* Muell. Arg. bark, temperature at 65 °C, pH 10.5, stir time of 1 hr., and 500 $\mu\text{g L}^{-1}$ of each tetracycline.

4.2.5 Effect of temperature

The temperature of the co-precipitation method affected the kinetic and thermodynamic conditions of the chemical reactions. The effect of temperature was investigated at 55, 60, 65, and 75 °C. The results are shown in Figure 18. It was found that the extraction efficiency increased with the temperature increase from 55 to 65 °C. This can be attributed to an increase in temperature, resulting in a decrease in the size of the nanoparticles produced, which was caused by the higher frequency of nuclei collisions, leading to a decrease particle aggregation. Conversely, the extraction efficiency decreased when the temperature increased from 65 to 75 °C because of the increase in nanoparticle size, which can be explained by the disruption of the magnetic growth mechanism and the redeposition of stable nuclei with particles [87]. Consequently, this resulted in a reduced contact area. Therefore, a temperature of 65 °C was chosen for the synthesis of MNPs.

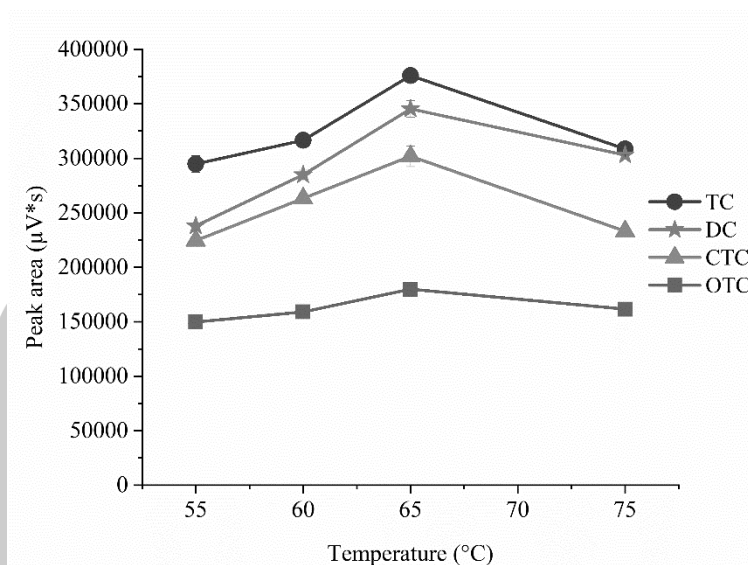


Figure 18 Effect of temperature. Conditions: concentration ratio of $\text{FeCl}_3:\text{FeSO}_4$ was 0.1 M:0.1 M, 2g of *Hevea brasiliensis* Muell. Arg. bark, flow rate at 4 mL min^{-1} , pH 10.5, stir time of 1 hr., and $500 \mu\text{g L}^{-1}$ of each tetracycline.

4.2.6 Effect of pH

The effect of pH was investigated in the range of 5.0 to 12.5 using 1 M NaOH for pH adjustment. The results revealed that the extraction efficiency increased with the rise in pH from 5.0 to 10.5 and then decreased, as illustrated in Figure 19. The increase in extraction efficiency can be explained by the heightened purity of the Fe_3O_4 phase, resulting in an increase in saturation magnetization [88]. Subsequently, extraction efficiency decreased when $\text{pH} > 10.5$ because the excess OH^- reacted with Fe^{2+} and Fe^{3+} to form the goethite ($\text{FeO}(\text{OH})$) phase, causing a decrease in the purity of the Fe_3O_4 phase. Hence, pH 10.5 was chosen as the optimum pH for the synthesis of MNPs.

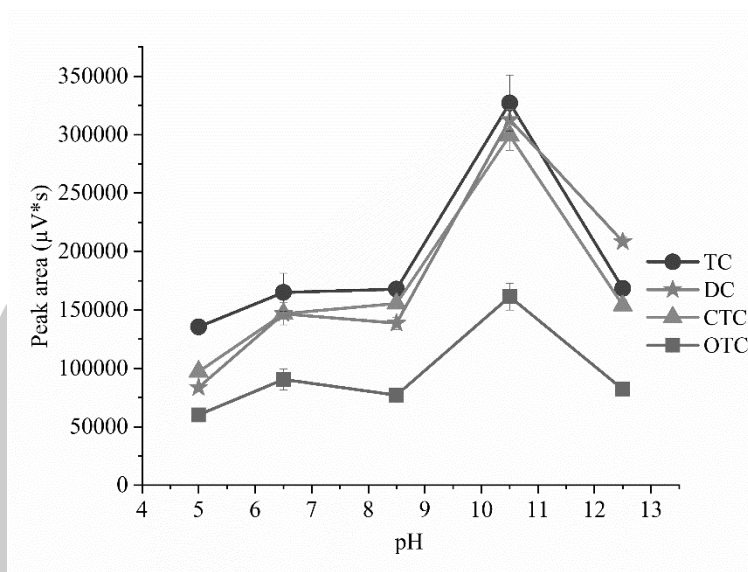


Figure 19 Effect of pH. Conditions: concentration ratio of $\text{FeCl}_3\text{:FeSO}_4$ was 0.1 M:0.1 M, 2g of *Hevea brasiliensis* Muell. Arg. bark, flow rate at 4 mL min^{-1} , temperature at 65°C , stir time of 1 hr., and $500 \mu\text{g L}^{-1}$ of each tetracycline.

4.2.7 Effect of stir time

The effect of stir time was studied in the range of 30 to 120 min, and the results are presented in Figure 20. It was observed that the highest extraction efficiency was achieved at a stir time of 60 min, indicating an equilibrium state in the reaction process at this duration. However, when the stir time exceeded 60 min, the extraction efficiency decreased due to nanoparticle agglomeration, leading to an increase in particle size [89]. Consequently, the MNP synthesis procedure was conducted with a stir time of 60 min.

พหุ ประสิทธิภาพ

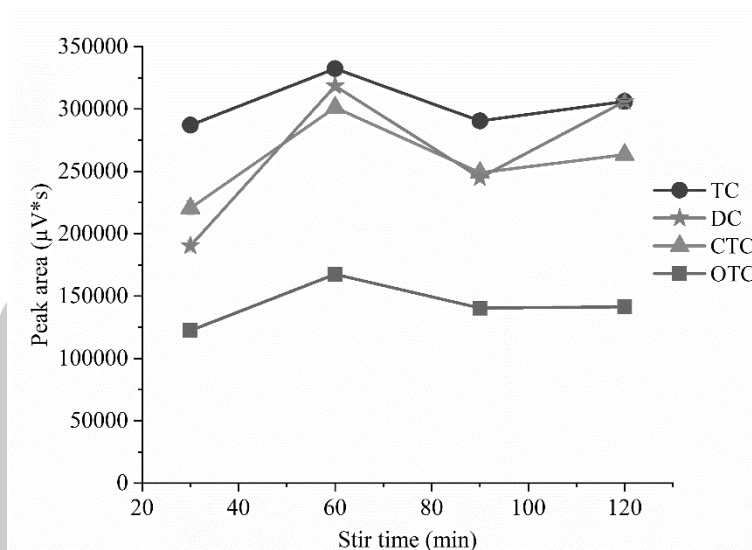


Figure 20 Effect of stir time. Conditions: concentration ratio of $\text{FeCl}_3:\text{FeSO}_4$ was 0.1 M:0.1 M, 2g of *Hevea brasiliensis* Muell. Arg. bark, flow rate at 4 mL min^{-1} , temperature at 65°C , pH 10.5, and $500 \mu\text{g L}^{-1}$ of each tetracycline.

The summarized of the optimum condition for MNPs synthesis by ultrasound-assisted continuous-flow was presented in Table 9.

Table 9 The optimum condition of natural phenolic-coated Fe_3O_4 magnetic nanoparticle synthesis for use as an adsorbent in dispersive solid phase extraction to extract tetracyclines.

Parameters	Optimum conditions
Temperature control	Ultrasonic bath
Synthesis method	Flow technique
Concentration ratio of FeCl_3 and $\text{FeSO}_4 \cdot 7\text{H}_2\text{O}$ (mol L^{-1})	0.1:0.1 ($\text{FeCl}_3:\text{FeSO}_4$)
Flow rate (mL min^{-1})	4.0
Temperature ($^\circ\text{C}$)	65
pH	10.5
Stir time (min)	60

4.3 Characterization of ultrasound-assisted continuous flow-synthesized natural phenolic-coated Fe₃O₄ MNPs

The functional group of ultrasound-assisted continuous flow-synthesized bare Fe₃O₄ MNPs, ultrasound-assisted continuous flow-synthesized natural phenolic-coated Fe₃O₄ MNPs before and after TCs extraction were investigated from FTIR spectra, as shown in Figure 21. The Fe-O stretching characteristics band of Fe₃O₄ can be observed at around 557 cm⁻¹ in all three spectra. The characteristic band of phenolics, including conjugated C=O stretching (1707 cm⁻¹), aromatic C=C stretching (1608 cm⁻¹) and C-O stretching (1381 and 1069 cm⁻¹) was appeared in the spectra of natural phenolic-coated Fe₃O₄ MNPs. Moreover, it can clearly observe the stretching vibrations of -O-H groups more than in the spectra of bare Fe₃O₄ MNPs. Therefore, these results show that the surface of Fe₃O₄ MNPs was successfully coated with natural phenolic compounds. Comparing the FTIR spectra of natural phenolic-coated Fe₃O₄ MNPs before and after TCs extraction. The adsorption band of O-H stretching at 3206 cm⁻¹ in the spectra of natural phenolic-coated Fe₃O₄ MNPs differed and shifted from the stretching vibrations of -O-H groups (3445 cm⁻¹) after TC extraction. The deformation absorption band peak of C-H stretching, C-C stretching, stretching vibrations of C-O, and O-H bending was observed at around 2948 to 2837 cm⁻¹ and between 1608 to 1069 cm⁻¹ in spectra of natural phenolic-coated Fe₃O₄ MNPs after TC extraction. These results demonstrate the existence of an interaction between TCs and functional groups of phenolics on the surface of Fe₃O₄ MNPs.

The crystallinity of ultrasound-assisted continuous flow-synthesized bare and natural phenolic-coated Fe₃O₄ MNPs was investigated, and the XRD pattern results are shown in Figure 22(a). The XRD patterns of both samples exhibited six diffraction peaks at 18.4°, 30.3°, 35.7°, 43.4°, 57.4 and 63.0°, corresponding to the planes (111), (220), (311), (400), (422), (511), and (440), respectively. Moreover, the XRD patterns of bare and natural phenolic-coated Fe₃O₄ MNPs were identical, indicating that the phenolic coating did not affect the phase transformation of Fe₃O₄. Additionally, the XRD pattern of each sample was compared with the 01-075-0449 reference database, and it was found that the diffraction peaks of each sample matched those of Fe₃O₄.

The magnetic properties of ultrasound-assisted continuous flow-synthesized bare and natural phenolic-coated Fe₃O₄ MNPs were evaluated using VSM. The results

presented in Figure 22(b) show that both synthesized Fe_3O_4 MNPs exhibited superparamagnetic behavior, and the saturation magnetization of bare Fe_3O_4 and natural phenolic-coated Fe_3O_4 MNPs were 96.4 and 87.8 emu g^{-1} , respectively. The reduction in saturation magnetization for Fe_3O_4 MNPs after coating with phenolic compounds could be explained by the presence of nonmagnetic phenolic molecules on the surface of Fe_3O_4 MNPs [90].

The surface charge of ultrasound-assisted continuous flow-synthesized natural phenolic-coated Fe_3O_4 MNPs before and after TCs extraction was measured using Zeta potential. The result demonstrated that the surface charge of the magnetic adsorbent was positive (5.6 ± 0.6 mV) before TCs extraction and increased to 8.9 ± 0.7 mV after TCs extraction.

In terms of morphological properties, the particle size of the natural phenolic-coated Fe_3O_4 MNPs synthesized using the ultrasound-assisted continuous flow method and the batch method was measured using TEM image analysis with the ImageJ program combined with data analysis with a Gaussian distribution. It was observed that the particle size of the natural phenolic-coated Fe_3O_4 MNPs synthesized using the ultrasound-assisted continuous flow method (7.5 ± 0.3 nm) was smaller than that of those synthesized using the batch method (14.7 ± 0.3 nm), as shown in Figure 23. Additionally, Figure 24(a) and (b) show TEM images of ultrasound-assisted continuous flow-synthesized natural phenolic-coated Fe_3O_4 MNPs before and after TCs extraction, respectively. It was found that the natural phenolic-coated Fe_3O_4 MNPs were spherical with average diameters of 7.5 ± 0.3 nm and increased in size to 22.5 ± 0.6 nm after TCs extraction. The results of pore structure and surface area analysis of ultrasound-assisted continuous flow-synthesized natural phenolic-coated Fe_3O_4 MNPs are shown in Figure 24(c). The obtained N_2 adsorption-desorption isotherms exhibit a type-V curve [91]. Moreover, the BET surface area, BJH Adsorption cumulative volume of pores ($\text{cm}^3 \text{g}^{-1}$), and BJH Adsorption average pore width ($4V/A$) were $45.3 \text{ m}^2 \text{g}^{-1}$, $0.16 \text{ cm}^3 \text{g}^{-1}$, and 150.6 \AA , respectively, classifying the pore size as mesopore ($20\text{--}500 \text{ \AA}$) [92].

Therefore, the results obtained from FTIR, TEM, and zeta potential analyses can explain the possible interactions in the extraction of TCs with ultrasound-assisted continuous flow-synthesized natural phenolic-coated Fe_3O_4 MNPs as follows: The

abundant hydroxyl (-O-H) functional groups in the structures of both the phenolic compounds coated on Fe_3O_4 and TCs can form hydrogen bonding interactions with each other. π - π interactions occur between the π electrons in the aromatic rings of phenolic compounds and those of TCs. Electrostatic interactions are formed between the positive charge of the magnetic adsorbent and the negative charge of TCs, which can be described under pH 5, where TCs exhibit properties as zwitterions (TCH_2^\pm), while the surface charge of ultrasound-assisted continuous flow-synthesized phenolic-coated Fe_3O_4 MNPs was positive (as determined by Zeta potential). Finally, the physical adsorption between the inner surface of the pores of MNPs and TCs molecules due to the pore size of the MNPs is 150.6 Å (as determined by BET), resulting in MNPs being able to adsorb tetracyclines with a size of $14.80 \times 9.00 \times 7.47$ Å [93].

The summarized graphitic layer extraction mechanism is presented in Figure 25.

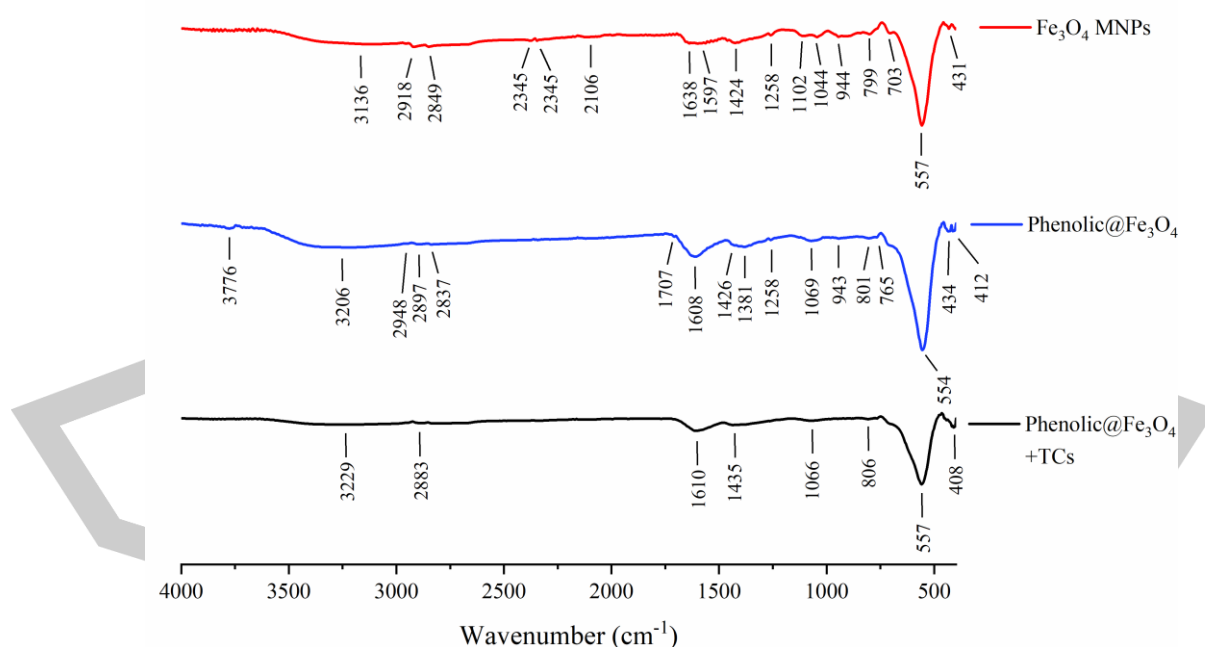


Figure 21 FTIR spectra of flow-synthesized bare Fe_3O_4 MNPs and natural phenolic-coated Fe_3O_4 MNPs before and after TCs extraction.

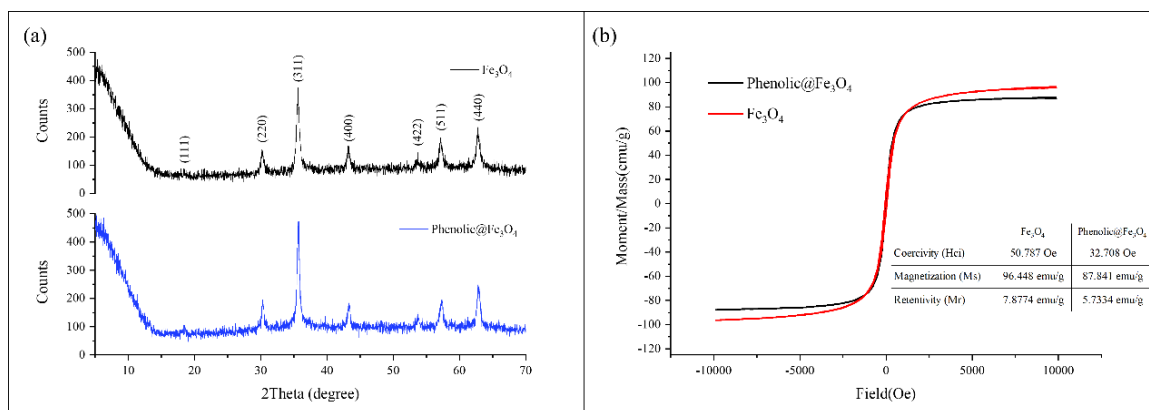


Figure 22 (a) XRD patterns of flow-synthesized bare and natural phenolic-coated Fe_3O_4 MNPs, (b) VSM magnetization of flow-synthesized bare and natural phenolic-coated Fe_3O_4 MNPs.

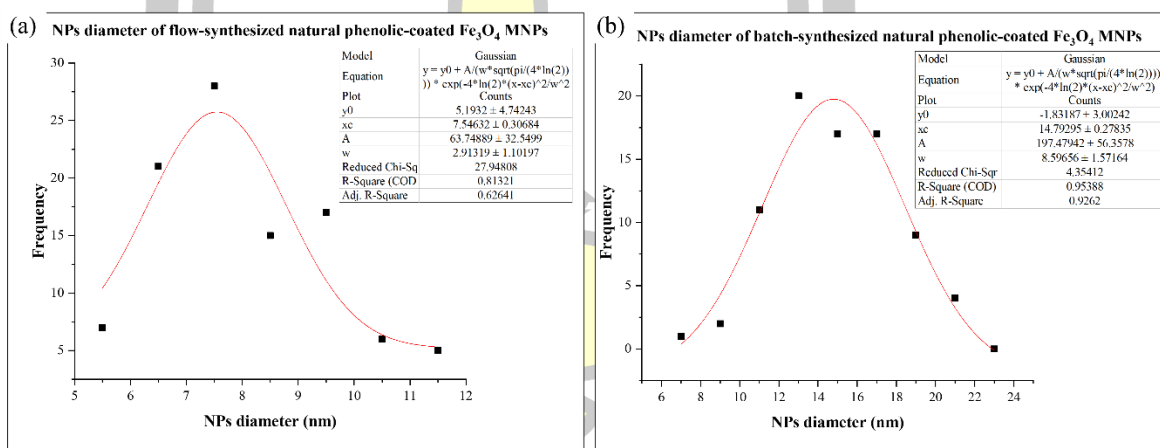


Figure 23 Gaussian distribution curves of (a) flow-synthesized and (b) batch-synthesized natural phenolic-coated Fe_3O_4 MNPs.

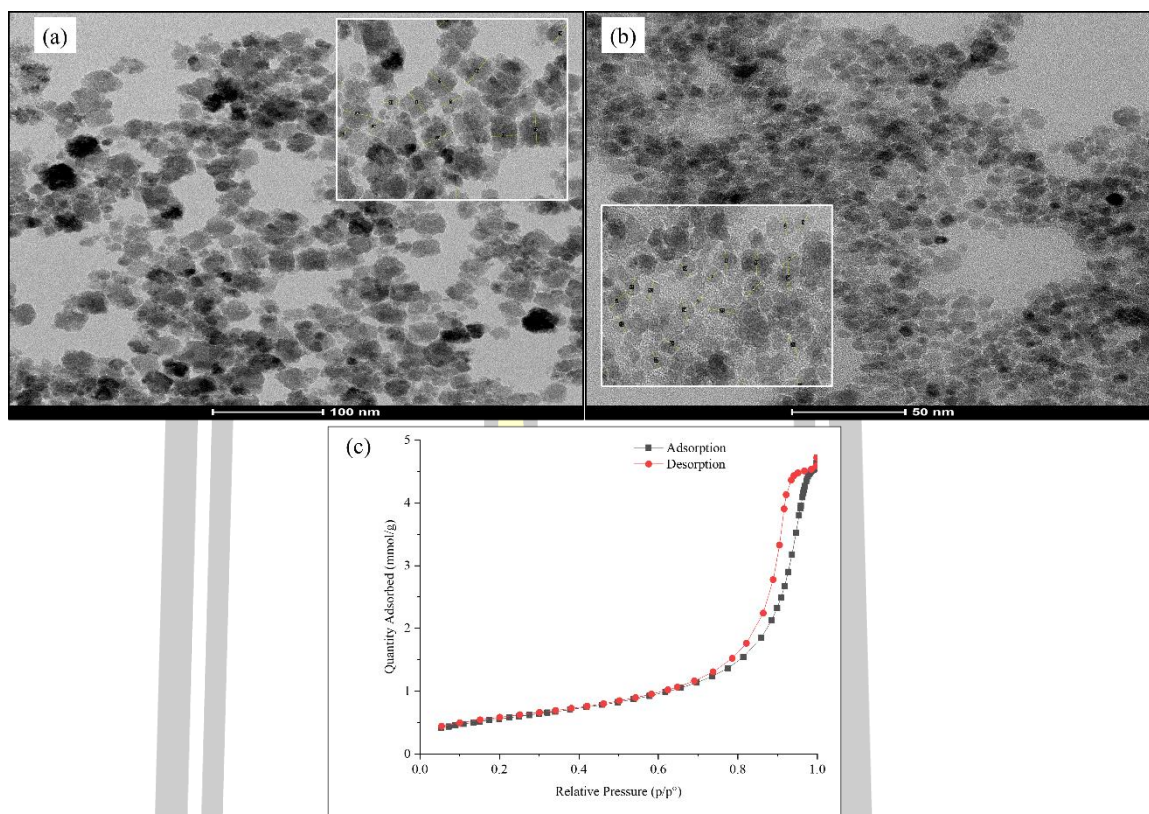
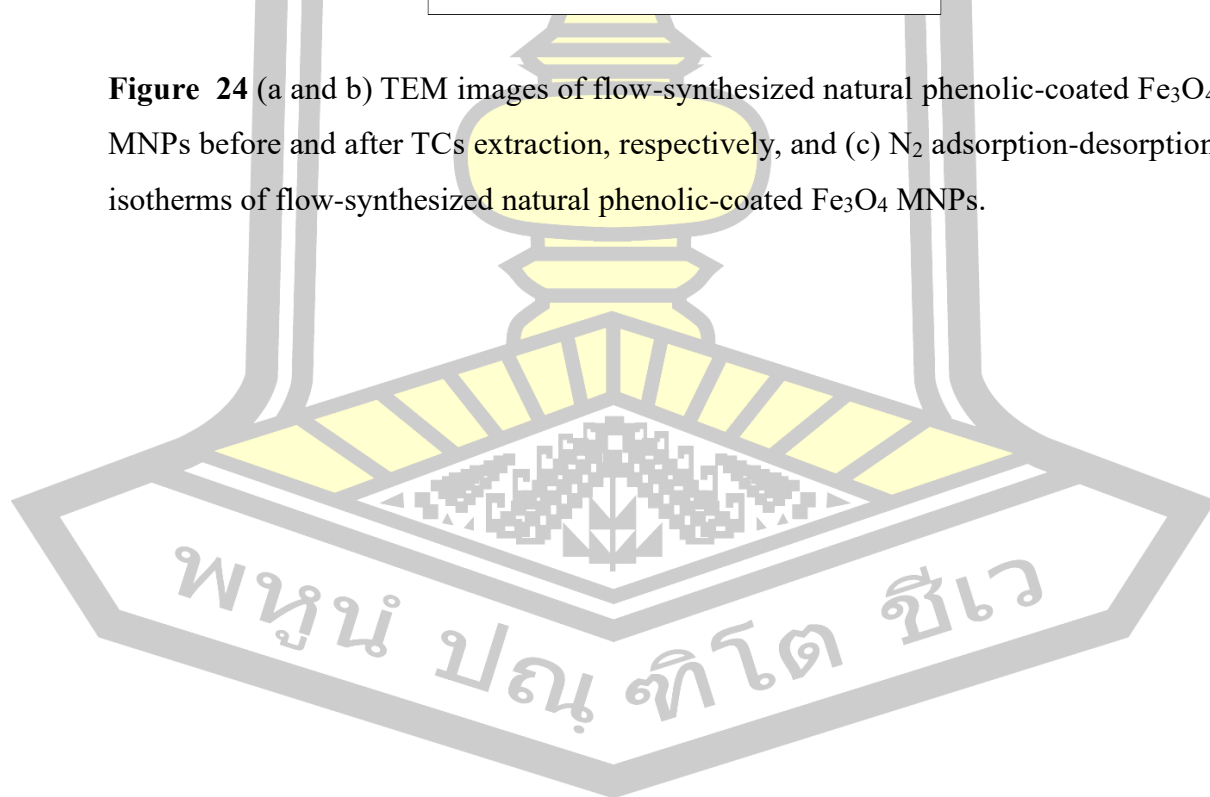


Figure 24 (a and b) TEM images of flow-synthesized natural phenolic-coated Fe_3O_4 MNPs before and after TCs extraction, respectively, and (c) N_2 adsorption-desorption isotherms of flow-synthesized natural phenolic-coated Fe_3O_4 MNPs.



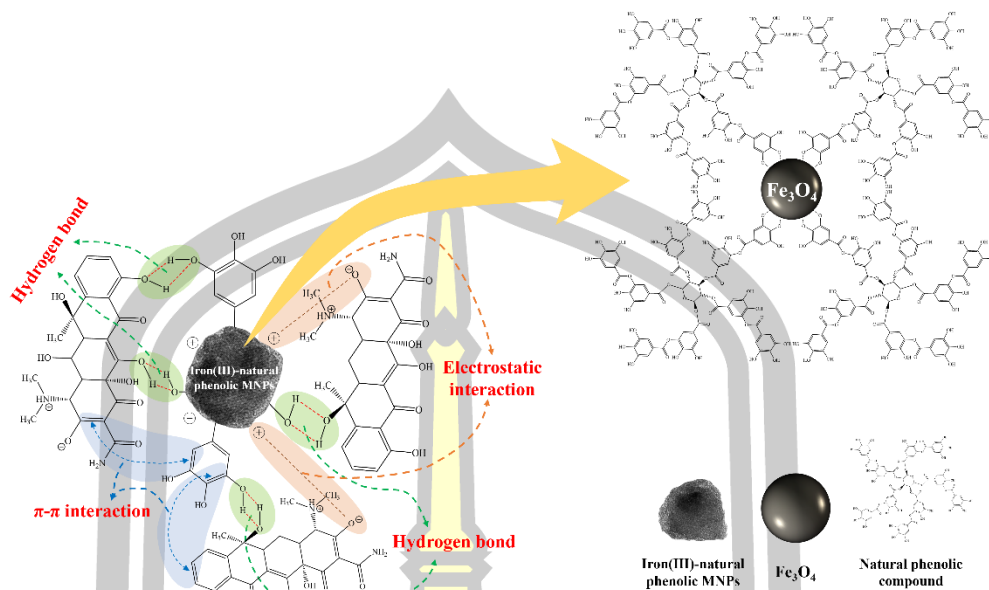


Figure 25 The summarized graphitic layer extraction mechanism between ultrasound-assisted continuous flow-synthesized natural phenolic-coated Fe_3O_4 MNPs and TCs analytes.

4.4 Optimization of the d-SPE procedure to TCs extraction using ultrasound-assisted continuous flow-synthesized natural phenolic-coated Fe_3O_4 MNPs

To achieve the highest extraction efficiency, the parameters affecting the extraction efficiency of the d-SPE method, including pH, honey weight, total volume, buffer solution volume, MNPs volume, ionic strength, vortex time, MNPs collection time, concentration, and volume of desorption solvent, were optimized. These parameters were optimized by the one-factor-at-a-time approach with three replicates. Additionally, the optimum conditions study was performed using the matrix-matched method with the addition of TC-free honey samples for each condition.

4.4.1 Effect of honey weight

To eliminate or reduce the effect of honey matrix on extraction efficiency, in this work, the optimum conditions and method validation were performed using the matrix-matched method with the addition of TCs-free honey samples. The effect of honey weight was evaluated at 1.0, 2.0, 3.0, 4.0, and 5.0 g. The results indicated that the extraction efficiency decreased as the honey weight increased, as shown in Figure 26. These results can be attributed

to an increase in viscosity, resulting in difficult dispersion of MNP sorbents throughout the sample solutions. Therefore, 2 g was used as the weight of honey because 2 g of honey contains more matrix than 1 g, but it can still provide a satisfactory extraction efficiency range.

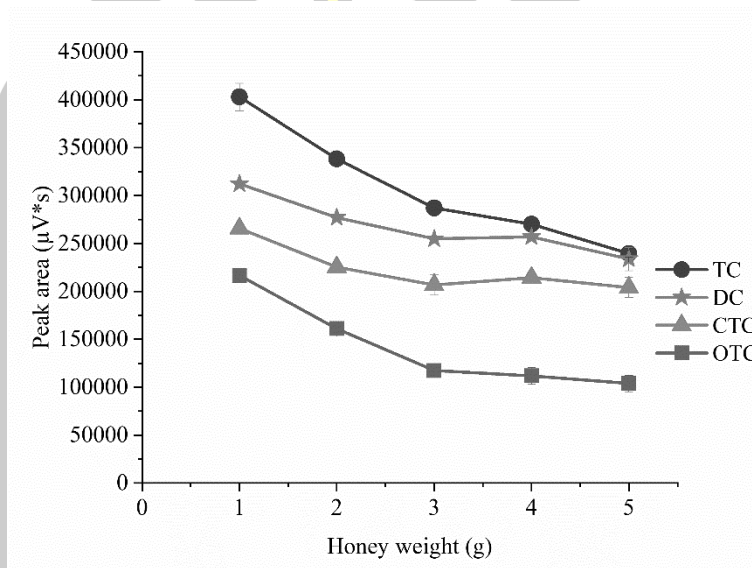


Figure 26 Effect of honey weight. Conditions: 100 μL of MNPs, 0.05 M acetate buffer pH 5.0, total volume was 10 mL, vortex 60 s, MNPs collection time was 2 min, 100 μL of 9% TFA in ACN, and 500 $\mu\text{g L}^{-1}$ of each tetracycline.

4.4.2 Effect of pH

The pH is an important parameter that affects the extraction efficiency and adsorption of analytes on the sorbent. It has influenced both the chemical structure of the TCs and the surface charge of the adsorbent. The $\text{pK}_{\text{a}1}$ of TCs is 3–4, $\text{pK}_{\text{a}2}$ is 7–8, and $\text{pK}_{\text{a}3}$ is 9–10, which is unique to each TC. At a pH below 3, TCs are positively charged. At pH between 3 and 8, they are presented in neutral (zwitterionic form), and at pH higher than 8, they have a negative charge [20], [21]. In this work, the effect of pH was investigated in the range of pH 3.0–7.0 using 5 mL of 0.05 mol L^{-1} acetate buffers (pH 3.0–5.0) and 0.05 mol L^{-1} phosphate buffers (pH 6.0–7.0). It was found that the extraction efficiency increased when the pH increased from 3.0 to 5.0 and decreased afterward when the pH was higher than 5.0, as shown in Figure 27. This occurred because, at a pH lower than 5.0, the functional group of the natural phenolic ligand might be

protonated, and active sites were occupied with protons [90]. Additionally, at a pH higher than 5.0, TCs were deprotonated, forming an anionic stage, resulting in a decreased hydrophobic interaction between TCs and MNPs [94]. Thus, pH 5.0 was chosen for further experiments.

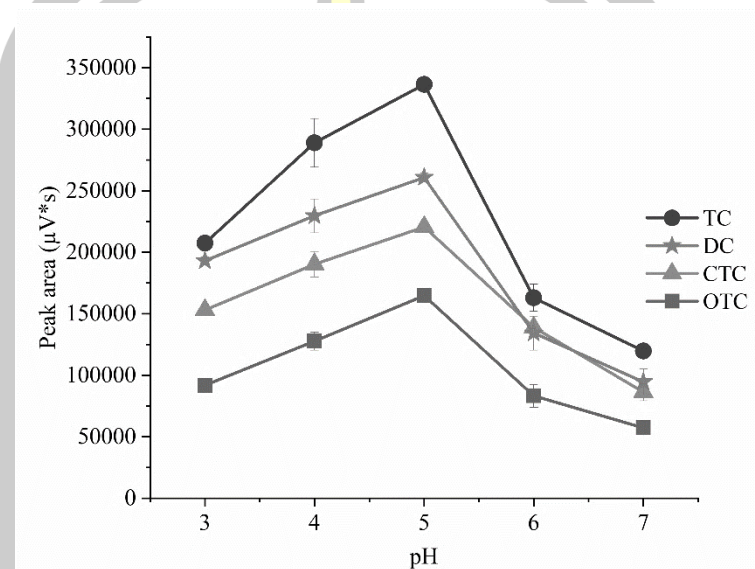


Figure 27 Effect of pH. Conditions: 2 g of honey, 100 μ L of MNPs, total volume was 10 mL, vortex 60 s, MNPs collection time was 2 min, 100 μ L of 9% TFA in ACN, and 500 μ g L⁻¹ of each tetracycline.

4.4.3 Effect of total volume

The effect of total volume was investigated in the range of 10 to 50 mL. The results are shown in Figure 28. It was found that the extraction efficiency increased with the increase in solution volume, which can be explained by the decrease in solution viscosity. Therefore, 40 mL was chosen as the total volume of the solution because it provided satisfactory extraction efficiency and higher precision compared to 50 mL.

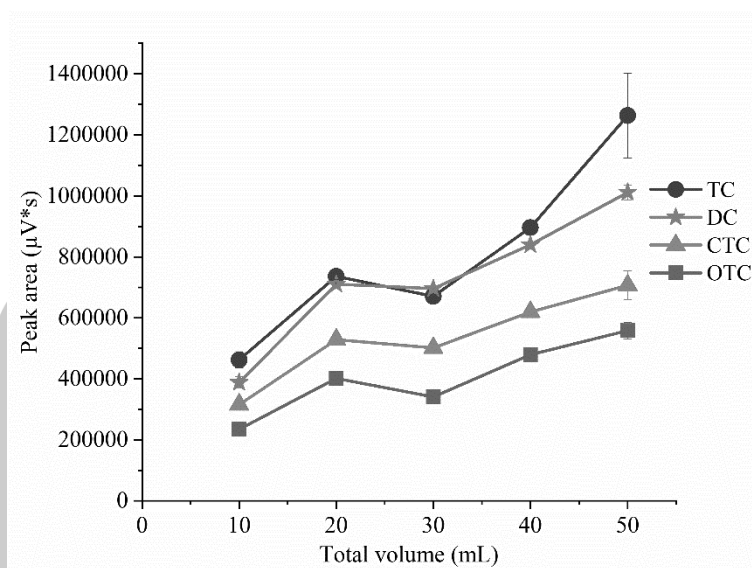
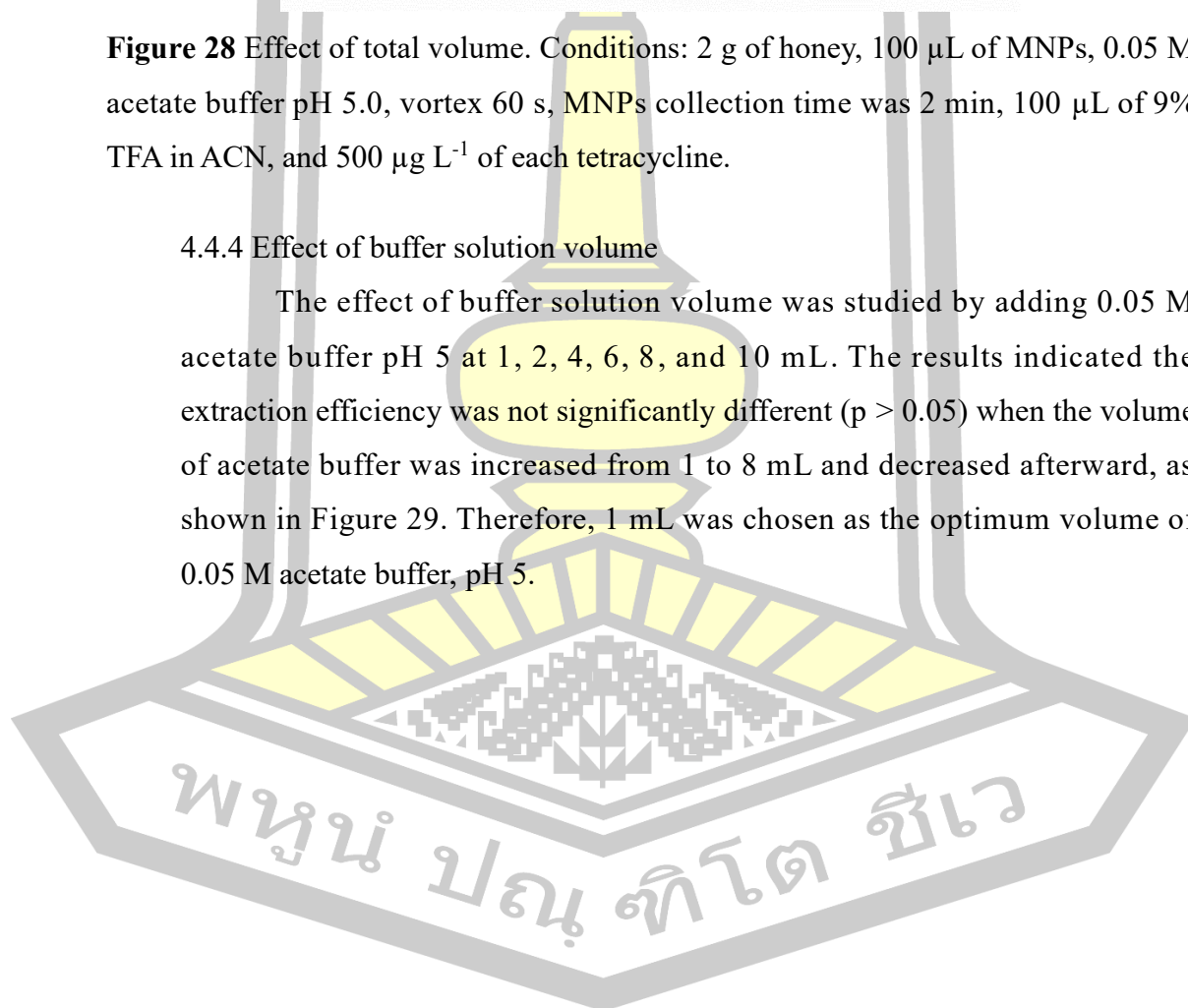


Figure 28 Effect of total volume. Conditions: 2 g of honey, 100 μL of MNPs, 0.05 M acetate buffer pH 5.0, vortex 60 s, MNPs collection time was 2 min, 100 μL of 9% TFA in ACN, and 500 $\mu\text{g L}^{-1}$ of each tetracycline.

4.4.4 Effect of buffer solution volume

The effect of buffer solution volume was studied by adding 0.05 M acetate buffer pH 5 at 1, 2, 4, 6, 8, and 10 mL. The results indicated the extraction efficiency was not significantly different ($p > 0.05$) when the volume of acetate buffer was increased from 1 to 8 mL and decreased afterward, as shown in Figure 29. Therefore, 1 mL was chosen as the optimum volume of 0.05 M acetate buffer, pH 5.



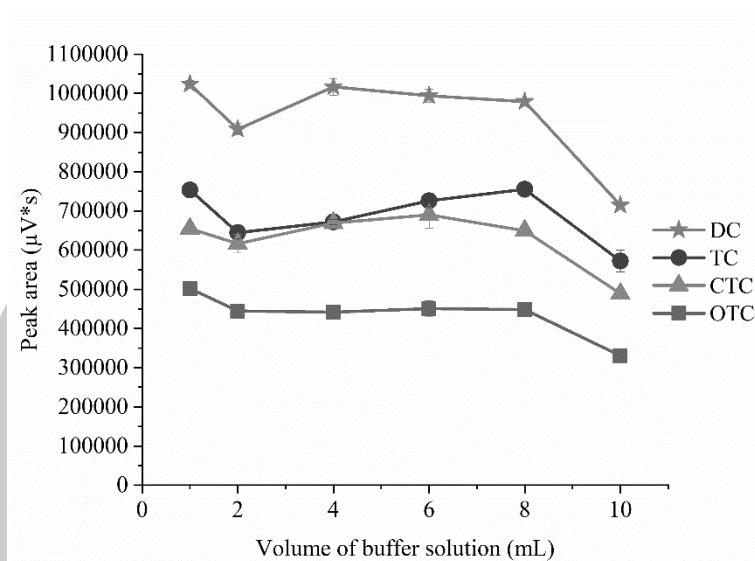
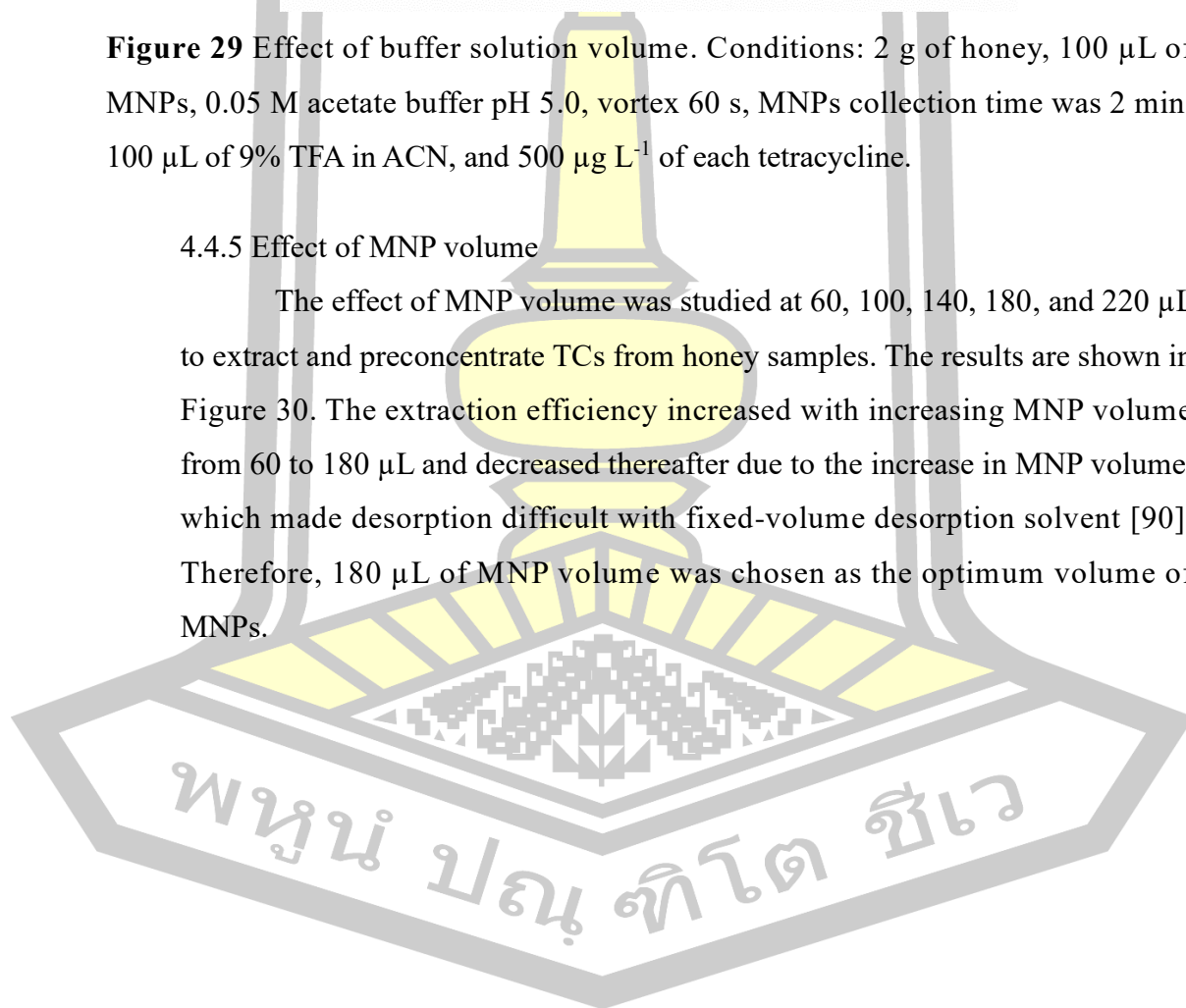


Figure 29 Effect of buffer solution volume. Conditions: 2 g of honey, 100 μL of MNPs, 0.05 M acetate buffer pH 5.0, vortex 60 s, MNPs collection time was 2 min, 100 μL of 9% TFA in ACN, and 500 $\mu\text{g L}^{-1}$ of each tetracycline.

4.4.5 Effect of MNP volume

The effect of MNP volume was studied at 60, 100, 140, 180, and 220 μL to extract and preconcentrate TCs from honey samples. The results are shown in Figure 30. The extraction efficiency increased with increasing MNP volume from 60 to 180 μL and decreased thereafter due to the increase in MNP volume, which made desorption difficult with fixed-volume desorption solvent [90]. Therefore, 180 μL of MNP volume was chosen as the optimum volume of MNPs.



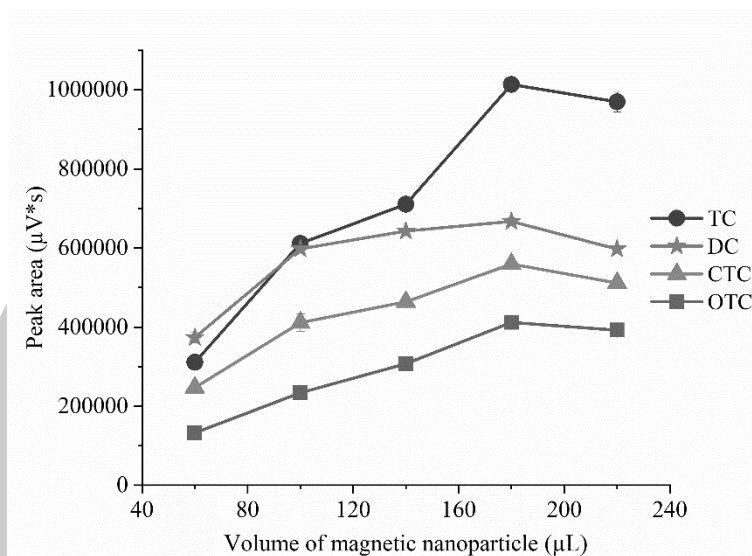
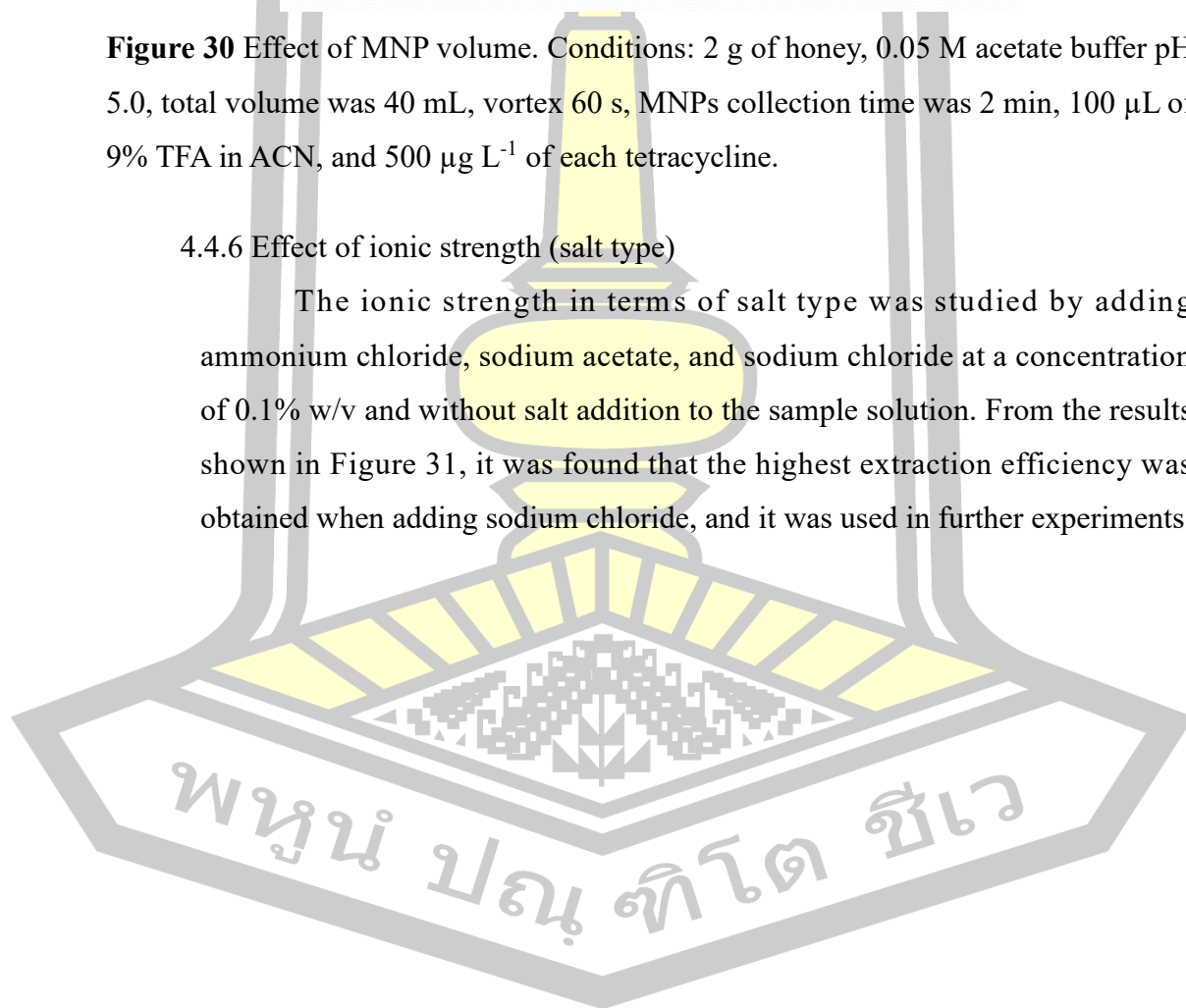


Figure 30 Effect of MNP volume. Conditions: 2 g of honey, 0.05 M acetate buffer pH 5.0, total volume was 40 mL, vortex 60 s, MNPs collection time was 2 min, 100 μL of 9% TFA in ACN, and 500 $\mu\text{g L}^{-1}$ of each tetracycline.

4.4.6 Effect of ionic strength (salt type)

The ionic strength in terms of salt type was studied by adding ammonium chloride, sodium acetate, and sodium chloride at a concentration of 0.1% w/v and without salt addition to the sample solution. From the results shown in Figure 31, it was found that the highest extraction efficiency was obtained when adding sodium chloride, and it was used in further experiments.



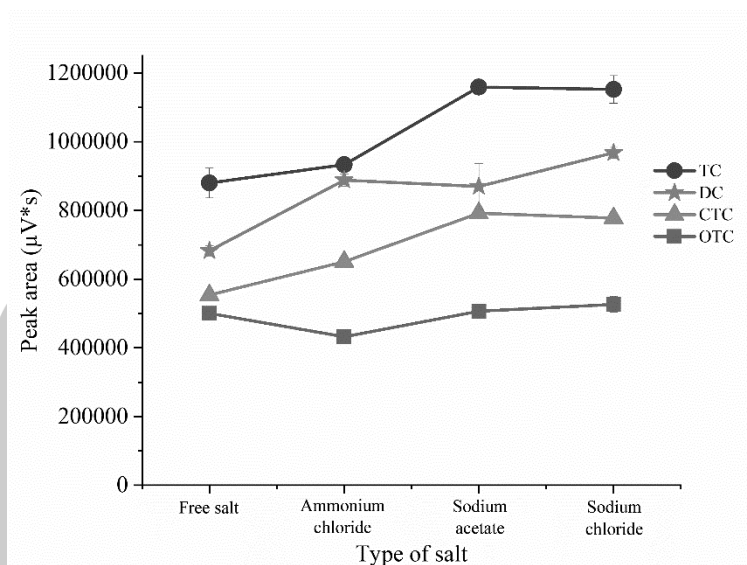


Figure 31 Effect of salt type. Conditions: 2 g of honey, 180 μL of MNPs, 0.05M acetate buffer pH 5.0, total volume was 40 mL, vortex 60 s, MNPs collection time was 2 min, 100 μL of 9% TFA in ACN, and 500 $\mu\text{g L}^{-1}$ of each tetracycline.

4.4.7 Effect of ionic strength (salt concentration)

The ionic strength in terms of salt concentration was investigated by adding sodium chloride at concentrations of 0.01, 0.05, 0.10, 0.15, and 0.20% (w/v). The results are demonstrated in Figure 32. The extraction efficiency increased when the NaCl concentration increased from 0.01 to 0.10%, which could be explained by the salting-out effect principle. After the concentration of salt was higher than 0.1% (w/v), the extraction efficiency decreased due to an increase in the viscosity of the sample solution, which made the sorbent difficult to disperse and reduced the interaction between the adsorbent and the analyte. Therefore, 0.10% (w/v) was used as the sodium chloride concentration.

พหุ ประถมศึกษา

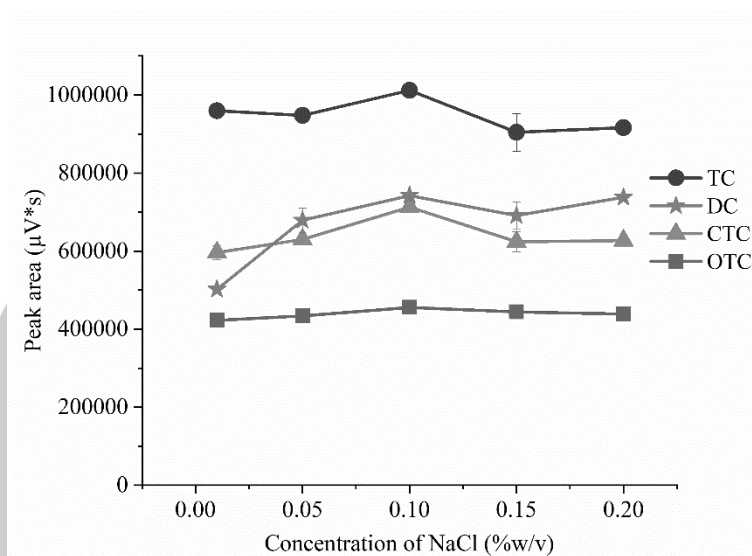


Figure 32 Effect of NaCl concentration. Conditions: 2 g of honey, 180 μL of MNPs, 0.05M acetate buffer pH 5.0, total volume was 40 mL, vortex 60 s, MNPs collection time was 2 min, 100 μL of 9% TFA in ACN, and 500 $\mu\text{g L}^{-1}$ of each tetracycline.

4.4.8 Effect of vortex time

The vortex is a procedure that accelerates the dispersion of the magnetic sorbent into the sample solution containing the analytes, resulting in increased interaction between the analyte and the adsorbent, which affects the extraction efficiency. In this work, the vortex time was investigated in the range of 10–90 s at a speed of 2000 rpm. The results are shown in Figure 33. It was found that the optimum condition of the vortex time was 10 s because it could give the highest extraction efficiency. Therefore, 10 s was used as the vortex time in the further experiments.

พหุ ประสิทธิภาพ

MNPs containing TCs should be collected completely or as much as possible to obtain the best extraction efficiency, accuracy, and precision. The magnetic nanoparticle collection time was studied in the range of 0.5–5 min. The results are shown in Figure 34. It was found that at 1–5 min, the extraction efficiency was not significantly different ($p > 0.05$). Therefore, 2 min was chosen as the suitable time for MNPs collection due to its short time and low standard deviation, which indicates that collecting MNPs was consistent.

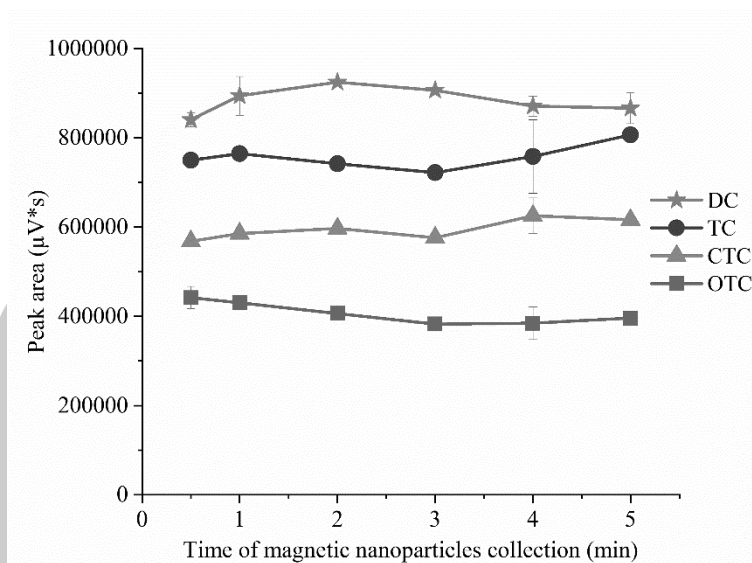


Figure 34 Effect of vortex time. Conditions: 2 g of honey, 180 μL of MNPs, 0.05M acetate buffer pH 5.0, total volume was 40 mL, 0.1% NaCl, vortex 10 s, 100 μL of 9% TFA in ACN, and 500 $\mu\text{g L}^{-1}$ of each tetracycline.

4.4.10 Effect of concentration of desorption solvent

In this work, TFA in ACN was used as a desorption solvent to desorb TCs on the MNPs before quantitation analysis by HPLC-UV. The concentration of TFA in ACN was studied in the range of 0.0–9.0% (v/v). It was found that 9% TFA in ACN was the concentration that yielded the highest extraction efficiency, as shown in Figure 35. The lower extraction efficiency was observed when TFA concentrations were less than 9% (v/v). It may result in the incomplete desorption of TCs from the adsorbent. Therefore, 9% (v/v) was used as the proper concentration of TFA in the ACN to desorb TCs from the adsorbent.

พหุ ประสิทธิภาพ

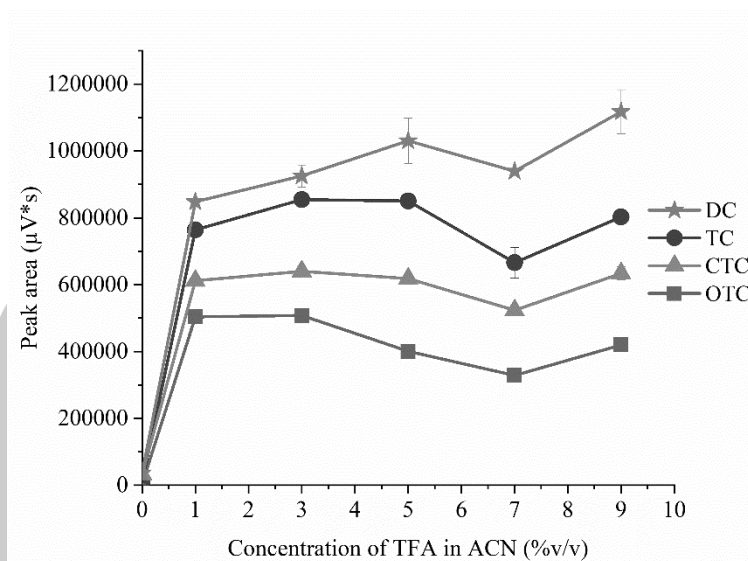
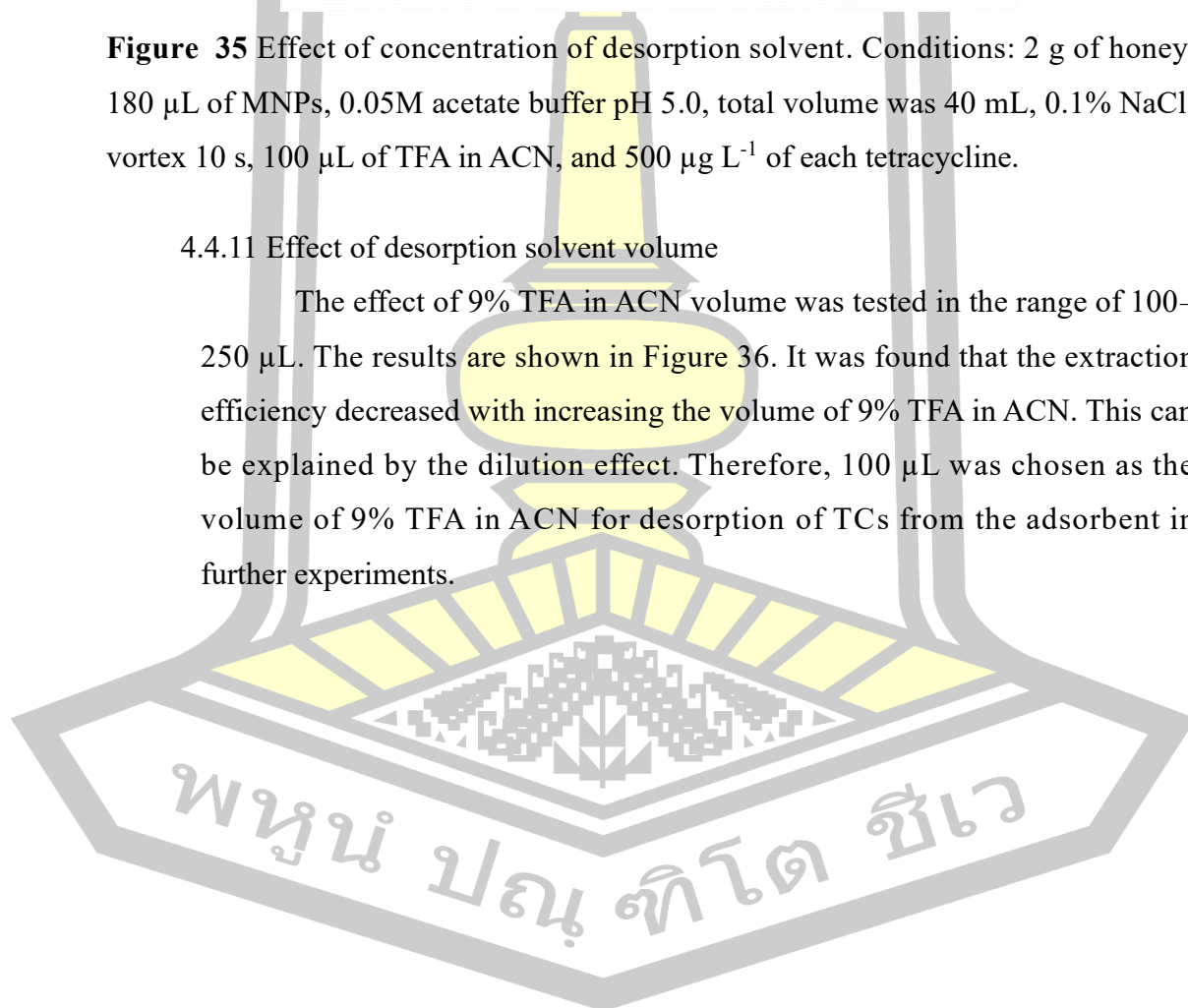


Figure 35 Effect of concentration of desorption solvent. Conditions: 2 g of honey, 180 μL of MNPs, 0.05M acetate buffer pH 5.0, total volume was 40 mL, 0.1% NaCl, vortex 10 s, 100 μL of TFA in ACN, and 500 $\mu\text{g L}^{-1}$ of each tetracycline.

4.4.11 Effect of desorption solvent volume

The effect of 9% TFA in ACN volume was tested in the range of 100–250 μL . The results are shown in Figure 36. It was found that the extraction efficiency decreased with increasing the volume of 9% TFA in ACN. This can be explained by the dilution effect. Therefore, 100 μL was chosen as the volume of 9% TFA in ACN for desorption of TCs from the adsorbent in further experiments.



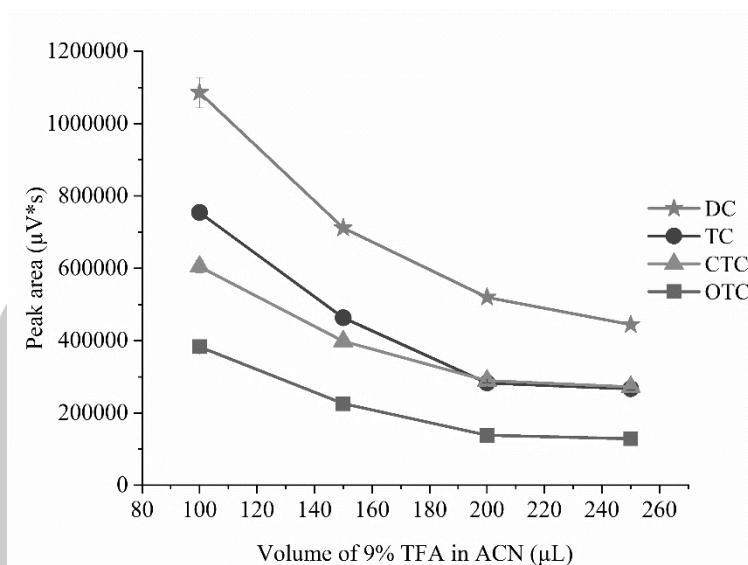


Figure 36 Effect of concentration of desorption solvent. Conditions: 2 g of honey, 180 μL of MNPs, 0.05M acetate buffer pH 5.0, a total volume was 40 mL, 0.1% NaCl, vortex 10 s, and 500 $\mu\text{g L}^{-1}$ of each tetracycline.

The summarized optimum condition for TCs extraction by d-SPE based on natural phenolic-coated Fe_3O_4 MNP sorbent obtained from ultrasound-assisted continuous flow-synthesis is presented in Table 10.

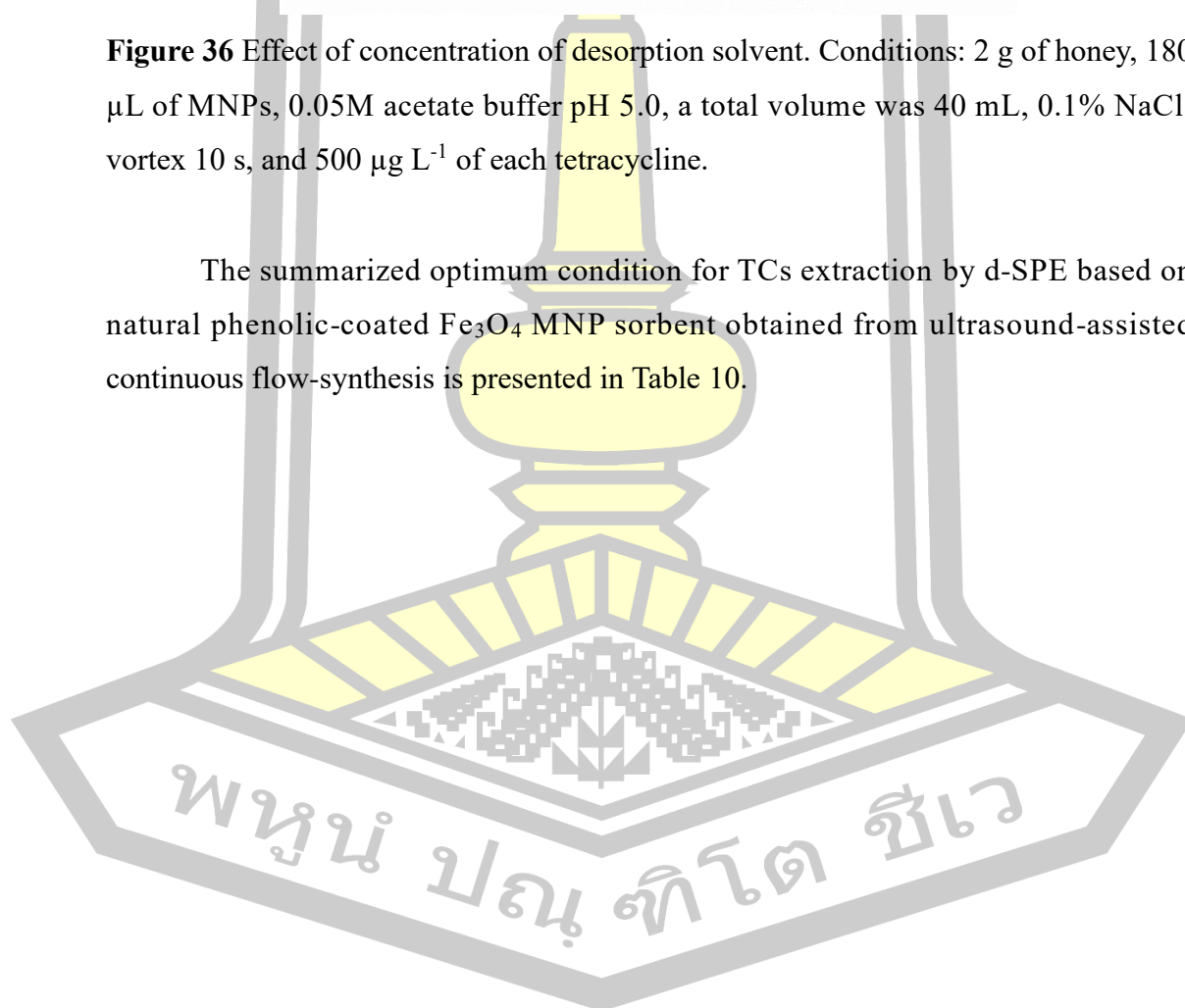


Table 10 The optimum condition of dispersive solid phase extraction for the extraction of tetracyclines using natural phenolic-coated Fe₃O₄ MNP sorbent from ultrasound-assisted continuous flow-synthesis.

Parameters	Optimum conditions
Honey sample weight (g)	2.0
pH of buffer solution	5.0
Total volume (mL)	40.0
Buffer solution volume (mL)	1.0
Magnetic nanoparticles volume (μL)	180.0
Ionic strength (salt type)	NaCl
Ionic strength (concentration of salt) (%(w/v))	0.10
Vortex time (s)	10.0
MNPs collection time (min)	2.0
Concentration of desorption solvent (TFA in ACN) (% (v/v))	9.0
Volume of desorption solvent (TFA in ACN) (μL)	100.0

4.5 Method validation

To ensure the performance of the proposed method for the extraction and preconcentration of TCs under the optimum conditions, the validation of the method was evaluated in terms of linearity, limit of detection (LOD), limit of quantitation (LOQ), precision (intra-day and inter-day), accuracy, and enrichment factor (EF). The results are summarized in Table 11. The calibration graph was constructed by the matrix-matched method using a blank honey sample. The linearity was in the range of 0.70–500 μg L⁻¹ for OTC and TC, and 1.00–500 μg L⁻¹ for CTC and DC, with the coefficient of determination (R²) greater than 0.9953 for all analytes. The LODs and LOQs were calculated based on a signal-to-noise ratio (S/N) of 3 and 10 were obtained at 0.50 μg L⁻¹ (10 μg kg⁻¹) and 0.70–1.00 μg L⁻¹ (14–20 μg kg⁻¹), respectively, and the LODs of the proposed method were equal to the EURL Guidance on minimum method performance requirements (MMPRs) for the analysis of TC residues in honey (10 μg kg⁻¹) [7]. The precision was investigated by performing 7 replicates of analysis for the mixed standard solution at 10, 50, and 100 μg L⁻¹ in the

same day (intra-day RSDs) and performing 3 replicates of analysis for the mixed standard solution at concentrations in the ranges 10–500 $\mu\text{g L}^{-1}$ in 5 consecutive days (inter-day RSDs). The results found that %RSD was less than 6.91% and 13.17% for intra- and inter-day precision, respectively. Recovery was used to assess accuracy by spiked TCs standard to honey samples at concentrations of 1.00, 3.00, and 5.00 $\mu\text{g L}^{-1}$ and found that recovery was in the range of 81.3–117.9%. Therefore, the precision and accuracy of the developed method were considered to be within the acceptable range (70–120%, RSD <20%) [95]. Furthermore, the EF was calculated in accordance with the ratio of the slope of the after-preconcentration calibration curve to the slope of the before-preconcentration calibration curve, and the results were obtained at 32.05, 63.71, 96.82, and 90.46 for the EF of OTC, TC, CTC, and DC, respectively. Additionally, the obtained chromatogram from the TCs standard solution analysis by direct injection method and the proposed method are shown in Figure 37.

Table 11 Method validation of the proposed method in terms of limit of detection, limit of quantitation, linear range, R^2 , enrichment factor, and precision for the determination of tetracyclines in honey matrix.

Analytes	LODs ^a ($\mu\text{g L}^{-1}$)	LOQs ^b ($\mu\text{g L}^{-1}$)	LR ^c ($\mu\text{g L}^{-1}$)	R^2 ^d	EF ^e	RSD ^f	
						Intra-day (n=7)	Inter-day (n=5×3)
OTC	0.50 (10 $\mu\text{g kg}^{-1}$)	0.70 (14 $\mu\text{g kg}^{-1}$)	0.70 – 500 (14 – 10 ⁴ $\mu\text{g kg}^{-1}$)	0.9965	32.05	4.50	6.72
TC	0.50 (10 $\mu\text{g kg}^{-1}$)	0.70 (14 $\mu\text{g kg}^{-1}$)	0.70 – 500 (14 – 10 ⁴ $\mu\text{g kg}^{-1}$)	0.9982	63.71	6.91	10.15
CTC	0.50 (10 $\mu\text{g kg}^{-1}$)	1.00 (20 $\mu\text{g kg}^{-1}$)	1.00 – 500 (20 – 10 ⁴ $\mu\text{g kg}^{-1}$)	0.9976	96.82	4.35	7.65
DC	0.50 (10 $\mu\text{g kg}^{-1}$)	1.00 (20 $\mu\text{g kg}^{-1}$)	1.00 – 500 (20 – 10 ⁴ $\mu\text{g kg}^{-1}$)	0.9953	90.46	2.59	13.17

^a Limit of detection ($\mu\text{g L}^{-1}$)

^b Limit of quantification ($\mu\text{g L}^{-1}$)

^c Linear range ($\mu\text{g L}^{-1}$)

^d Coefficient of determination (R^2)

^e Enrichment factor = slope of the calibration curve with extraction / slope of the calibration curve without extraction

^f Relative standard deviation percent (RSD)

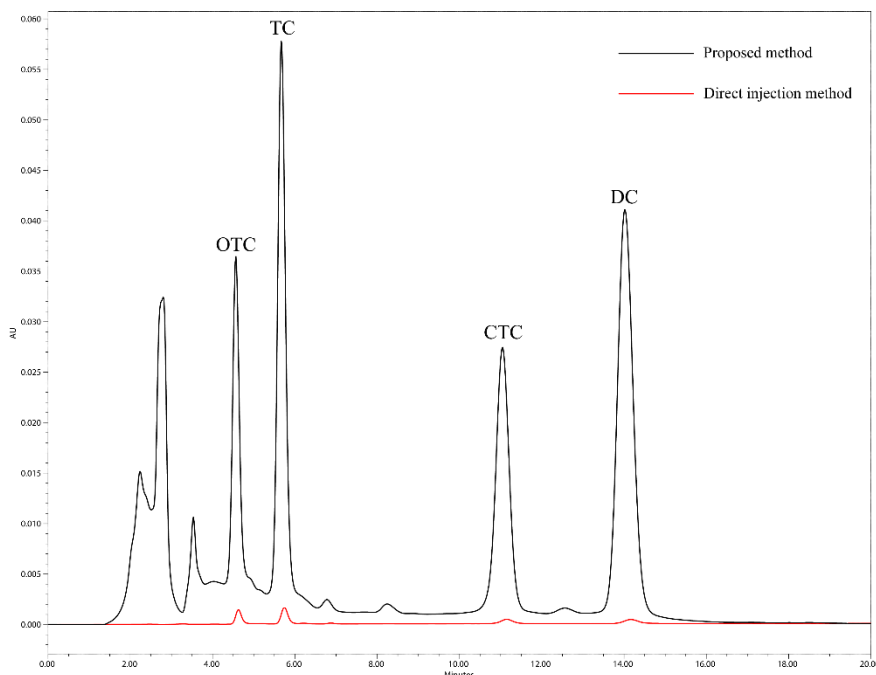


Figure 37 Chromatogram of tetracyclines standard solution analysis by direct injection method and preconcentrated by the proposed method ($500 \mu\text{g L}^{-1}$ of each tetracycline).

4.6 Stability of the natural phenolic-coated Fe_3O_4 MNP

The stability of the natural phenolic-coated Fe_3O_4 MNP was assessed by comparing the results of using the intra-batch of the natural phenolic-coated Fe_3O_4 MNP, which was synthesized as an adsorbent in the TC extraction procedure, as described in Section 3.5. The results in Figure 38 indicate that the developed sorbent demonstrated close extraction efficiency for TCs over a 20-day period. The precision, measured as the relative standard deviation (%RSD), was less than 17% for all analytes. Hence, the results demonstrate that the natural phenolic-coated Fe_3O_4 MNP has satisfactory stability.

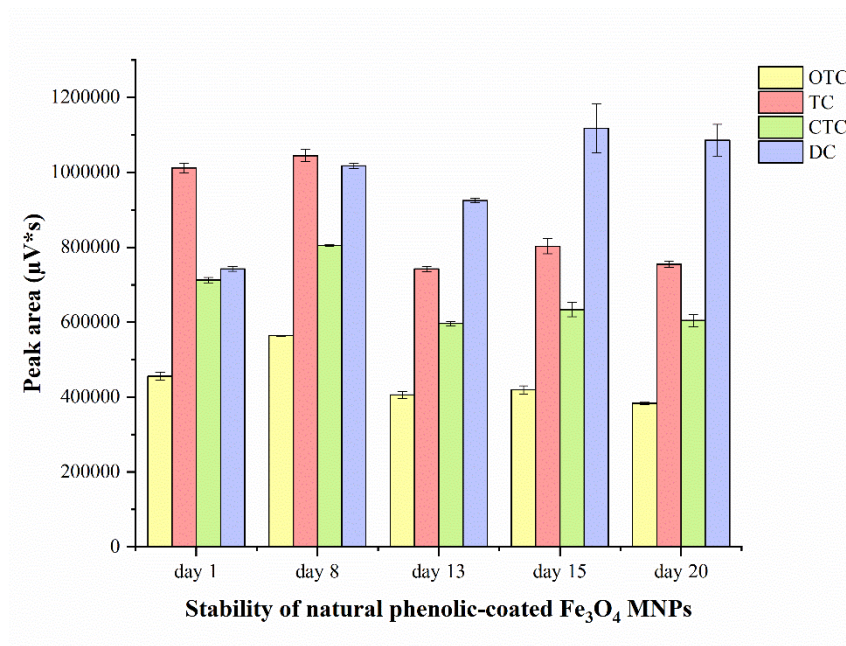


Figure 38 Peak area of all TCs after being extracted and enriched over a 15-day period by intra-batch-synthesized MNPs.

4.7 Application of the developed method to honey samples

Twelve samples of honey were purchased from department stores and convenience stores within Maha Sarakham province and nearby provinces. The honey samples weighing 2.0 g were analyzed for quantitation of the four tetracyclines (OTC, TC, CTC, and DC) using a method developed under appropriate conditions as described above. The quantitation of four residues of TCs in honey was analyzed by our developed method combined with HPLC-UV. The accuracy was evaluated by spiking TCs at three concentration levels (1.00, 3.00, and 5.00 $\mu\text{g L}^{-1}$) each analyte into the sample. The results are presented in Table 12. It was observed that TC was not detected in any of the samples. However, OTC was detected only in sample 12 at a concentration of 0.90 $\mu\text{g L}^{-1}$ (18 $\mu\text{g kg}^{-1}$). Three samples (3, 11, and 12) detected CTC at concentrations ranging from 2.40 to 6.40 $\mu\text{g L}^{-1}$ (48 to 128 $\mu\text{g kg}^{-1}$). CTC was found below the LOQ in sample 8. DC was detected at 1.00–2.40 $\mu\text{g L}^{-1}$ (20–48 $\mu\text{g kg}^{-1}$) in samples 4, 11, and 12, and DC was obtained below the LOQ in samples 1, 2, 6, and 8. Therefore, from the results of the determination of tetracycline residues in twelve honey samples, it was found that only CTC detected in samples 11 and 12 had a concentration exceeding the maximum residue limits (MRLs) (50 $\mu\text{g kg}^{-1}$) [6].

Representation chromatograms of honey samples spiked with standard TCs at 0.05, 0.15, and 0.25 $\mu\text{g L}^{-1}$, are shown in Figure 39.

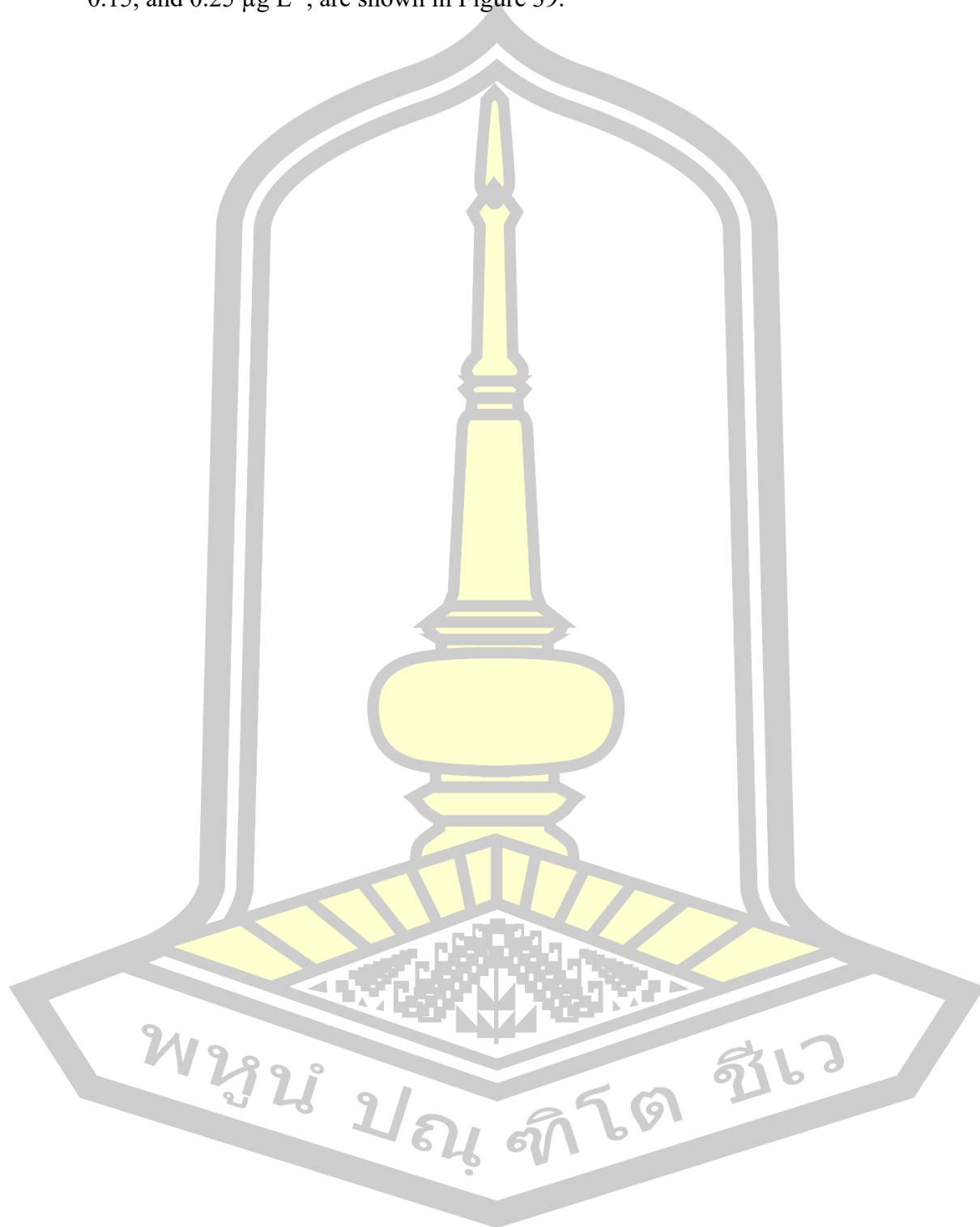


Table 12 Application of the developed method for determination of TCs in real honey samples.

Sample	Spiked (µg/L)	Oxytetracycline			Tetracycline			Chlortetracycline			Doxycycline		
		Found (µg/L)	Recovery (%)	%RSD	Found (µg/L)	Recovery (%)	%RSD	Found (µg/L)	Recovery (%)	%RSD	Found (µg/L)	Recovery (%)	%RSD
Honey 1	0.0	N.D.	-	-	N.D.	-	-	N.D.	-	-	<LOQ	-	-
	1.0	0.1	96.6	5	1.0	97.1	6	1.1	112.9	5	1.9	99.4	3
	3.0	2.7	91.1	7	3.0	100.2	3	2.8	93.0	5	3.4	83.3	5
	5.0	4.5	90.3	7	4.9	97.5	3	4.5	90.0	1	5.1	85.0	5
Honey 2	0.0	N.D.	-	-	N.D.	-	-	N.D.	-	-	<LOQ	-	-
	1.0	1.0	100.2	1	1.2	114.7	7	1.1	109.9	0.2	1.6	106.6	8
	3.0	2.6	87.8	5	2.6	87.2	3	2.4	81.4	2	3.0	81.5	6
	5.0	4.8	95.3	3	5.2	104.4	1	4.2	84.0	1	4.7	83.4	9
Honey 3	0.0	N.D.	-	-	N.D.	-	-	2.4 (48)*	-	-	N.D.	-	-
	1.0	0.9	91.7	3	1.0	97.8	6	3.5	110.2	4	0.9	86.4	9
	3.0	2.6	88.5	9	3.3	111.2	4	5.0	86.4	8	2.6	86.1	5
	5.0	5.0	99.1	1	5.1	101.7	1	7.0	92.9	5	4.2	83.2	3
Honey 4	0.0	N.D.	-	-	N.D.	-	-	N.D.	-	-	1.0 (20)*	-	-
	1.0	0.9	92.6	6	0.9	93.00	4	0.9	87.2	8	2.0	95.1	6
	3.0	3.4	111.8	3	3.4	112.7	5	2.7	90.5	3	3.8	91.6	4
	5.0	5.0	99.1	3	5.1	102.2	1	4.1	82.2	1	5.2	82.7	9
Honey 5	0.0	N.D.	-	-	N.D.	-	-	N.D.	-	-	N.D.	-	-
	1.0	1.1	105.6	8	1.2	117.4	1	1.2	115.7	1	1.1	106.8	1
	3.0	3.5	117.9	3	3.5	116.9	3	3.2	105.1	2	2.9	97.9	3
	5.0	5.7	113.6	2	5.8	116.3	2	5.0	100.7	2	5.8	115.4	3
Honey 6	0.0	N.D.	-	-	N.D.	-	-	N.D.	-	-	<LOQ	-	-
	1.0	1.0	100.8	8	1.1	107.9	2	1.1	105.9	1	1.4	88.3	6
	3.0	3.4	115.0	0.3	3.5	116.4	1	3.2	107.3	3	3.1	85.8	3
	5.0	4.9	98.0	2	5.6	112.5	2	4.7	93.7	3	4.7	83.7	4

N.D.: Not detected ()*: µg/kg

Table 12 (continued)

Sample	Spiked (µg/L)	Oxytetracycline			Tetracycline			Chlortetracycline			Doxycycline		
		Found (µg/L)	Recovery (%)	%RSD	Found (µg/L)	Recovery (%)	%RSD	Found (µg/L)	Recovery (%)	%RSD	Found (µg/L)	Recovery (%)	%RSD
Honey 7	0.0	N.D.	-	-	N.D.	-	-	N.D.	-	-	N.D.	-	-
	1.0	1.0	103.5	10	1.0	98.3	5	1.1	106.1	2	0.9	88.4	8
	3.0	2.8	92.6	5	2.9	97.6	4	2.8	93.3	5	2.4	81.8	1
	5.0	4.3	86.4	2	4.8	97.0	3	4.8	96.6	1	4.3	86.1	3
Honey 8	0.0	N.D.	-	-	N.D.	-	-	<LOQ	-	-	<LOQ	-	-
	1.0	1.1	100.9	5	0.9	86.9	8	1.8	102.9	9	1.6	97.2	7
	3.0	3.0	100.8	10	2.5	82.7	7	3.8	100.9	3	3.4	95.0	3
	5.0	4.4	88.8	6	4.1	81.3	3	5.3	91.4	3	4.7	82.0	3
Honey 9	0.0	N.D.	-	-	N.D.	-	-	N.D.	-	-	N.D.	-	-
	1.0	1.0	102.8	4	0.8	84.7	3	1.0	105.0	4	1.0	95.0	5
	3.0	2.8	94.1	7	3.2	107.6	4	3.2	105.1	3	2.5	84.5	1
	5.0	5.1	102.6	1	5.2	104.5	6	5.0	101.0	3	4.4	88.1	5
Honey 10	0.0	N.D.	-	-	N.D.	-	-	N.D.	-	-	N.D.	-	-
	1.0	1.0	101.2	1	1.1	108.2	1	1.1	110.0	2	0.9	87.3	5
	3.0	3.2	108.4	0.3	3.3	109.2	4	3.2	106.4	5	2.9	98.1	6
	5.0	4.8	95.5	6	5.3	105.4	2	5.6	111.2	4	4.7	93.7	2
Honey 11	0.0	N.D.	-	-	N.D.	-	-	5.0	-	-	2.0	-	-
	1.0	1.0	103.1	9	1.0	101.6	1	(100)	97.1	6	2.9	94.7	8
	3.0	3.0	99.8	2	3.0	100.9	2	7.6	85.7	7	4.5	85.7	5
	5.0	4.6	91.4	2	4.8	96.6	5	10.0	101.0	6	6.6	93.0	1
Honey 12	0.0	0.9 (18)	-	-	N.D.	-	-	6.4 (128)	-	-	2.4 (48)	-	-
	1.0	1.8	84.7	7	0.9	90.1	7.5	7.3	90.7	6	3.4	100.2	6
	3.0	3.9	99.9	5	2.8	91.6	4.5	8.9	83.6	5	5.4	99.7	5
	5.0	6.2	105.9	4	4.9	98.7	6.8	11.5	102.4	2	7.1	94.3	4

N.D.: Not detected ()*: µg/kg

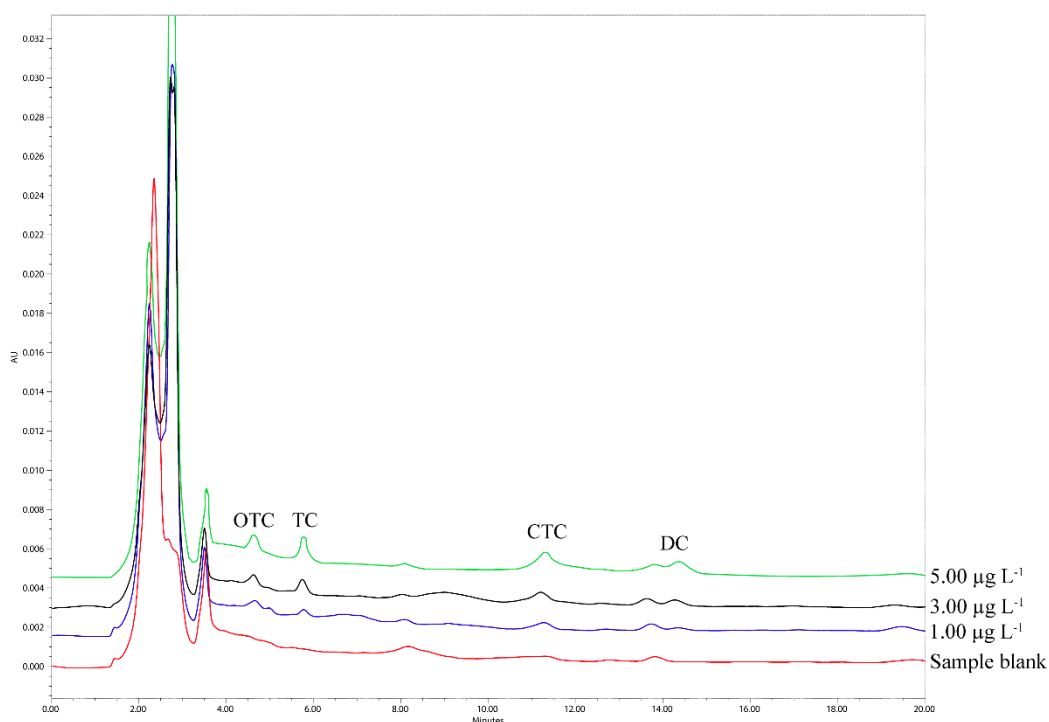


Figure 39 Representation chromatograms of honey samples spiked with standard TCs at 1.00, 3.00, and 5.00 $\mu\text{g L}^{-1}$.

4.8 Comparison of the analytical performance of the developed sample preparation with the previous method

Magnetic nanoparticles as adsorbents for the determination of TCs have been previously reported in several works. To confirm the performance of the developed method, it was compared with previously reported results, as summarized in Table 13. The ultrasound-assisted continuous flow-synthesized natural phenolic-coated Fe_3O_4 MNPs demonstrated a capability to provide lower LODs and LOQs compared to using surfactant-coated Fe_3O_4 MNPs [12], $\text{C}_{18}/\text{SiO}_2/\text{Fe}_3\text{O}_4$ MNPs [94], and water-soluble amino functionalized MNP [96] as adsorbents in the TCs extraction. Moreover, the developed method exhibited a higher enrichment factor and a wider linearity range than many comparable methods. Additionally, the suggested method provided the advantages of utilizing reagents derived from agricultural waste, increasing its environmental friendliness, and importantly, this research is the first work that uses natural phenolic-coated Fe_3O_4 MNPs for extracting and enriching TCs.

Therefore, the proposed method provides another suitable alternative method for the determination of TCs in honey samples.

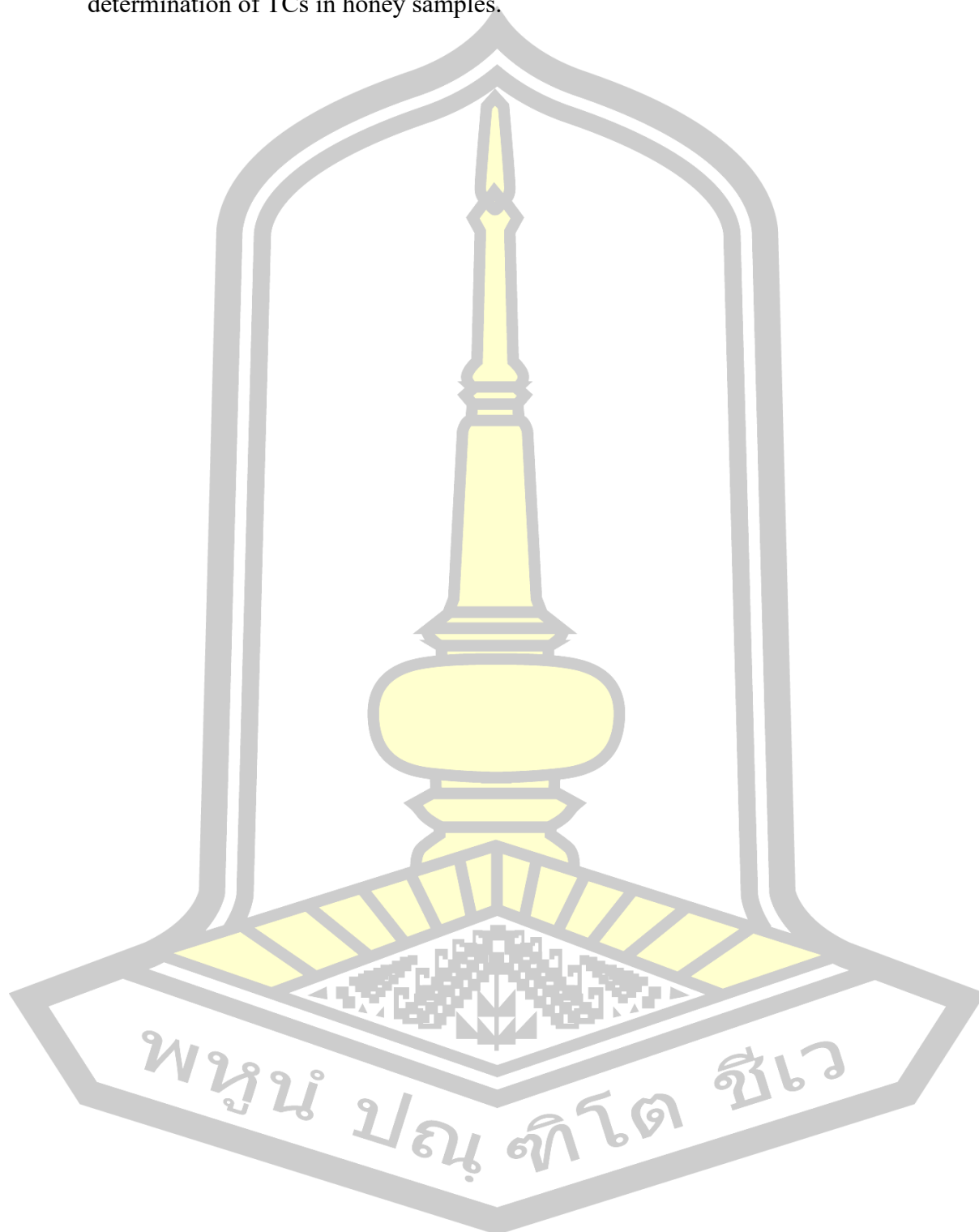


Table 13 Comparison of the analytical performance method between the proposed methods and other previously reported methods for using magnetic nanoparticles for tetracycline analysis.

Sorbents	Sample	Analytes	LODs ^a	LOQs ^b	LR ^c	EF ^d	Recovery (%)	RSD ^e	Reference
Surfactant-coated Fe ₃ O ₄ MNPs	Human serum	OTC	0.03 mg L ⁻¹	Not shown	0.10–10 mg L ⁻¹		97–108		
		TC	0.08 mg L ⁻¹	Not shown	0.25–10 mg L ⁻¹	Not shown	90–112	1–6% (intra-day) <8% (inter-day)	[12]
		DC	0.03 mg L ⁻¹	Not shown	0.10–10 mg L ⁻¹		99–115		
C ₁₈ /SiO ₂ /Fe ₃ O ₄ MNPs	Water	OTC	2.0 µg L ⁻¹	8.0 µg L ⁻¹	2.0–1000 µg L ⁻¹		83–88	<10%	
		TC	10.0 µg L ⁻¹	40.0 µg L ⁻¹	10.0–1000 µg L ⁻¹	5	83–87	(repeatability) <6%	[94]
		DC	10.0 µg L ⁻¹	40.0 µg L ⁻¹	10.0–1000 µg L ⁻¹		82–87	(reproducibility)	
Carboxyl-modified MNPs	Water	OTC	12.0 ng L ⁻¹	40.1 ng L ⁻¹	0.1–200 µg L ⁻¹		99–105		
		TC	19.6 ng L ⁻¹	65.4 ng L ⁻¹	0.1–200 µg L ⁻¹		98–111		
		CTC	74.1 ng L ⁻¹	247.0 ng L ⁻¹	0.5–200 µg L ⁻¹		97–111	<9% (intra-day) <12% (inter-day)	[97]
		DC	12.4 ng L ⁻¹	41.4 ng L ⁻¹	0.1–200 µg L ⁻¹	204 – 276	97–106		
		DMC	21.2 ng L ⁻¹	72.6 ng L ⁻¹	0.1–200 µg L ⁻¹		96–103		
		MC	19.2 ng L ⁻¹	64.1 ng L ⁻¹	0.1–200 µg L ⁻¹		96–106		
C-nanofiber-coated MNPs	Milk	CP	3.02 ng mL ⁻¹	9.63 ng mL ⁻¹	10–600 ng mL ⁻¹	124	93–104		
		TC	3.52 ng mL ⁻¹	9.83 ng mL ⁻¹	10–600 ng mL ⁻¹	109	95–105	<4%	[98]

^a Limit of detection, ^b Limit of quantification, ^c Linear range, ^d Enrichment factor, ^e Relative standard deviation.

OTC: Oxytetracycline, TC: Tetracycline, CTC: Chlortetracycline, DC: Doxycycline, DMC: Demeclocycline, MC: Metacycline and CP: Chloramphenicol.

Table 13 (continued)

Sorbents	Sample	Analytes	LODs ^a	LOQs ^b	LR ^c	EF ^d	Recovery (%)	RSD ^e	Reference
Fe ₃ O ₄ @SiO ₂ @FeO magnetic nanocomposite	Water	OTC	0.027 µg L ⁻¹	0.133 µg L ⁻¹	0.133–333 µg L ⁻¹	23	91–95		
		TC	0.027 µg L ⁻¹	0.133 µg L ⁻¹	0.133–333 µg L ⁻¹	25	93–103	<2% (intra-day) <4% (inter-day)	[99]
		CTC	0.107 µg L ⁻¹	0.267 µg L ⁻¹	0.267–333 µg L ⁻¹	24	94–105		
Water-soluble amino functionalized MNP	Milk	OTC	40 µg L ⁻¹	50 µg L ⁻¹	50–2500 µg L ⁻¹		93–96		
		TC	40 µg L ⁻¹	50 µg L ⁻¹	50–2500 µg L ⁻¹	Not shown	98–108		
		CTC	40 µg L ⁻¹	50 µg L ⁻¹	50–2500 µg L ⁻¹		88–90	≤2.2%	[96]
		DC	40 µg L ⁻¹	50 µg L ⁻¹	50–2500 µg L ⁻¹		88–90		
Natural-phenolic-coated Fe ₃ O ₄ MNPs	Honey	OTC	0.5 µg L ⁻¹ (10 µg kg ⁻¹)	0.7 µg L ⁻¹ (14 µg kg ⁻¹)	0.7–500 µg L ⁻¹ (14–10 ⁴ µg kg ⁻¹)	32	85–118		
		TC	0.5 µg L ⁻¹ (10 µg kg ⁻¹)	0.7 µg L ⁻¹ (14 µg kg ⁻¹)	0.7–500 µg L ⁻¹ (14–10 ⁴ µg kg ⁻¹)	64	81–117	<7% (intra-day) <14% (inter-day)	This work
		CTC	0.5 µg L ⁻¹ (10 µg kg ⁻¹)	1.0 µg L ⁻¹ (20 µg kg ⁻¹)	1.0–500 µg L ⁻¹ (20–10 ⁴ µg kg ⁻¹)	97	81–116		
		DC	0.5 µg L ⁻¹ (10 µg kg ⁻¹)	1.0 µg L ⁻¹ (20 µg kg ⁻¹)	1.0–500 µg L ⁻¹ (20–10 ⁴ µg kg ⁻¹)	90	82–115		

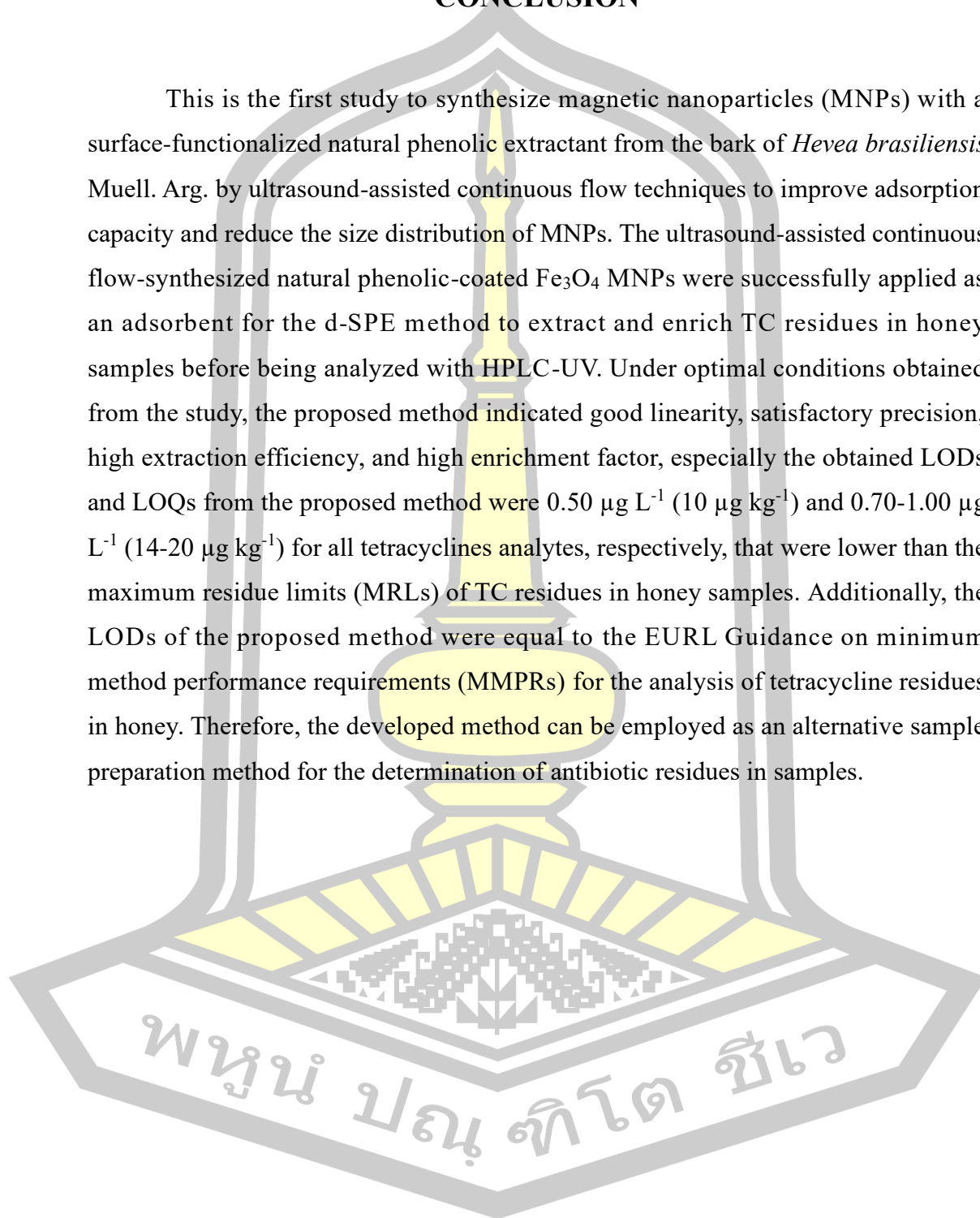
^a Limit of detection, ^b Limit of quantification, ^c Linear range, ^d Enrichment factor, ^e Relative standard deviation.

OTC: Oxytetracycline, TC: Tetracycline, CTC: Chlortetracycline, DC: Doxycycline.

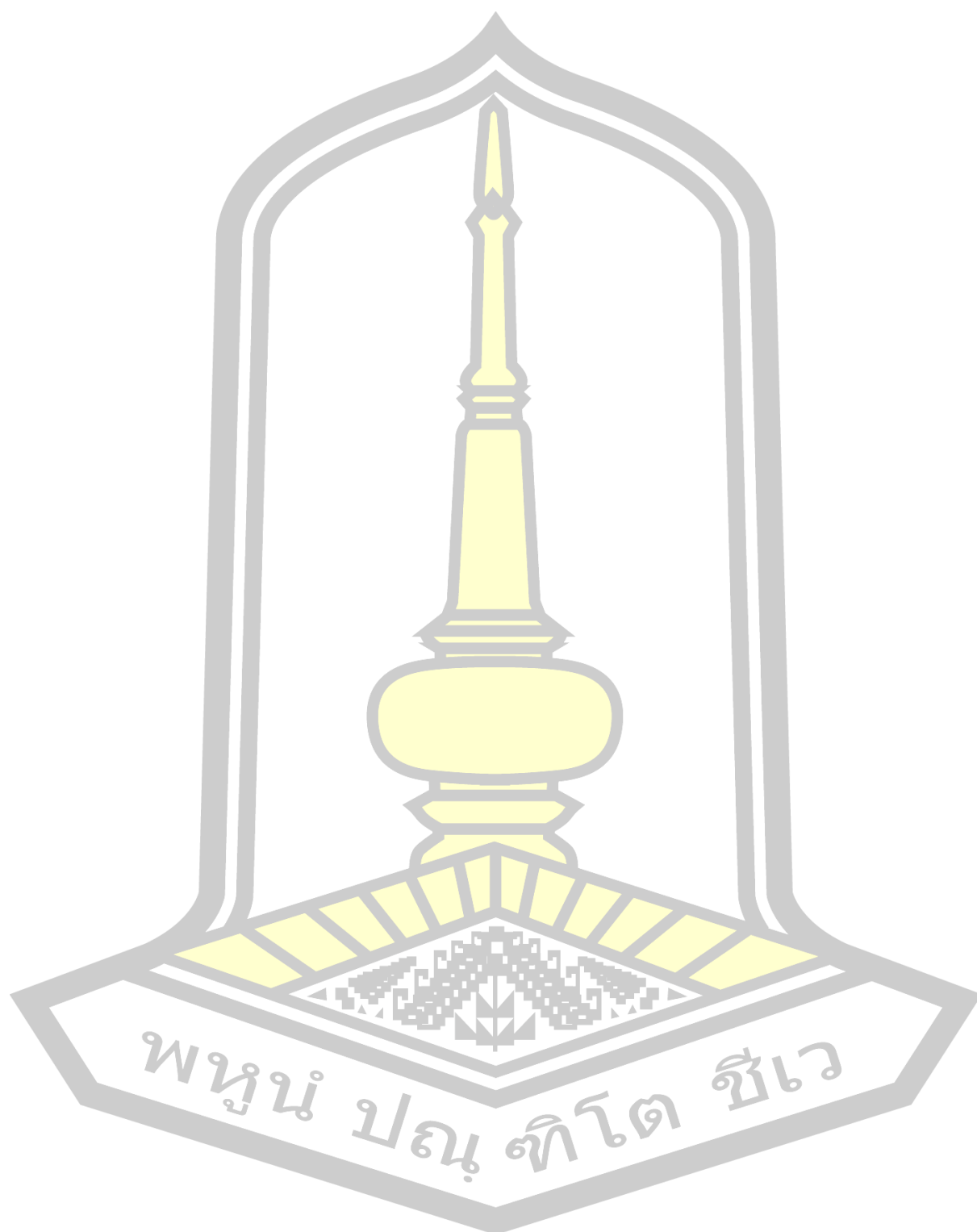
CHAPTER V

CONCLUSION

This is the first study to synthesize magnetic nanoparticles (MNPs) with a surface-functionalized natural phenolic extractant from the bark of *Hevea brasiliensis* Muell. Arg. by ultrasound-assisted continuous flow techniques to improve adsorption capacity and reduce the size distribution of MNPs. The ultrasound-assisted continuous flow-synthesized natural phenolic-coated Fe₃O₄ MNPs were successfully applied as an adsorbent for the d-SPE method to extract and enrich TC residues in honey samples before being analyzed with HPLC-UV. Under optimal conditions obtained from the study, the proposed method indicated good linearity, satisfactory precision, high extraction efficiency, and high enrichment factor, especially the obtained LODs and LOQs from the proposed method were 0.50 µg L⁻¹ (10 µg kg⁻¹) and 0.70-1.00 µg L⁻¹ (14-20 µg kg⁻¹) for all tetracyclines analytes, respectively, that were lower than the maximum residue limits (MRLs) of TC residues in honey samples. Additionally, the LODs of the proposed method were equal to the EURL Guidance on minimum method performance requirements (MMPRs) for the analysis of tetracycline residues in honey. Therefore, the developed method can be employed as an alternative sample preparation method for the determination of antibiotic residues in samples.



REFERENCES



REFERENCES

- [1] M. Hamed Sango Ally and M. Anna, "Determination of Tetracycline Residues in Honey from Tabora and Singida Regions Tanzania Produced Using Modern Beehives," *Int. J. Food Eng. Technol.*, vol. 4, no. 2, p. 32, 2020, doi: 10.11648/j.ijfet.20200402.14.
- [2] D. M. Aljedani, "Antibiotic treatment (Tetracycline) effect on bio-efficiency of the larvae honey bee (*Apis mellifera jemenatica*)," *Saudi J. Biol. Sci.*, vol. 29, no. 3, pp. 1477–1486, 2022, doi: 10.1016/j.sjbs.2021.11.024.
- [3] A. C. Martel, S. Zeggane, P. Drajnudel, J. P. Faucon, and M. Aubert, "Tetracycline residues in honey after hive treatment," *Food Addit. Contam.*, vol. 23, no. 3, pp. 265–273, 2006, doi: 10.1080/02652030500469048.
- [4] N. Phiroonsoontorn, S. Sansuk, Y. Santaladchaiyakit, and S. Srijaranai, "The use of dissolvable layered double hydroxide components in an in situ solid-phase extraction for chromatographic determination of tetracyclines in water and milk samples," *J. Chromatogr. A*, vol. 1519, pp. 38–44, 2017, doi: 10.1016/j.chroma.2017.09.005.
- [5] H. Sereshti, S. Semnani Jazani, N. Nouri, and G. Shams, "Dispersive liquid–liquid microextraction based on hydrophobic deep eutectic solvents: Application for tetracyclines monitoring in milk," *Microchem. J.*, vol. 158, no. June, p. 105269, 2020, doi: 10.1016/j.microc.2020.105269.
- [6] Y. Yang, S. Yin, L. Wu, Y. Li, and C. Sun, "Application of ionic liquid-based air-assisted dispersive liquid–liquid microextraction combined with high-performance liquid chromatography for the determination of six tetracyclines in honey," *Eur. Food Res. Technol.*, vol. 247, no. 11, pp. 2777–2785, 2021, doi: 10.1007/s00217-021-03838-3.
- [7] E. Union and R. Laboratories, "EURL GUIDANCE ON MINIMUM METHOD PERFORMANCE REQUIREMENTS (MMPRs) FOR SPECIFIC PHARMACOLOGICALLY ACTIVE SUBSTANCES IN SPECIFIC ANIMAL MATRICES," no. 37, 2022.
- [8] H. Sereshti, F. Karami, and N. Nouri, "A green dispersive liquid-liquid microextraction based on deep eutectic solvents doped with β -cyclodextrin: Application for determination of tetracyclines in water samples," *Microchem. J.*, vol.

163, no. December 2020, p. 105914, 2021, doi: 10.1016/j.microc.2020.105914.

- [9] R. S. Valverde, M. D. G. García, M. M. Galera, and H. C. Goicoechea, "Determination of tetracyclines in surface water by partial least squares using multivariate calibration transfer to correct the effect of solid phase preconcentration in photochemically induced fluorescence signals," *Anal. Chim. Acta*, vol. 562, no. 1, pp. 85–93, 2006, doi: 10.1016/j.aca.2006.01.035.
- [10] S. ang Supharoek, K. Ponhong, B. Weerasuk, W. Siriangkawut, and K. Grudpan, "A new spectrophotometric method based on peroxidase enzymatic reaction to determine tetracycline in pharmaceutical and water samples," *J. Iran. Chem. Soc.*, vol. 17, no. 9, pp. 2385–2395, 2020, doi: 10.1007/s13738-020-01934-x.
- [11] Z. Wang *et al.*, "High through-put determination of 28 veterinary antibiotic residues in swine wastewater by one-step dispersive solid phase extraction sample cleanup coupled with ultra-performance liquid chromatography-tandem mass spectrometry," *Chemosphere*, 2019, doi: 10.1016/j.chemosphere.2019.05.047.
- [12] K. Cherkashina, M. Voznesenskiy, O. Osmolovskaya, C. Vakh, and A. Bulatov, "Effect of surfactant coating of Fe₃O₄ nanoparticles on magnetic dispersive micro-solid phase extraction of tetracyclines from human serum," *Talanta*, vol. 214, p. 120861, 2020, doi: 10.1016/j.talanta.2020.120861.
- [13] T. Khezeli and A. Daneshfar, "Development of dispersive micro-solid phase extraction based on micro and nano sorbents," *TrAC - Trends Anal. Chem.*, vol. 89, pp. 99–118, 2017, doi: 10.1016/j.trac.2017.01.004.
- [14] B. Ahmed *et al.*, "Synthesis of gallotannin capped iron oxide nanoparticles and their broad spectrum biological applications," *RSC Adv.*, vol. 11, no. 17, pp. 9880–9893, 2021, doi: 10.1039/d1ra00220a.
- [15] S. O. S. Mookantsa, S. Dube, and M. M. Nindi, "Talanta Development and application of a dispersive liquid – liquid microextraction method for the determination of tetracyclines in beef by liquid chromatography mass spectrometry," *Talanta*, vol. 148, pp. 321–328, 2016, doi: 10.1016/j.talanta.2015.11.006.
- [16] F. Nguyen, A. L. Starosta, S. Arenz, D. Sohmen, A. Dönhöfer, and D. N. Wilson, "Tetracycline antibiotics and resistance mechanisms," vol. 395, no. 5, pp. 559–575, 2014, doi: 10.1515/hsz-2013-0292.

- [17] R. Following and H. Therapy, "Tetracycline Antibiotics : Mode of Action , Applications , Molecular Biology , and Epidemiology of Bacterial Resistance," vol. 65, no. 2, pp. 232–260, 2001, doi: 10.1128/MMBR.65.2.232.
- [18] D. Fuoco, "Classification Framework and Chemical Biology of Tetracycline-Structure-Based Drugs," pp. 1–13, 2012, doi: 10.3390/antibiotics1010001.
- [19] A. Önal, "Overview on liquid chromatographic analysis of tetracycline residues in food matrices," *Food Chem.*, vol. 127, no. 1, pp. 197–203, 2011, doi: 10.1016/j.foodchem.2011.01.002.
- [20] K. J. Choi, H. J. Son, and S. H. Kim, "Ionic treatment for removal of sulfonamide and tetracycline classes of antibiotic," *Sci. Total Environ.*, vol. 387, no. 1–3, pp. 247–256, 2007, doi: 10.1016/j.scitotenv.2007.07.024.
- [21] J. Chico, F. van Holthoon, and T. Zuidema, "Ion Suppression Study for Tetracyclines in Feed," *Chromatogr. Res. Int.*, vol. 2012, pp. 1–9, 2012, doi: 10.1155/2012/135854.
- [22] M. Pérez-Rodríguez, R. G. Pellerano, L. Pezza, and H. R. Pezza, "An overview of the main foodstuff sample preparation technologies for tetracycline residue determination," *Talanta*, vol. 182, no. January, pp. 1–21, 2018, doi: 10.1016/j.talanta.2018.01.058.
- [23] N. Pastor-Navarro, Á. Maquieira, and R. Puchades, "Review on immunoanalytical determination of tetracycline and sulfonamide residues in edible products," *Anal. Bioanal. Chem.*, vol. 395, no. 4, pp. 907–920, 2009, doi: 10.1007/s00216-009-2901-y.
- [24] H. Chen *et al.*, "Ratiometric fluorescence and visual determination of tetracycline antibiotics based on Y^{3+} and copper nanoclusters–induced cascade signal amplification," *Microchim. Acta*, vol. 189, no. 9, pp. 1–8, 2022, doi: 10.1007/s00604-022-05447-7.
- [25] F. Alanazi, R. Almugbel, H. M. Maher, F. M. Alodaib, and N. Z. Alzoman, "Determination of tetracycline, oxytetracycline and chlortetracycline residues in seafood products of Saudi Arabia using high performance liquid chromatography–Photo diode array detection," *Saudi Pharm. J.*, vol. 29, no. 6, pp. 566–575, 2021, doi: 10.1016/j.jsps.2021.04.017.
- [26] "MAXIMUM RESIDUE LIMITS (MRLs) AND RISK MANAGEMENT RECOMMENDATIONS (RMRs) FOR RESIDUES OF VETERINARY DRUGS IN

FOODS CAC/MRL 2-2015 Updated as at the 38 Session of the Codex Alimentarius Commission (July 2015),” no. July, 2015.

- [27] “ARCHIVED List of Maximum Residue Limits (MRLs) for Veterinary Drugs in Foods – [May 31, 2021] - Canada.ca.” <https://www.canada.ca/en/health-canada/services/drugs-health-products/veterinary-drugs/maximum-residue-limits-mrls/list-maximum-residue-limits-mrls-veterinary-drugs-foods-may-31-2021.html> (accessed Jan. 29, 2023).
- [28] R. Smith, “Commission Regulation (EU) No 330/2010,” *Core EU Legis.*, no. 2377, pp. 157–163, 2015, doi: 10.1007/978-1-137-54482-7_12.
- [29] “Announcement No. 235 of the Ministry of Agriculture regarding to the maximum residue limits of veterinary drugs in animal foods. | FAOLEX.” <https://www.fao.org/faolex/results/details/en/c/LEX-FAOC176367> (accessed Jan. 29, 2023).
- [30] Brazil, “Plano de Nacional de Controle de Resíduos e Contaminantes PNCRC / Animal,” 2014. <https://www.gov.br/agricultura/pt-br/assuntos/inspecao/produtos-animal/plano-de-nacional-de-controle-de-residuos-e-contaminantes/documentos-da-pncrc/pncrc-2014.pdf> (accessed Jan. 29, 2023).
- [31] L. A. de la Rosa, J. O. Moreno-Escamilla, J. Rodrigo-García, and E. Alvarez-Parrilla, *Phenolic compounds*. Elsevier Inc., 2018.
- [32] A. Basli, N. Belkacem, and I. Amrani, “Health Benefits of Phenolic Compounds Against Cancers,” *Phenolic Compd. - Biol. Act.*, 2017, doi: 10.5772/67232.
- [33] R. Y. Gan *et al.*, *Bioactive compounds and beneficial functions of sprouted grains*. Elsevier Inc., 2018.
- [34] K.-T. Chung *et al.*, “Critical Reviews in Food Science and Nutrition Tannins and Human Health: A Review Tannins and Human Health: A Review,” *Crit. Rev. Food Sci. Nutr.*, vol. 386, no. 386, pp. 37–41, 1998, [Online]. Available: <http://www.tandfonline.com/loi/bfsn20%5Cnhttp://dx.doi.org/10.1080/10408699891274273%5Cnhttp://%5Cnwww.tandfonline.com/>.
- [35] U . S . F O R E S T S E R V I C E , “ T a n n i n s . ” https://www.fs.usda.gov/wildflowers/ethnobotany/tannins.shtml?fbclid=IwAR1DRqKS-hj-Pb2qh13gm4IGgoX-qWrQTFQIZlevbx__dE9wVXEwwy48oLs (accessed Feb.

12, 2023).

- [36] T. Okuda and H. Ito, “Tannins of Constant Structure in Medicinal and Food Plants—Hydrolyzable Tannins and Polyphenols Related to Tannins,” *Molecules*, vol. 16, no. 3, pp. 2191–2217, Mar. 2011, doi: 10.3390/molecules16032191.
- [37] I. Ky, A. Le Floch, L. Zeng, L. Pechamat, M. Jourdes, and P. L. Teissedre, “Tannins,” *Encycl. Food Heal.*, pp. 247–255, 2015, doi: 10.1016/B978-0-12-384947-2.00683-8.
- [38] G. D. Hill, “PLANT ANTINUTRITIONAL FACTORS | Characteristics,” *Encycl. Food Sci. Nutr.*, no. 1948, pp. 4578–4587, 2003, doi: 10.1016/b0-12-227055-x/01318-3.
- [39] C. Crestini and H. Lange, “A novel and efficient immobilised tannase coated by the layer-by-layer technique in the hydrolysis of gallotannins and ellagitannins,” *Microchem. J.*, vol. 123, pp. 139–147, 2015, doi: 10.1016/j.microc.2015.05.025.
- [40] by D. Harley Naumann and M. Mort Kothmann, “MOLECULAR WEIGHT OF CONDENSED TANNINS FROM WARM-SEASON PERENNIAL LEGUMES AND ITS EFFECT ON CONDENSED TANNIN BIOLOGICAL ACTIVITY A Dissertation,” no. August, 2013.
- [41] L. Vaysse, F. Bonfils, J. Sainte-Beuve, and M. Cartault, *Natural Rubber*, vol. 10. Elsevier B.V., 2012.
- [42] K. P. P. Nair, *Rubber (Hevea brasiliensis)*. 2010.
- [43] P. Venkatachalam, N. Geetha, P. Sangeetha, and A. Thulaseedharan, “Natural rubber producing plants: An overview,” *African J. Biotechnol.*, vol. 12, no. 12, pp. 1297–1310, 2013, doi: 10.5897/AJBX12.016.
- [44] C. Dutsadee and C. Nunta, “Induction of peroxidase, scopoletin, phenolic compounds and resistance in *Hevea brasiliensis* by elicitor and a novel protein elicitor purified from *Phytophthora palmivora*,” *Physiol. Mol. Plant Pathol.*, vol. 72, no. 4–6, pp. 179–187, 2008, doi: 10.1016/j.pmpp.2008.09.002.
- [45] W. Zuraida, W. Mohd, N. Nadia, S. Jusoh, and N. Amira, “ANTIOXIDANT ACTIVITY , TOTAL PHENOLIC AND FLAVONOID CONTENT FROM LEAVES AND SEED EXTRACTS OF *Hevea brasiliensis* CLONE,” vol. 9, no. 1, pp. 1–7, 2021.
- [46] M. H. Simatupang, U. Schmitt, and A. Kasim, “WOOD EXTRACTIVES OF

RUBBERWOOD (HEVEA BRASILIENSIS) AND THEIR INFLUENCES ON THE SETTING OF THE INORGANIC BINDER IN GYPSUM-BONDED PARTICLEBOARDS,” *J. Trop. For. Sci.*, vol. 6, no. 3, pp. 269–285, Nov. 1994, [Online]. Available: <http://www.jstor.org/stable/43582437>.

- [47] L. F. Salomé Abarca, P. G. L. Klinkhamer, and Y. H. Choi, “Plant Latex, from Ecological Interests to Bioactive Chemical Resources,” *Planta Med.*, vol. 85, no. 11–12, pp. 856–868, 2019, doi: 10.1055/a-0923-8215.
- [48] B. Arabsorkhi and H. Sereshti, “Determination of tetracycline and cefotaxime residues in honey by micro-solid phase extraction based on electrospun nanofibers coupled with HPLC,” *Microchem. J.*, vol. 140, no. April, pp. 241–247, 2018, doi: 10.1016/j.microc.2018.04.030.
- [49] K. Ridgway, S. P. D. Lalljie, and R. M. Smith, “Sample preparation techniques for the determination of trace residues and contaminants in foods,” *J. Chromatogr. A*, vol. 1153, no. 1–2, pp. 36–53, 2007, doi: 10.1016/j.chroma.2007.01.134.
- [50] G. T. Peres, S. Rath, and F. G. R. Reyes, “A HPLC with fluorescence detection method for the determination of tetracyclines residues and evaluation of their stability in honey,” *Food Control*, vol. 21, no. 5, pp. 620–625, 2010, doi: 10.1016/j.foodcont.2009.09.006.
- [51] J. Li *et al.*, “Determination of tetracyclines residues in honey by on-line solid-phase extraction high-performance liquid chromatography,” *Talanta*, vol. 75, no. 5, pp. 1245–1252, 2008, doi: 10.1016/j.talanta.2008.01.027.
- [52] Y. H. Pang, Z. Y. Lv, J. C. Sun, C. Yang, and X. F. Shen, “Collaborative compounding of metal–organic frameworks for dispersive solid-phase extraction HPLC–MS/MS determination of tetracyclines in honey,” *Food Chem.*, vol. 355, no. November 2020, 2021, doi: 10.1016/j.foodchem.2021.129411.
- [53] Y. Yang, G. Lin, L. Liu, and T. Lin, “Rapid determination of multi-antibiotic residues in honey based on modified QuEChERS method coupled with UPLC–MS/MS,” *Food Chem.*, vol. 374, no. 67, p. 131733, 2022, doi: 10.1016/j.foodchem.2021.131733.
- [54] C. Tu *et al.*, “Determination of Tetracycline in Water and Honey by Iron(II, III)/Aptamer-Based Magnetic Solid-Phase Extraction with High-Performance Liquid Chromatography Analysis,” *Anal. Lett.*, vol. 52, no. 10, pp. 1653–1669, 2019, doi: 10.1080/00032719.2018.1560458.

- [55] J. J. Xu *et al.*, “Determination of Tetracycline Antibiotic Residues in Honey and Milk by Miniaturized Solid Phase Extraction Using Chitosan-Modified Graphitized Multiwalled Carbon Nanotubes,” *J. Agric. Food Chem.*, vol. 64, no. 12, pp. 2647–2654, 2016, doi: 10.1021/acs.jafc.6b00748.
- [56] N. Taokaenchan and S. Sangsrichan, “HPLC-Fluorescence Detection Method for Quantitative Determination of Tetracycline Antibiotic Residues in Honey Department of Chemistry, Faculty of Science, Maejo University, a value of 0.1 mg/kg was introduced as the allowed residual quantity of te,” vol. 6, no. 2, pp. 147–155, 2010.
- [57] G. Krepper, G. D. Pierini, M. F. Pistonesi, and M. S. Di Nezio, “‘In-situ’ antimony film electrode for the determination of tetracyclines in Argentinean honey samples,” *Sensors Actuators, B Chem.*, vol. 241, pp. 560–566, 2017, doi: 10.1016/j.snb.2016.10.125.
- [58] M. F. Lanjwani, N. Altunay, and M. Tuzen, “Preparation of fatty acid-based ternary deep eutectic solvents: Application for determination of tetracycline residue in water, honey and milk samples by using vortex-assisted microextraction,” *Food Chem.*, vol. 400, no. May 2022, p. 134085, 2023, doi: 10.1016/j.foodchem.2022.134085.
- [59] B. Socas-Rodríguez, A. V. Herrera-Herrera, M. Asensio-Ramos, and J. Hernández-Borges, “Dispersive Solid-Phase Extraction,” *Anal. Sep. Sci.*, pp. 1525–1570, 2015, doi: 10.1002/9783527678129.assep056.
- [60] G. Islas, I. S. Ibarra, P. Hernandez, J. M. Miranda, and A. Cepeda, “Dispersive Solid Phase Extraction for the Analysis of Veterinary Drugs Applied to Food Samples: A Review,” *Int. J. Anal. Chem.*, vol. 2017, p. 8215271, 2017, doi: 10.1155/2017/8215271.
- [61] P. Ścigalski and P. Kosobucki, “Recent Materials Developed for Dispersive Solid Phase Extraction,” *Molecules*, vol. 25, no. 21, pp. 1–26, 2020, doi: 10.3390/molecules25214869.
- [62] M. Ghorbani, M. Aghamohammadhassan, H. Ghorbani, and A. Zabihi, “Trends in sorbent development for dispersive micro-solid phase extraction,” *Microchem. J.*, vol. 158, no. April, p. 105250, 2020, doi: 10.1016/j.microc.2020.105250.
- [63] B. Hu, M. He, and B. Chen, *Magnetic nanoparticle sorbents*. Elsevier Inc., 2019.
- [64] M. Faraji, M. Shirani, and H. Rashidi-Nodeh, “The recent advances in magnetic

- sorbents and their applications,” *TrAC - Trends Anal. Chem.*, vol. 141, p. 116302, 2021, doi: 10.1016/j.trac.2021.116302.
- [65] S. Liu, C. Ma, M. Ma, and F. Xu, *12 - Magnetic Nanocomposite Adsorbents*. Elsevier Inc., 2019.
- [66] R. Keçili, F. Ghorbani-Bidkorbeh, İ. Dolak, G. Canpolat, M. Karabörk, and C. M. Hussain, “Functionalized magnetic nanoparticles as powerful sorbents and stationary phases for the extraction and chromatographic applications,” *TrAC - Trends Anal. Chem.*, vol. 143, 2021, doi: 10.1016/j.trac.2021.116380.
- [67] R. Gérardy *et al.*, “Continuous Flow Organic Chemistry: Successes and Pitfalls at the Interface with Current Societal Challenges,” *European J. Org. Chem.*, vol. 2018, no. 20, pp. 2301–2351, 2018, doi: 10.1002/ejoc.201800149.
- [68] A. Mokkarat, S. Kruanetr, and U. Sakee, “Simple continuous flow synthesis of 3-indolyl naphthoquinone using acid catalysts,” *Synth. Commun.*, vol. 51, no. 15, pp. 2324–2335, 2021, doi: 10.1080/00397911.2021.1934701.
- [69] J. I. Yoshida, A. Nagaki, and D. Yamada, “Continuous flow synthesis,” *Drug Discov. Today Technol.*, vol. 10, no. 1, pp. e53–e59, 2013, doi: 10.1016/j.ddtec.2012.10.013.
- [70] J. H. Bang and K. S. Suslick, “Applications of ultrasound to the synthesis of nanostructured materials,” *Adv. Mater.*, vol. 22, no. 10, pp. 1039–1059, 2010, doi: 10.1002/adma.200904093.
- [71] A. R. Deshmukh, A. Gupta, and B. S. Kim, “Ultrasound Assisted Green Synthesis of Silver and Iron Oxide Nanoparticles Using Fenugreek Seed Extract and Their Enhanced Antibacterial and Antioxidant Activities,” *Biomed Res. Int.*, vol. 2019, 2019, doi: 10.1155/2019/1714358.
- [72] Q. Yan, M. Qiu, X. Chen, and Y. Fan, “Ultrasound assisted synthesis of size-controlled aqueous colloids for the fabrication of nanoporous zirconia membrane,” *Front. Chem.*, vol. 7, no. MAY, pp. 1–10, 2019, doi: 10.3389/fchem.2019.00337.
- [73] C. Vaitsis *et al.*, “Ultrasound-Assisted Preparation Methods of Nanoparticles for Energy-Related Applications,” in *Nanotechnology and the Environment*, M. Sen, Ed. Rijeka: IntechOpen, 2020, p. Ch. 5.
- [74] S. G. Babu, B. Neppolian, and M. Ashokkumar, *Ultrasound-assisted synthesis of nanoparticles for energy and environmental applications #14*, no. October. 2016.

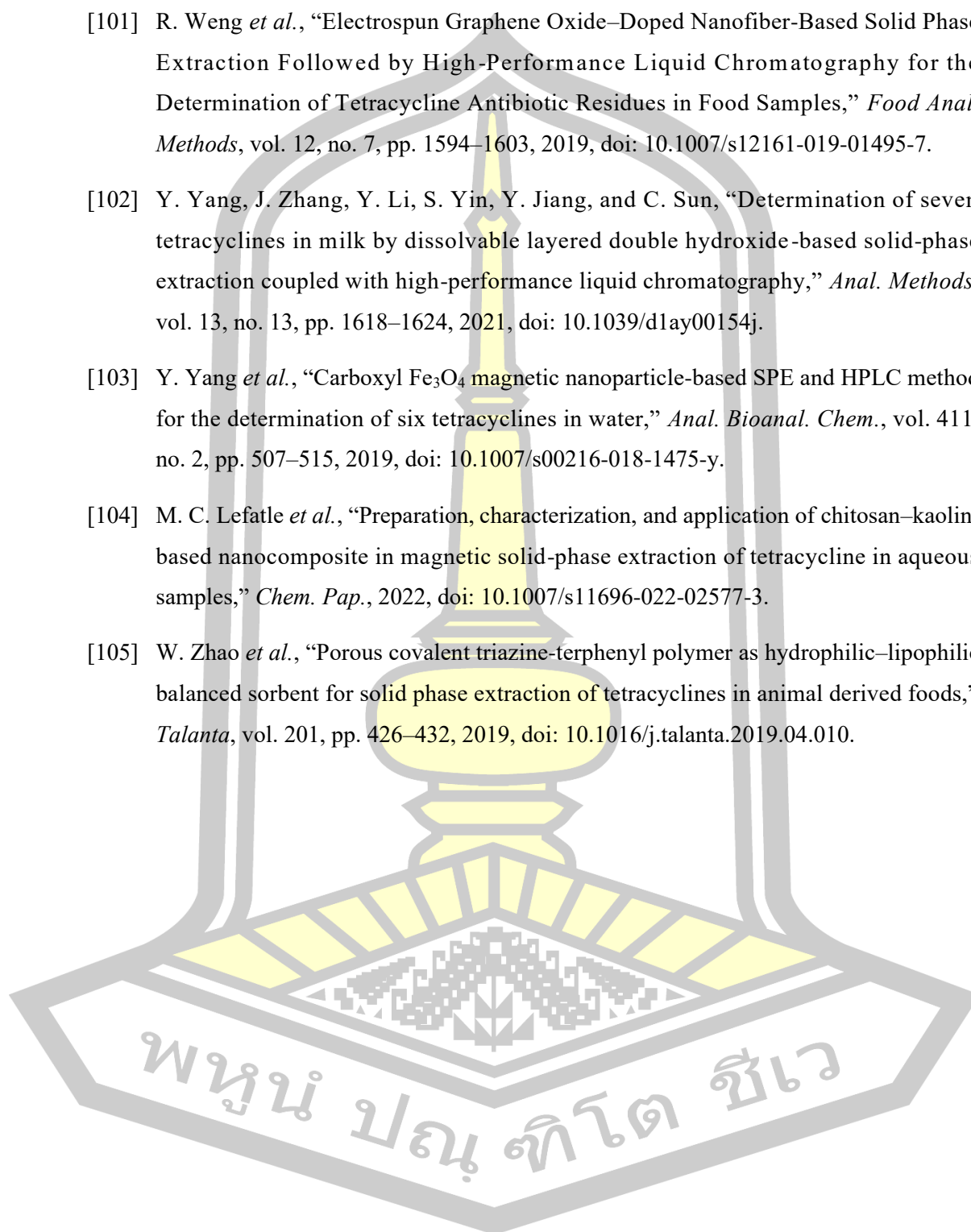
- [75] R. Herrera-Becerra, J. L. Rius, and C. Zorrilla, "Tannin biosynthesis of iron oxide nanoparticles," *Appl. Phys. A Mater. Sci. Process.*, vol. 100, no. 2, pp. 453–459, 2010, doi: 10.1007/s00339-010-5903-x.
- [76] C. Pucci *et al.*, "Tannic Acid-Iron Complex-Based Nanoparticles as a Novel Tool against Oxidative Stress," *ACS Appl. Mater. Interfaces*, vol. 14, no. 14, pp. 15927–15941, 2022, doi: 10.1021/acsami.1c24576.
- [77] K. Saowalak, T. Titipun, T. Somchai, and P. Chalermchai, "Iron(III)-Tannic Molecular Nanoparticles Enhance Autophagy effect and T1 MRI Contrast in Liver Cell Lines," *Sci. Rep.*, vol. 8, no. 1, pp. 1–13, 2018, doi: 10.1038/s41598-018-25108-1.
- [78] P. Ding *et al.*, "Tannic Acid (TA)-Functionalized Magnetic Nanoparticles for EpCAM-Independent Circulating Tumor Cell (CTC) Isolation from Patients with Different Cancers," *ACS Appl. Mater. Interfaces*, vol. 13, no. 3, pp. 3694–3700, 2021, doi: 10.1021/acsami.0c20916.
- [79] M. Nemati, M. A. Farajzadeh, and M. R. Afshar Mogaddam, "Development of a surfactant-assisted dispersive solid phase extraction using deep eutectic solvent to extract four tetracycline antibiotics residues in milk samples," *J. Sep. Sci.*, vol. 44, no. 10, pp. 2121–2130, 2021, doi: 10.1002/jssc.202001218.
- [80] E. Soleimanirad, A. Badameh, A. Raoufi, and M. Ebrahimi, "Simultaneous determination of four antibiotics in human urine and hair samples employing a simple and efficient dispersive micro solid-phase extraction-high performance liquid chromatography," *Pharmacol. Reports*, vol. 74, no. 5, pp. 1069–1082, 2022, doi: 10.1007/s43440-022-00404-w.
- [81] N. Ma *et al.*, "Determination of Tetracyclines in Chicken by Dispersive Solid Phase Microextraction Based on Metal-Organic Frameworks/Molecularly Imprinted Nanopolymer and Ultra Performance Liquid Chromatography," *Food Anal. Methods*, vol. 13, no. 5, pp. 1211–1219, 2020, doi: 10.1007/s12161-020-01744-0.
- [82] Y. Sun, J. Tian, L. Wang, H. Yan, F. Qiao, and X. Qiao, "One pot synthesis of magnetic graphene/carbon nanotube composites as magnetic dispersive solid-phase extraction adsorbent for rapid determination of oxytetracycline in sewage water," *J. Chromatogr. A*, vol. 1422, pp. 53–59, 2015, doi: 10.1016/j.chroma.2015.10.035.
- [83] G. R. Jamieson, S. Arora, and D. Bhanot, "HPLC e-Book," *Introd. to High Perform.*

Liq. Chromatogr. by Lab-Training.com, pp. 1–40, 2014.

- [84] “The Principle of High-Performance Liquid Chromatography (HPLC) - Creative Proteomics.” <https://www.creative-proteomics.com/pronalyse/the-principle-of-high-performance-liquid-chromatography-hplc.html> (accessed Feb. 18, 2023).
- [85] X. Wang, F. Liu, W. Liang, and W. Zhang, “Characterization of Electromagnetic Catalysis and Degradation of Algogenic Odor Using Fe_3O_4 Nanoparticles with Tannin Coating,” *ACS ES&T Eng.*, vol. 1, no. 11, pp. 1542–1552, 2021, doi: 10.1021/acsestengg.1c00191.
- [86] J. L. Li, D. C. Li, S. L. Zhang, H. C. Cui, and C. Wang, “Analysis of the factors affecting the magnetic characteristics of nano- Fe_3O_4 particles,” *Chinese Sci. Bull.*, vol. 56, no. 8, pp. 803–810, 2011, doi: 10.1007/s11434-010-4126-z.
- [87] B. H. Hui and M. N. Salimi, “Production of Iron Oxide Nanoparticles by Co-Precipitation method with Optimization Studies of Processing Temperature, pH and Stirring Rate,” *IOP Conf. Ser. Mater. Sci. Eng.*, vol. 743, no. 1, 2020, doi: 10.1088/1757-899X/743/1/012036.
- [88] S. Z. H. Shah, U. Khan, S. Riaz, and S. Naseem, *Effect of pH on Iron Oxide Nanoparticles*, vol. 2, no. 10. Elsevier Ltd., 2015.
- [89] A. A. Wibowo, H. Sutanto, P. Priyono, A. N. Syahida, F. D. D. Irianti, and I. Alkian, “The effect of 6 hours stirring time on natural iron sand base on magnetics Fe_3O_4 nanoparticle by sonification,” *J. Phys. Conf. Ser.*, vol. 1943, no. 1, 2021, doi: 10.1088/1742-6596/1943/1/012015.
- [90] M. Bagtash, Y. Yamini, E. Tahmasebi, J. Zolgharnein, and Z. Dalirnasab, “Magnetite nanoparticles coated with tannic acid as a viable sorbent for solid-phase extraction of Cd^{2+} , Co^{2+} and Cr^{3+} ,” *Microchim. Acta*, vol. 183, no. 1, pp. 449–456, 2016, doi: 10.1007/s00604-015-1667-5.
- [91] M. D. Donohue and G. L. Aranovich, “Classification of Gibbs adsorption isotherms,” *Adv. Colloid Interface Sci.*, vol. 76–77, pp. 137–152, 1998, doi: 10.1016/S0001-8686(98)00044-X.
- [92] M. V. Goycoolea, M. M. Hueb, and C. Ruah, “Definitions and terminology,” *Otolaryngol. Clin. North Am.*, vol. 24, no. 4, pp. 757–761, 1991, doi: 10.4324/b23292-3.

- [93] C. Li *et al.*, “Adsorption of two antibiotics on biochar prepared in air-containing atmosphere: Influence of biochar porosity and molecular size of antibiotics,” *J. Mol. Liq.*, vol. 274, pp. 353–361, 2019, doi: 10.1016/j.molliq.2018.10.142.
- [94] W. Kaewsuwan, P. Kanatharana, and O. Bunkoed, “Dispersive magnetic solid phase extraction using octadecyl coated silica magnetite nanoparticles for the extraction of tetracyclines in water samples,” *J. Anal. Chem.*, vol. 72, no. 9, pp. 957–965, Sep. 2017, doi: 10.1134/S1061934817090143.
- [95] Fao, “Guidelines on performance criteria for methods of analysis for the determination of pesticide residues in food and feed,” *Codex Aliment.*, pp. 1–13, 2017, [Online]. Available: http://www.fao.org/fao-who-codexalimentarius/sh-proxy/fr/?lnk=1&url=https://workspace.fao.org/sites/codex/Standards/CAC+GL+90-2017/CXG_090e.pdf.
- [96] H. zhi Tang, Y. hui Wang, S. Li, J. Wu, Z. xian Gao, and H. ying Zhou, “Development and application of magnetic solid phase extraction in tandem with liquid–liquid extraction method for determination of four tetracyclines by HPLC with UV detection,” *J. Food Sci. Technol.*, vol. 57, no. 8, pp. 2884–2893, 2020, doi: 10.1007/s13197-020-04320-w.
- [97] H. C. Ri *et al.*, “A reciprocating magnetic field assisted on-line solid-phase extraction coupled with liquid chromatography-tandem mass spectrometry determination of trace tetracyclines in water,” *Anal. Chim. Acta*, vol. 1182, p. 338957, 2021, doi: 10.1016/j.aca.2021.338957.
- [98] B. Vuran *et al.*, “Determination of chloramphenicol and tetracycline residues in milk samples by means of nanofiber coated magnetic particles prior to high-performance liquid chromatography-diode array detection,” *Talanta*, vol. 230, no. November 2020, p. 122307, 2021, doi: 10.1016/j.talanta.2021.122307.
- [99] L. Lian, J. Lv, X. Wang, and D. Lou, “Magnetic solid–phase extraction of tetracyclines using ferrous oxide coated magnetic silica microspheres from water samples,” *J. Chromatogr. A*, vol. 1534, pp. 1–9, 2018, doi: 10.1016/j.chroma.2017.12.041.
- [100] E. Marinou, V. F. Samanidou, and I. N. Papadoyannis, “Development of a high pressure liquid chromatography with diode array detection method for the determination of four tetracycline residues in milk by using QuEChERS dispersive

- extraction,” *Separations*, vol. 6, no. 2, 2019, doi: 10.3390/separations6020021.
- [101] R. Weng *et al.*, “Electrospun Graphene Oxide–Doped Nanofiber-Based Solid Phase Extraction Followed by High-Performance Liquid Chromatography for the Determination of Tetracycline Antibiotic Residues in Food Samples,” *Food Anal. Methods*, vol. 12, no. 7, pp. 1594–1603, 2019, doi: 10.1007/s12161-019-01495-7.
- [102] Y. Yang, J. Zhang, Y. Li, S. Yin, Y. Jiang, and C. Sun, “Determination of seven tetracyclines in milk by dissolvable layered double hydroxide-based solid-phase extraction coupled with high-performance liquid chromatography,” *Anal. Methods*, vol. 13, no. 13, pp. 1618–1624, 2021, doi: 10.1039/d1ay00154j.
- [103] Y. Yang *et al.*, “Carboxyl Fe_3O_4 magnetic nanoparticle-based SPE and HPLC method for the determination of six tetracyclines in water,” *Anal. Bioanal. Chem.*, vol. 411, no. 2, pp. 507–515, 2019, doi: 10.1007/s00216-018-1475-y.
- [104] M. C. Lefatle *et al.*, “Preparation, characterization, and application of chitosan–kaolin-based nanocomposite in magnetic solid-phase extraction of tetracycline in aqueous samples,” *Chem. Pap.*, 2022, doi: 10.1007/s11696-022-02577-3.
- [105] W. Zhao *et al.*, “Porous covalent triazine-terphenyl polymer as hydrophilic–lipophilic balanced sorbent for solid phase extraction of tetracyclines in animal derived foods,” *Talanta*, vol. 201, pp. 426–432, 2019, doi: 10.1016/j.talanta.2019.04.010.



BIOGRAPHY

NAME	Tammanoon Nilnit
DATE OF BIRTH	17 April 1999
PLACE OF BIRTH	Kuchinarai district, Kalasin province
ADDRESS	167 Village No. 2 Joomjung Sub-district, Kuchinarai district, Kalasin, 46110.
POSITION	Student
PLACE OF WORK	Mahasarakham University
EDUCATION	2015-2017 High School Certificate equivalent, Buakhao School, Kalasin, Thailand 2018-2021 Bachelor of Science, Mahasarakham University, Maha Sarakham, Thailand 2022-Present Master of Science, Mahasarakham University, Maha Sarakham, Thailand
Research grants & awards	Centre of Excellence for Innovation in Chemistry
Research output	-

